UNIVERSIDADE DE SÃO PAULO
FACULDADE DE ODONTOLOGIA DE BAURU

NÁDIA GHINELLI AMÔR

Characterization of the functional relationship between macrophages, cancer stem cells and epithelial-to-mesenchymal transition in oral squamous cell carcinoma

Caracterização da relação funcional entre macrófagos, fenótipo célula-tronco de câncer e fenômeno de transição epitélio-mesenquimal no carcinoma epidermóide de boca

BAURU
2019

NÁDIA GHINELLI AMÔR

Characterization of the functional relationship between macrophages, cancer stem cells and epithelial-to-mesenchymal transition in oral squamous cell carcinoma

Caracterização da relação funcional entre macrófagos, fenótipo célula-tronco de câncer e fenômeno de transição epitélio-mesenquimal no carcinoma epidermóide de boca

Tese constituída por artigos apresentada a Faculdade de Odontologia de Bauru da Universidade de São Paulo para obtenção do título de Doutor em Ciências no Programa de Ciências Odontológicas Aplicadas, na área de concentração Biologia Oral.

Orientador: Profa. Dra. Camila de Oliveira Rodini Pegoraro

BAURU
2019

Amôr, Nádia Ghinelli
Characterization of the functional relationship between macrophages, cancer stem cells and epithelial-to-mesenchymal transition in oral squamous cell carcinoma / Nádia Ghinelli Amôr. – Bauru, 2019.
126 p. : il. ; 31cm.

Tese (Doutorado) – Faculdade de Odontologia de Bauru. Universidade de São Paulo

Orientadora: Profa. Dra. Camila de Oliveira Rodini Pegoraro

Comitê de Ética da FOB-USP
Protocolo nº: 002/2017
Data: 05/05/2017

O presente trabalho foi realizado com o apoio da Coordenação de Aperfeiçoamento de Pessoal de Nível Superior – Brasil (CAPES) – Código de Financiamento 001.

O presente trabalho também recebeu apoio financeiro da Fundação de Amparo à Pesquisa do Estado de São Paulo, por meio do Auxílio Jovem Pesquisador e do Conselho Nacional de Desenvolvimento Científico e Tecnológico, por meio do auxílio Universal (C.R.O. 2013/07245-9 e 424158/2016-7, respectivamente)

ERRATA

FOLHA DE APROVAÇÃO

DEDICATÓRIA

Ao Rapha...

AGRADECIMENTOS

A minha orientadora, **Profa. Dra. Camila Rodini**, por tamanha confiança depositada em mim, pela oportunidade diária de aprendizagem e por todo carinho e zelo que sempre demonstrou pela equipe. Exemplo vivo de como liderar e inspirar um grupo e não de apenas chefiá-lo.

Aos meus colegas de equipe, **Rafael Ortiz** e **Nathália Lopes**, que me acolheram prontamente tornando a minha mudança a mais leve possível e se tornaram pessoas essenciais na minha vida acadêmica e pessoal. A **Luciana Saito** pessoa incrível que tenho o prazer de conviver dentro e fora do laboratório. Um exemplo vivo de resiliência!

Ao **Rodrigo Buzzo**, que me ajudou durante a execução de todo o meu projeto! Sempre ouvindo meus desabafos e acalmando minha ansiedade!! Agradeço pela grande oportunidade de compartilhar meus conhecimentos e ajuda-lo no início de sua vida acadêmica/científica.

Aos amigos **Claudinha, Franco** e **Karen** que sempre me incentivaram a buscar mais e sempre compartilharam comigo suas experiências e conhecimentos. Muito obrigada mesmo! Sinto muito a falta de vocês no meu dia-a-dia.

Aos professores do Laboratório de Histologia, **Prof. Rumio Taga**, **Prof. Dr. Gerson Francisco de Assis** e **Prof. Dr. Gustavo Pompermaier Garlet** por todos os conselhos e aprendizado diário.

As queridas técnicas e secretária do Laboratório de Histologia, **Patrícia Germino**, **Danielle Ceolin, Dra. Tânia Mary Cestari e Maria Teresa**, que além de todo o apoio técnico-científico sempre pude contar com a amizade e carinho!

A todos os amigos do Laboratório de Histologia, **Angélica**, **Jéssica**, **Suelen**, **Paulinha**, **Danizinha**, **Ever** e **Vinícius**, pela convivência, pela troca de conhecimentos e principalmente pela amizade, pelas risadas e pelos doces na Tetê!!

A **Profa. Dra. Vanessa Soares Lara**, por todo apoio, carinho e palavras de incentivo.

Ao **Dr. Thiago José Dionísio** do laboratório de Farmacologia por toda ajuda na execução/análise dos meus PCRs e ensaios Multiplex.

Aos funcionários e amigos do CIP por todo apoio e companheirismo.

Aos funcionários do Biotério, Sr. **Luis Silva**, Sr. **Erasmo Silva** e Sr. **Richard Simões** pela ajuda com a manutenção dos meus camundongos.

Aos funcionários e amigos do Laboratório de Microbiologia/Imunologia, **Dalvinha**, **André, Grazi** e **Vanessa**, pela amizade incondicional.

Aos meus amigos e familiares que sempre me apoiam e celebram as vitórias comigo!

AGRADECIMENTOS INSTITUCIONAIS

Ao **Prof. Dr. Vahan Agopyan**, digníssimo reitor da Universidade de São Paulo.

Ao **Prof. Dr. Pedro Vitoriano de Oliveira**, digníssimo Secretário Geral da Universidade de São Paulo.

Ao **Prof. Dr. Carlos Ferreira dos Santos**, digníssimo Diretor da Faculdade de Odontologia de Bauru da Universidade de São Paulo.

A **Prof. Dr. Marco Antonio Hungaro Duarte**, digníssimo Coordenador do Programa de Pós-Graduação em Ciências Odontológicas Aplicadas.

A **Profa. Dra. Izabel Regina Fischer Rubira de Bullen**, digníssima Presidente da Comissão de Pós-Graduação, da Faculdade de Odontologia de Bauru da Universidade de São Paulo.

Ao **Prof. Dr. Rodrigo Cardoso de Oliveira**, digníssimo chefe do Departamento de Ciências Biológicas da Faculdade de Odontologia de Bauru da Universidade de São Paulo.

A **Coordenação de Aperfeiçoamento de Pessoal de Nível Superior** (CAPES) pela bolsa concedida.

A **Fundação de Amparo à Pesquisa do Estado de São Paulo** (FAPESP), pelo auxílio concedido (processo número 2013/07245-9, C. O. R.).

Ao Conselho Nacional de Desenvolvimento Científico e Tecnológico (CNPq) pelo auxílio financeiro concedido (processo número 424158/2016-7, C. O. R.).

“Perde-se a riqueza, algo se perdeu.

Perde-se a honra, algo se perdeu.

Perde-se a coragem, tudo se perdeu.”

Johann Wolfgang Von Goethe

ABSTRACT

Characterization of the functional relationship between macrophages, cancer stem cells and epithelial-to-mesenchymal transition in oral squamous cell carcinoma

Oral squamous cell carcinoma (OSCC) is one of the most common malignant neoplasms of the head and neck, and the major prognostic factor is the presence of metastatic lesions in cervical lymph nodes. Studies have shown that cancer stem cells (CSCs) might be involved with migration and invasion process through the epithelial-to-mesenchymal transition (EMT) in tumor cells. It is known that cellular and soluble components of tumor microenvironment influence the EMT process, and macrophages represent the major class of cells that are recruited to the tumor site in different cancers. Furthermore, TGF-β signaling has been described as a critical regulator of EMT in cancer cells and can sustain CSCs properties. In view of that, the purpose of this study was to determine the functional relationship between CSC, EMT, and macrophages in OSCC. In paper 1, we analyzed the *in vitro* and *in vivo* behavior of two CSCs subpopulations, $CD44^{High}ESA^{Low}$ and $CD44^{High}ESA^{High}$ sorted from the OSCC cell line, LUC4. Our findings suggested that the subpopulation $CD44^{High}ESA^{High}$ is the one that carries the most stemness features. However, what induced or sustained that phenotype remained to be clarified. In paper 2, the influence of macrophages on CSCs was analyzed by directly co-culturing the subpopulations of CSC with macrophages or culturing CSC with conditioned medium from macrophages. Our results suggested that macrophages promote EMT in CSC, and that influence was probably mediated by TGF-β signaling. Altogether, our results showed that tumor heterogeneity must be considered and deeply characterized to better determine the therapeutic approach.

Keywords: Squamous cell carcinoma. Neoplastic Stem Cells. Epithelial-Mesenchymal Transition. Macrophages. Transforming Growth Factor beta.

RESUMO

O carcinoma epidermóide de boca (CEB) é uma das neoplasias malignas mais comuns da região da cabeça e do pescoço e o fator prognóstico com impacto mais significante nessa doença é a presença de metástase em linfonodos cervicais. Evidências mostram que células-tronco de câncer (CSCs, do inglês *cancer stem cells*) podem estar envolvidas nos processos de migração e invasão por meio da ativação do fenômeno de transição epitélio-mesenquimal (TEM) nas células tumorais. Sabe-se, que o processo de TEM pode ser influenciado por componentes celulares e solúveis presentes no microambiente tumoral e que, dentre as células infiltrantes, os macrófagos representam a principal população leucocitária recrutada, sendo detectado em maior número em diferentes neoplasias. Ademais, a sinalização mediada por TGF-β tem sido descrita como essencial para regulação de TEM em células tumorais bem como para a manutenção das propriedades, diferenciação e função das CSCs. Nesse contexto, a proposta deste estudo foi determinar a relação funcional entre CSC, TEM e macrófagos em CEB. No artigo 1, analisamos o comportamento *in vivo* e *in vitro* de duas subpopulações de CSC, $CD44^{High}ESA^{High}$ e $CD44^{High}ESA^{Low}$, presentes na linhagem de CEB LUC4. Nossos achados sugeriram que a subpopulação $CD44^{Hig}ESA^{High}$ é a subpopulação que mais carrega características de células-tronco. Entretanto, o que induz ou sustenta esse fenótipo ainda não foi esclarecido. No artigo 2, a influência dos macrófagos nas CSC foi analisada através da co-cultura direta das subpopulações de CSC com macrófagos ou por meio da cultura das CSC com médio condicionado obtido da cultura de macrófagos. Nossos resultados demonstraram que os macrófagos promovem TEM nas CSC e que essa influência é mediada pela sinalização de TGF-β. Juntos, nossos resultados demonstraram a importância de se considerar a heterogeneidade tumoral para melhor traçar estratégias terapêuticas.

Palavras-chave: Carcinoma Epidermóide. Células-Tronco Neoplásicas. Transição Epitelial-Mesenquimal. Macrófagos. Fator de Crescimento Transformador beta.

LISTA DE ILUSTRAÇÕES

LISTA DE ABREVIATURA E SIGLAS

ALDH1	Aldehyde dehydrogenase one
CCL	C-C motif chemokine ligand
CD	Cluster of differentiation
CM	Conditioned medium
CSC	Cancer stem-cell
CSF	Colony-stimulating factor
CXCL	C-X-C motif chemokine ligand
ECM	Extracellular matrix
EMT	Epithelial-to-mesenchymal transition
ESA	Epithelial-specific antigen
GM-CSF	Granulocyte-macrophage colony-stimulating factor
IFN-γ	Interferon gamma
IL	Interleukin
LPS	Lipopolysaccharide
MET	Mesenchymal-to-epithelial transition
MIP	Macrophage inflammatory protein
MMP	Metalloproteinase
NK	Natural killer
OSCC	Oral squamous cell carcinoma
PKA	Protein kinase A
SC	Stem-cell
TAC	Transiently amplifying cells
TAM	Tumor-associated macrophages
TGF-β	Tumor growth factor beta
Th	T helper
TLR	Toll-like receptor
TNF-α	Tumor necrosis factor alpha
VEGF	Vascular endothelial growth factor

TABLE OF CONTENTS

1 Introduction

The oral mucosa is the moist lining of the oral cavity continuous with the skin at the lips and the gut lining the larynx. It consists of two parts: the outer vestibule, bounded by the lips and cheeks, and the oral cavity proper, divided in the superior zone with the hard and soft palates, and the floor of the mouth and base of the tongue forming the inferior border (NANCI, 2013). Microscopically, the oral mucosa is composed of oral epithelium and underlying connective tissue, named lamina propria. The oral epithelium is formed by layers of firmly attached cells (keratinocytes) organized in sheets by intercellular connections that form the adherents' junctions, tight junctions, and desmosomes enabling epithelial cells to communicate (NANCI, 2013; SHIN; FOGG; MARGOLIS, 2006). The stratified epithelium is divided into superficial cell layer, granular cell layer (only in hard palate), prickle cell layer, and basal cell layer (NANCI, 2013). This organization confers a fundamental role of the epithelium as a mechanical barrier between the outside environment and underlying tissues, which are continuously exposed to pathological microorganisms.

The interface between the epithelium and the lamina propria is irregular, with projections entering into the lamina propria called connective tissue papillae (NANCI, 2013). Due to its frequently stress exposure, the lamina propria contains a very particular immune system network. The oral immune compartments are organized as a mucosal-associated lymphoid tissue (MALT) and consist of buccal mucosa, salivary glands, and Waldeyer´s ring, mainly composed by palatine tonsils and adenoids (LU; JACOBSON, 2007). The interaction between epithelium and lamina propria is achieved by the expression of trans-membrane integrins that bind to ligands present in the extracellular matrix (ECM), providing a link with the cellular cytoskeleton (GIANCOTTI; TARONE, 2003). In addition, focal adhesions and hemidesmosomes regulate the dynamics of adhesion and detachment of cells to their underlying ECM, thus mediating cell migration, stratification, and differentiation (FUCHS; RAGHAVAN, 2002; WATT, 2002).

The oral epithelium homeostasis is regulated by specific cell programs that control cell division, differentiation, and cell death, and it is in a continually renewing process. The maintenance of most adult epithelial tissues is hierarchically organized and depends on a subpopulation of unipotent cells called stem cells (SC) (BLANPAIN; HORSLEY; FUCHS, 2007; MCCAFFREY;

MACARA, 2011; RODINI; LOPES; LARA; MACKENZIE, 2017). Epithelial stem cells (ESC) are undifferentiated cells, and during homeostasis remain dormant demanding external signals to become activated. Once activated, stem cells have unlimited proliferating potential and may divide asymmetrically or symmetrically. Asymmetrically division generates another quiescent epithelial stem cell that will require a new round of signals to become activated, as well as one daughter cell committed to differentiation, named transiently-amplifying cells (TAC), that will proliferate for a limited period and then differentiate to maintain the organ structure (Figure 1a). The symmetrical pattern of division generates two daughter cells that may be both stem cells or both lineage-committed cells/TAC (JONES; KLEIN, 2013; MCCAFFREY; MACARA, 2011) (Figure 1b).

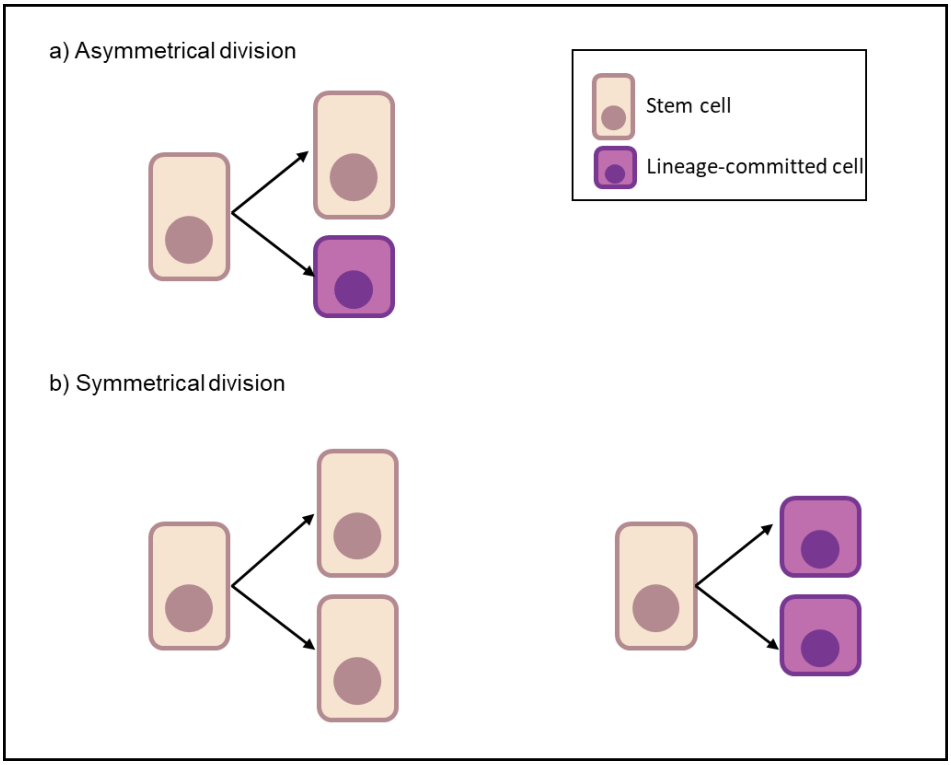

Figure 1. Models of epithelial SC divisions. (a) Asymmetrical division generating one SC (light brown cell) and one lineage-committed cell (purple cell). (b) Symmetrical divisions are generating ether two SCs or two lineage-committed cells.

The balance of self-renewal and differentiation is orchestrated mainly by Wnt/β-catenin and Notch signaling pathways (BLANPAIN; HORSLEY; FUCHS, 2007), and deregulation of any of these pathways are frequently associated with cancer development (REYA; CLEVERS, 2005; VENKATESH; NATARAJ;

THANGARAJ; KARTHIKEYAN et al., 2018). Once SC possesses increased proliferation and differentiation capacities that contribute to cellular tissue heterogeneity, it is reasonable to assume an association between stem cells and cancer development. Indeed, the presence of cancer stem cells (CSC) have been described and characterized in many types of carcinomas, and there is a considerable amount of work establishing markers for CSC identification, including the ones that develop in the oral cavity, like oral squamous cell carcinomas (OSCC) (HERMANN; HUBER; HERRLER; AICHER et al., 2007; KROHN; SONG; MUEHLBERG; DROLL et al., 2009; YANAMOTO; KAWASAKI; YAMADA; YOSHITOMI et al., 2011).

One of the greatest drivers of the OSCC outcome is the timing of diagnosis and, consequently, the beginning of treatment. Unfortunately, most OSCC patients are diagnosed at a late phase, which significantly decreases survival and patient quality of life (WANGSA; RYOTT; AVALL-LUNDQVIST; PETERSSON et al., 2008). In 2015, more than 4,000 OSCC patients died in Brazil, accounting for 3.5 % of all cancer deaths (Instituto Nacional de Câncer - INCA, 2019). In 2018, it was estimated 11,200 new cases of oral cancer between men in Brazil, ranking in fifth between all cancers (Instituto Nacional de Câncer - INCA, 2019), and despite all advances in cancer diagnosis and therapeutics approaches, the overall 5-year survival rate remains the lowest among malignancies (SASAHIRA; KIRITA, 2018).

The presence of cervical lymph nodes metastases is one of the most significant prognostic factors in OSCC. Lymph node metastasis occurs in 25 % to 65 % of OSCC patients (HANNEN; VAN DER LAAK; MANNI; PAHLPLATZ et al., 2001; ORTIZ; LOPES; AMÔR; PONCE et al., 2018); therefore, prediction of tumor invasiveness through clinical-pathological and immunohistochemistry analysis might influence the treatment and improve the prognosis of OSCC patients (MATTIJSSEN; PETERS; SCHALKWIJK; MANNI et al., 1993; NAKAYAMA; SASAKI; MESE; ALCALDE et al., 1998; OKAMOTO; NISHIMINE; KISHI; KIRITA et al., 2002). Studies have shown that tumor recurrence and metastasis, as well as treatment failure, might be related to the heterogeneity patterns among tumor cells (DRIESSENS; BECK; CAAUWE; SIMONS et al., 2012; FIDLER; KRIPKE, 1977; HEPPNER, 1984). Intra-tumoral heterogeneity is

resulted from intrinsic differences generated from genetic and epigenetic changes and can be explained by two models: the stochastic model (clonal expansion), in which all cells that form tumor mass are capable of undefined proliferation rate and can generate a new tumors (NOWELL, 1976); or the CSC theory, that suggests that tumors developed and progress starting from a specific undifferentiated cancer cell subpopulation and only this subpopulation is capable of proliferate and initiate a new tumor, thus conferring an hierarchical organization of tumor growth similar to epithelial maintenance/renewal (REYA; MORRISON; CLARKE; WEISSMAN, 2001).

In the past few years, studies were conducted in an attempt to prove both theories. The existence of premalignant lesions among surgical edges may result in local recurrence and also secondary tumors and can be explained by the stochastic model (ALBERS; CHEN; KOBERLE; QIAN et al., 2012). On the other hand, prolonged exposition of oral mucosa to nicotine resulted in increased expression of SC markers in epithelial cells, sustaining the CSC hypothesis (YU; CHANG, 2013). The CSC model takes advantage of the embryogenesis concept to explain the tumorigenesis process. In this context, the most important characteristics of this model are: [1] only a few fractions of cancer cells possess tumor-initiating capacity when transplanted in immunodeficient mice; [2] the CSCs can be isolated from the bulk of cancer cells trough specific membrane markers; [3] tumor generated from CSC contains both CSC and non-CSCs derived from original tumor and; [4] CSC subpopulations can be serially transplanted in multiple generations, suggesting their self-renewal potential (PRINCE; AILLES, 2008).

It was demonstrated that CSCs are also capable of establishing metastases. $CD44^{+}CD24^{-/low}$ CSCs (CD, cluster of differentiation) isolated from breast cancer and orthotopic inoculated in immunodeficient mice generate both primary tumors and subsequent lung metastases (LIU; PATEL; PRESCHER; PATSIALOU et al., 2010). Similarly, orthotopic implantation of pancreatic CSCs generate liver metastasis in mouse model (HERMANN; HUBER; HERRLER; AICHER et al., 2007). However, only a specific CSC subtype seems to be capable of detaching from the primary tumor and colonize distant organs, and their genetic signature might predict their invasive capacity. In OSCC, a study

identified four subpopulations of cancer cells: $CD44^{High}ESA^{High}$ (ESA, epithelial-specific antigen) cells, which presents epithelial features and can undergo epithelial-to-mesenchymal transition (EMT) generating $CD44^{High}ESA^{Low}ALDH1^{+}$ (ALDH1, aldehyde dehydrogenase 1) cells. $CD44^{High}ESA^{Low}ALDH1^{+}$ has mesenchymal characteristics and can either undergo mesenchymal-to-epithelial transition (MET) or generates $ALDH1^{-}$ cells. The authors also described the presence of non-tumorigenic cells defined by the low expression of CD44 (BIDDLE; LIANG; GAMMON; FAZIL et al., 2011), suggesting a significant difference between CSCs sub-fractions that probably dictates the course of malignant progression.

Although the mechanisms by which cancer cells detach from primary tumors and invade underlying tissues and disseminate through the body are not completely understood, it is known that the migratory phenotype is a normal/physiological process and essential for body development (SHIOZAWA; NIE; PIENTA; MORGAN et al., 2013). Most of the adult epithelial tissues retains some aspects of migration through the EMT. In general, cells in EMT exhibit downregulation of epithelial markers, including E-cadherin, desmoplakin, cytokeratin, claudin, β-catenin; in contrast with the upregulation of mesenchymal markers, such as N-cadherin, Vimentin, fibronectin and Snail 1/2 (GRILLE; BELLACOSA; UPSON; KLEIN-SZANTO et al., 2003; IKENOUCHI; MATSUDA; FURUSE; TSUKITA, 2003; THIERY, 2002). Even though EMT is an integral part of the natural process of development, it can be activated in pathological scenarios, like fibrosis and tumor invasion and metastasis; however, what triggers EMT in OSCC is not well characterized.

It has been suggested that CSCs migrate through EMT. Indeed, immortalized epithelial cancer cells activated EMT through the expression of FoxC2, Zeb, and N-cadherin; all of them CSCs related (MOREL; LIÈVRE; THOMAS; HINKAL et al., 2008). In addition, it has been already proposed that transcription factors of CSCs from carcinomas can regulate EMT, including Slug, Snail, and Twist, and orchestrate intercellular alterations such as Vimentin expression, inhibition of E-cadherin and nuclear translocation of β-catenin (THIERY, 2003). Thus, during EMT, CSCs lose their polarity and intercellular junctions, acquiring migratory/mesenchymal phenotype and dissipate through

vascular/lymphatic circulation, reaching distant organs, where they revert their mesenchymal phenotype to epithelial undergoing MET and establish new tumor that recalls the primary one (BRABLETZ; JUNG; SPADERNA; HLUBEK et al., 2005). In view of that, EMT comprises a fundamental role in tumor progression and can easily facilitate metastasis of CSC (RODINI; LOPES; LARA; MACKENZIE, 2017).

Cells and soluble factors present in the tumor microenvironment can regulate the beginning and maintenance of CSC and EMT phenotype, and might contribute to tumor progression (KANG; MASSAGUE, 2004; THIERY, 2003). In particular, myeloid cells, mostly monocytes/macrophages, have been pointed out as key elements for tumor progression (DENARDO; RUFFELL, 2019). Monocytes are recruited to the inflammatory site and can be polarized into two different phenotypes: M1 or M2 macrophages. M1-polarized macrophages, also known as classically activated macrophages, are differentiated via Th1 (T helper) cytokines, such as IFN-γ (interferon-gamma) and TNF-α (tumor necrosis factor-alpha), and/or by toll-like receptors (TLR) activated by bacterium components, like LPS (lipopolysaccharide), and produce mainly pro-inflammatory cytokines, including IL (interleukin)-12, IL-1β, IL-6, and TNF-α (SICA; MANTOVANI, 2012). On the other hand, in response to IL-4, IL-10, and/or IL-13, macrophages are polarized towards M2-phenotype, or alternatively activated macrophages, and participate in Th2-type immune response, including humoral immunity, and assist tissue healing and remodeling (GORDON; MARTINEZ, 2010). M2 macrophages are characterized by the expression of scavenger receptors, mannose and galactose receptors, arginase pathway activation, and production of IL-10 and TGF-β (tumor growth factor-beta), VEGF (vascular endothelial growth factor) and matrix metalloproteinases (MMP) (GORDON; MARTINEZ, 2010; SICA; MANTOVANI, 2012).

Monocyte recruitment is mediated by chemokines, like CCL2 (C-C motif chemokine ligand), CCL5, CXCL12 (C-X-C motif chemokine ligand), CSF-1 (colony-stimulating factor), and components of the complement cascade (BONAVITA; GALDIERO; JAILLON; MANTOVANI, 2015; BONAVITA; GENTILE; RUBINO; MAINA et al., 2015) and, once within the tumor microenvironment, cancer cells promptly promotes monocyte differentiation towards to tumor-

associated macrophages (TAM). It is known that TAMs share traits with M2 macrophages (BISWAS; MANTOVANI, 2010), which in turn promote tumor progression and metastasis via increased angiogenesis, producing growth factors and matrix remodeling by MMPs, as well suppressing anti-tumor immune response mediated by T lymphocytes (POLLARD, 2004). In addition, TAMs can modulate EMT in cancer scenarios. It has been demonstrated that breast cancer cells in EMT activated macrophages through GM-CSF (granulocyte-macrophage colony-stimulating factor) secretion (SU; LIU; CHEN; CHEN et al., 2014). Once activated, these macrophages release CCL18, which in turn induces EMT in tumor cells *in vitro*, conferring a positive feedback loop between macrophages and cancer cells (SU; LIU; CHEN; CHEN et al., 2014). In hepatocellular carcinoma and pancreatic adenocarcinoma cells, TAMs reduced the E-cadherin expression and increased Vimentin expression (FAN; JING; YU; KOU et al., 2014), which are EMT-associated features. More importantly, the presence of $CD206^+$ macrophages in OSCC patients was reported to be positively correlated with worst prognosis (HAQUE; MORIYAMA; KUBOTA; ISHIGURO et al., 2019). These studies highlight that the macrophages phenotype induced by tumor has a crucial role in tumor development and progression. However, the precise relation between CSC, EMT, TAMs, and the mechanisms and factors that influence and coordinate such relation in OSCC is not completely understood.

The TGF-β cytokine represents one of the greatest mediators of embryonic development and is responsible for adult tissue homeostasis (HELDIN; LANDSTROM; MOUSTAKAS, 2009). It is recognized a specific contribution of TGF-β during tumor development, cellular invasion, immune suppression, and modification of tumor microenvironment (BIERIE; MOSES, 2010; MASSAGUE, 2008; VAN MEIR; HADJIPANAYIS; NORDEN; SHU et al., 2010). The signaling mediated by TGF-β has been described as essential for maintenance, differentiation, and function of CSCs in different types of carcinomas, as well as regulators of EMT in normal and tumor cells (EHATA; JOHANSSON; KATAYAMA; KOIKE et al., 2011; KATSUNO; LAMOUILLE; DERYNCK, 2013; LONARDO; HERMANN; MUELLER; HUBER et al., 2011; ZHANG; LIU; WANG; ZHAO et al., 2013) TGF-β increases the self-renewal capacity and tumor initiation ability of CSC in glioblastoma (IKUSHIMA; TODO; INO; TAKAHASHI et al.,

2009), breast cancer (BRUNA; GREENWOOD; LE QUESNE; TESCHENDORFF et al., 2012), liver cancer (WU; DING; CHEN; SUN et al., 2012), and also in OSCC cell lines (BIDDLE; GAMMON; LIANG; COSTEA et al., 2016). TGF-β is a regulator of the genetic program of EMT, so TGF-β-driven EMT is sufficient to generate migratory CSCs and maintain the stemness features of cancer cells (CUFI; VAZQUEZ-MARTIN; OLIVERAS-FERRAROS; MARTIN-CASTILLO et al., 2010). Importantly, it has been demonstrated that TGF-β blockade in colon tumor cells revert the EMT phenotype *in vitro* and similar results were obtained with *in vivo* models of skin and breast cancers (OFT; HEIDER; BEUG, 1998; PORTELLA; CUMMING; LIDDELL; CUI et al., 1998).

Once stromal cells, including fibroblasts, endothelial, and immune cells are considerable sources of TGF-β in tumor microenvironment (DALAL; KEOWN; GREENBERG, 1993; RONCA; VAN GINDERACHTER; TURTOI, 2018), all these cellular and soluble elements must direct or indirectly influence each other and play fundamental role in the control and maintenance of phenotypic alterations associated with CSCs and EMT phenotypes, and consequently influence the invasiveness/migratory behavior of tumor cells. In this context, the aim of the present study was to analyze the *in vivo* and *in vitro* behavior of the CSC that were in EMT or not, and to investigate whether macrophages and TGF-β induce and potentiate CSCs and EMT phenotypes in an OSCC cell line.

2 Articles

The articles presented in this Thesis were written according to the Oncogene instructions and guidelines for article submission:

2.1 ARTICLE 1 – **Cancer stem-cells subpopulations differentially affect oral squamous carcinoma behavior *in vivo* and *in vitro*** (Submitted)

2.2 ARTICLE 2 – **Macrophages promote aggressive behavior on tumor cells via TGF-β signaling in oral squamous cell carcinoma** (In preparation)

Cancer stem-cells subpopulations differentially affect oral squamous carcinoma behavior *in vivo* and *in vitro*

Nádia Ghinelli Amôr, Rodrigo Fonseca Buzo, Rafael Carneiro Ortiz, Nathália Martins Lopes, Luciana Mieli Saito, and Camila Oliveira Rodini*

Department of Biological Sciences, Bauru School of Dentistry, University of São Paulo, Al. Dr. Octávio Pinheiro Brisolla, 9-75, Bauru, SP, Brazil

*Correspondence should be addressed to: Camila Rodini, DDS, MSc, Ph.D., Department of Biological Sciences, Bauru School of Dentistry, University of São Paulo, Av. Octávio Pinheiro Brisolla, 9-75, Bauru/SP, Brazil. Tel: +55 14 3235 8259; Email: carodini@usp.br

Running title: Cancer heterogeneity and tumorigenesis

Keywords: Oral squamous cell carcinoma. Cancer stem-cell. Epithelial-mesenchymal transition. Xenograft. CD44. CD326.

Abstract

Oral squamous cell carcinoma (OSCC) is one of the most common malignant neoplasms of the head and neck. Tumor heterogeneity has been pointed as an essential factor in cancer development and explains, at least in part, the divergent outcomes observed among patients. Cancer stem cells (CSC) represent a single fraction of cancer cells that are responsible for generating other tumor cells, and due to its ability to divide asymmetrically, they may contribute directly to tumor heterogeneity. Using the stem-cell marker CD44 and the epithelial marker ESA, we characterized two distinct phenotypes of CSC (epithelial, Epi-CSC, and epithelial-mesenchymal transition, EMT-CSC) in OSCC cell lines (CA1, LUC4, and SCC-9), by *means of immunofluorescence* and *flow cytometry*. *In vitro* findings from LUC4 cells showed that the Epi-CSC phenotype was more proliferative and generated more holoclones than the EMT-phenotype. Despite the unexpected similar migratory capacity evaluated by *wound healing assay*, both phenotypes displayed very different patterns of invasion by *3D culture and invasion assays,* demonstrating how the phenotype might affect the behavior of tumor cells. When orthotopically inoculated in immunodeficient mice´s (NOD/SCID) tongues, both subpopulations originated squamous cell carcinoma; however, EMT-CSC subpopulation formed smaller tumors than Epi-CSC, and they were detected only in 75 % of xenografted mice. It suggests that Epi-CSC are the cells responsible for reestablishing the tumor, therefore the more important CSC subpopulation for tumorigenesis. Finally, the co-culture of LUC4 whole population with macrophages increased the frequency of the EMT-CSC subpopulation, demonstrating a critical role of these immune cells in EMT regulation in OSCC. Altogether, our findings reveal how distinct phenotypes of

tumor cells can dictate tumor course and imply that tumor heterogeneity and individuality must be considered when designing patient to patient treatment.

Introduction

Oral squamous cell carcinoma (OSCC), which arises within the oral cavity, including the tongue, upper and lower gingiva, oral floor, palate, and buccal mucosa, is the most common malignancy of the head and neck [1]. Despite advances in cancer diagnosis and therapeutics, the overall 5-year survival rate remains the lowest among malignancies [2], and it is associated with a high rate of cervical lymph nodes metastasis, which occurs in 25-65 % of OSCC patients [3, 4]. Personalized antitumor therapies considering intrinsic characteristics from each patient have been revealed as a promising approach to improve cancer treatment, especially immunotherapies [5, 6]. Additionally, the knowledge about the biology and molecular mechanisms underlying cancer development, progression, and metastasis is fundamental for designing this kind of individualized treatment.

Although the clonal expansion of cancer was the most accepted theory for many decades, studies revealed that subclones of cancer cells from the same tumor are very different regarding growth rate, immunogenicity, drug response, and ability to metastasize [7]. The variability of resources within the tumor, such as nutrients and oxygen, can be the driver that generates intra-tumoral heterogeneity [8, 9]. Furthermore, it was demonstrated the existence of subpopulations of cancer cells with different tumor-initiating capacities [10, 11]. Tumor-initiating cells are frequently described as cancer-stem cells (CSC) once they share some of the stemness features, such as extensive self-renewal

properties and multilineage differentiation potential, being able of sustaining the tumor heterogeneity by dividing either symmetrically or asymmetrically [11, 12].

CSCs are involved with tumor formation and growth, being associated with recurrence, chemo and radioresistance, and metastasis [13-15]. Metastasis is a multi-step process that involves local invasion, intravasation, survival in the circulation, extravasation, and distant site colonization [12]. Studies demonstrate that carcinoma cells can invade surrounding tissues trough the epithelial-mesenchymal transition program (EMT) [16, 17]. Considering that these same cells must restart their tumor-initiating program to establish secondary tumors, it is reasonable to assume that they might retain some of the CSCs traits, like tumor-initiating capacity. Indeed, tumor cells undergoing EMT exhibit CSCs proprieties [18, 19]. It has been already demonstrated that transcription factors of CSCs from carcinomas can regulate EMT, including Slug, Snail, and Twist and orchestrate intercellular alterations such as Vimentin expression, inhibition of E-cadherin and nuclear translocation of β-catenin [20]. Moreover, the presence of macrophages is frequently found at the invasive front of aggressive cancers [21], where tumor cells undergoing EMT are founded [22], suggesting that macrophages might contribute to the invasive behavior of carcinoma cells.

Using CSCs and EMT markers, Biddle et al. [23] have shown the existence of four different subclones of CSC in OSCC, and described the dynamics that regulate the transition between them. This study aimed to better characterize and functionally describe how two CSC phenotypes from OSCC cell lines, $CD44^{High}ESA^{High}$ (Epi-CSC) and $CD44^{High}ESA^{Low}$ (EMT-CSC), affect tumor cell behavior *in vivo* and *in vitro* contributing to intra-tumoral heterogeneity. Herein, high expression of CD44 and ESA represents a highly tumorigenic subpopulation

of cancer cells, and macrophages are a potential inducer of EMT phenotype in OSCC.

Results

The proportion of epithelial and mesenchymal phenotypes differ among OSCC cell lines

Loss of E-cadherin expression with concomitant Vimentin induction is frequently present in carcinoma cells undergoing EMT, including OSCC [24, 25]. In order to identify possible subpopulations in OSCC, we analyzed the expression of E-cadherin and Vimentin by immunofluorescence in three different OSCC cell lines, CA1, LUC4, and SCC-9. The E-cadherin expression was weak and very similar among cell lines, and the confluence of the culture did not affect its expression (Fig. 1). On the other hand, cells at higher densities displayed weaker staining for Vimentin, suggesting that cultures in low densities might have increased EMT (Fig. 1). Interestingly, the presence of Vimentin-positive cells was more prominent in LUC4 cells, especially in tumor cells that exhibit fibroblast-like morphology, followed by SCC-9 and CA1, which had an insignificant number of stained cells suggesting a robust epithelial phenotype by CA1 cells and high EMT in LUC4 cells (Fig. 1). To better quantify the presence of EMT cells, we evaluated the expression of CD44 (CSC marker) and ESA (CD326, epithelial marker) by flow cytometry (Fig. 2). Cells were plated at low and high densities, and after 72 h, the cultures were ~ 50-60 % and ~ 80-90 % confluent, respectively (Fig. 2a). By flow cytometry, we distinguished EMT ($CD44^{High}ESA^{Low}$, EMT-CSC) and epithelial ($CD44^{High}ESA^{High}$, Epi-CSC) CSC subpopulations among OSCC cell lines (Fig. 2b). The presence of both subpopulations was not influenced by cell confluency

in all three cell lines (Fig. 2c). As seen by immunofluorescence, CA1 cell line was more epithelial (92.4 – 98.3 %) than SCC-9 and LUC4 cells, which displayed similar percentages of Epi-CSC cells (Fig. 2c). Regarding EMT, LUC4 had the highest percentage of EMT-CSC cells (38.9 – 79.6 %) (Fig. 2c). The ratio of both subpopulations, $CD44^{High}ESA^{High}$ and $CD44^{High}ESA^{Low}$, was analyzed: the close the ratio mean was of 1, the more homogenous the subpopulations were distributed within the cell line. Epi-CSC and EMT-CSC were equally distributed within LUC4 cells, exhibiting an epithelial/mesenchymal ratio of around 0.5, while CA1 varied between 389.16 – 390.01 and SCC-9 between 4.53 – 6.74 (Fig. 2d). Based on these findings, only the LUC4 cell line was further investigated and corresponded to the subsequent results.

Epi-CSC and EMT-CSC act uniquely* in vitro*, exhibiting a different pattern of proliferation and invasive behavior

Due to the increased heterogeneity displayed by the LUC4 cell line, we decided to analyze how both LUC4 CSC phenotypes, Epi-CSC and EMT-CSC, behaved in gold standards *in vitro* assays. As expected, the Epi-CSC subpopulation displayed the common epithelial morphology, such as polygonal shape, growth tightly packed and presented intercellular bridges (Fig. 3a). In contrast, the EMT-CSC subpopulation exhibited spindly/fibroblastic morphology without evident signs of intercellular junctions (Fig. 3a). Regarding colony generation capacity, both subpopulations generated the three types of colonies: holoclones, meroclones, and paraclones (Fig. 3b). However, the Epi-CSC subpopulation generated higher numbers of colonies regardless of their morphology compared to EMT-CSC (Fig. 3c). Interestingly, Epi-CSC formed a significantly higher

percentage of holoclones than EMT-CSC (Fig. 3d). On the other hand, EMT-CSC displayed an increased frequency of paraclone formation (Fig. 3e). Despite the similar rate of migration exhibited by both subpopulations (Fig. 3e-f), Epi-CSC cells were more proliferative than EMT-CSC at 48h and 72h periods (Fig. 3g). Moreover, these two subpopulations displayed very different invasion patterns in 3D culture: Epi-CSC invaded as collective cells; EMT-CSC preferentially invaded as single cells (Fig. 3h). These results suggested that Epi-CSC phenotype is the potential tumorigenic clone presented in the LUC4 cell line.

Epi-CSC and EMT-CSC have different tumor-initiating capacities

To investigate the tumorigenic capacity of both subpopulations, Epi and EMT-CSC from LUC4 cells were orthotopic xenografted into the tongue of NOD/SCID mice (Fig. 4a). Neither the appetite (Fig. 4b) nor weight (Fig. 4c) was affected by the xenograft of both subpopulations indicating that the OSCC did not significantly affect their normal physiology. Although both subpopulations generated tumors, reflecting the *in vitro* observations, the EMT-CSC phenotype was less effective in generating tumors once we could detect OSCC only in 75 % of inoculated mice, in contrast to 100 % of mice inoculated with Epi-CSC cells (Fig. 4d). Moreover, tumors generated by Epi-CSC cells were significantly larger than tumors generated by EMT-CSC (Fig. 4e-f). Regarding the clinicopathological features of the tumors, both subpopulations originated squamous cell carcinoma of the tongue, and no fibrous capsule was observed (Fig. 5a-d). Both tumors showed increased cell heterogeneity, slightly basophilic cytoplasm, variable pleomorphism, hyperchromatic nuclei, and loss of nuclear-cytoplasmic ratio (Fig. 5e-t). Both subpopulations produced areas of well-differentiated tumor cells with

several corneal pearls at central regions (Fig. 5e-h). Remarkably, the Epi-CSC subpopulation also formed moderately differentiated tumor areas, characterized by the increased number of cellular and structural alterations, such as multinucleated cells (Fig. 5i) and, abnormal mitosis (Fig. 5j). Controversially, central regions of EMT-CSC tumors did not show several structural and cellular alterations; tumor cells at basal layers of tumor islands seemed to be more cuboidal compared to parabasal tumor layers (Fig. 5k-l). Regarding invasive tumor front (ITF), muscular invasion was observed in both tumors (Fig. 5m-p). As seen in the *in vitro* 3D invasion assay described above, tumors originated from epithelial phenotype invaded as groups of tumor islands (Fig. 5m) with several figures of abnormal mitosis (Fig. 5l-n). In contrast, tumors cells from the mesenchymal phenotype invaded as small clusters of tumor cells (Fig. 5o-p). Noteworthy, in deep ITF of Epi-CSC tumors, cells seemed to be less adherent and invaded as a smaller cluster of cells (Fig. 5r). It is important to note that EMT-CSC tumors distantly invaded from primary tumors (Fig. 5s) and appeared to spread toward blood vessels (Fig. 5t). In summary, these findings demonstrated that Epi-CSC cells are more tumorigenic than EMT-CSC.

Epi-CSC and EMT-CSC start to reassemble tumor heterogeneity both* in vitro *and* in vivo, *and macrophages induce the EMT-CSC phenotype

Finally, we wonder if the phenotype of Epi-CSC and EMT-CSC cells could individually restore cellular heterogeneity both *in vitro* and *in vivo*, and investigated what could affect the balance towards one or another subpopulation. After 60 days, both Epi-CSC and EMT-CSC cultures seem to slightly start to restore original tumor heterogeneity as seen by flow cytometry: both dot plots

presented a new cluster of cells separately from the majority of the tumor cells (Fig.6a). The dot plots from tumor cells recovered from the tongue presented even more heterogeneous cells regarding CD44 and ESA expression (Fig. 6b), suggesting a possible microenvironment influence upon their phenotype. Interestingly, Epi-CSC phenotype seems to be more heterogeneous, since the cells were more scattered along the ESA axis than EMT-CSC. Once macrophages are the major immune cell population that infiltrates tumor microenvironment [26] and they are described as a potent inducer of EMT [27], we analyzed if macrophages could affect the balance of Epi-/EMT-CSC *in vitro* (Fig. 7a). Our results demonstrated that LUC4 cells indirectly cultivated with macrophages displayed decreased percentages of Epi-CSC (Fig. 7b) concomitant with an increased percentage of EMT-CSC cells (Fig. 7c) even after only 24 h of co-culture, corroborating the notion that macrophages induce EMT in carcinoma cells.

Discussion

Different theories explain the phenotypic variability detected among tumor cells from the same patient. It is well documented that many types of tumors contain cancer cells with several phenotypes that reflect aspects of the differentiation that normally occurs in physiological conditions creating a hierarchical organization known as cancer stem cell model [28]. Many biomarkers are used to identify CSC among distinct types of cancers. For head and neck cancer, Prince et al. [29] have demonstrated stem-cell features in $CD44^+$ cancer cells. When xenografted in immunocompromised mice, only $CD44^+$ cells were able to generate tumors with similar characteristics to the original one. In

accordance to Biddle et al [23], adding the epithelial marker ESA (CD326, also known as EpCAM), we described two cancer cells phenotypes, Epi-CSC ($CD44^{High}ESA^{High}$) and EMT-CSC ($CD44^{High}ESA^{Low}$) in OSCC cell lines. Epi-CSC displayed several features typically observed in stem cells, including high proliferation activity and tumor-initiating capacity. Despite the knowledge that carcinoma cells in EMT are the most aggressive phenotype due to their ability of invade and migrate through the body [30], our results provide evidence that the Epi-CSC are the more tumorigenic subclone and thus should be considered as a potential target for future therapies.

Recent studies on CSC have correlated stem cell properties with the morphology of colonies generated from single cells [31, 32], and CSC was demonstrated to reside mostly in holoclones [33-35]. Our results showed that Epi-CSC phenotype formed considerably more holoclones than EMT-CSC, suggesting that Epi-CSC cells retain more stem cell features than EMT-CSC, despite their similar expression of the well-known CSC marker, CD44. On the other hand, EMT-CSC presented higher percentage of paraclones, allowing us to associate paraclone formation with EMT state. Another relevant characteristic of CSC is its unlimited proliferative activity [11]. Again, Epi-CSC cells were significantly more proliferative than EMT-CSC, suggesting that the Epi-CSC phenotype is more tumorigenic than the EMT-CSC one. In accordance with our work, cancer cells $CD44^{+}ESA^{+}$ were also demonstrated to be highly tumorigenic and described as cancer stem cells in pancreatic [36] and breast cancer [37].

Despite the well-described migration capacity of carcinoma cells in EMT [30], EMT-CSC migrated at the same ratio as Epi-CSC in the present study. However, regarding invasive behavior, they invaded the solid matrix very

differently; while Epi-CSC collectively invaded, that means invaded as a compact group of cells, EMT-CSC invaded as single cells. A considerable amount of work pointed single-cell invasion, typically observed in carcinoma cells in EMT, as essential for cancer metastasis [38-40]. However, tumor border of carcinomas is frequently dominated by multicellular agglomerates and, consequently, there is a predominance of collective cell invasion [41]. In addition, the presence of tumor cell emboli in lymph and blood vessels suggests that collective invasion may be necessary for tumor spread [42].

To finally determine whether these two phenotypes indeed have tumor-initiating capacity, both subpopulations were xenografted into the tongues of NOD/SCID mice. As expected, the Epi-CSC phenotype effectively generates tumors in all xenografted mice. On the other hand, only 75 % of mice inoculated with the EMT-CSC phenotype formed tumors. Knaack et al., [43] obtained similar results, since they observed efficiently tumor formation when inoculating holoclone in immunocompromised mice and only few animals inoculated with paraclones formed tumor. At the end of the experimental period, the tumors generated by Epi-CSC cells were considerably larger than the ones formed by EMT-CSC, probably due to its high proliferative activity. Although we did not analyze ALDH1 expression on EMT-CSC cells, Biddle et al. [23] demonstrated that some subclones of $CD44^{High}ESA^{Low}$ cells did not express ALDH-1 and do not undergo mesenchymal-epithelial transition, thus cannot generate tumor. Once normal epithelial stem-cells are responsible for restore tissue heterogeneity [44], we assume that CSC should also be able to reestablish tumor

heterogeneity. Indeed, analysis of tumor cells recovered from the tongue of the mice revealed a heterogenous pattern of cells regarding CD44 and ESA

expression. Tumors recovered from Epi-CSC-xenografted mice seem to be more heterogeneous than the tumors recovered from EMT-CSC inoculated mice. Similar results were obtained in studies with breast cancer [37], where the authors documented a high capacity of tumorigenic $ESA^{+}CD44^{+}CD24^{-}$ cells in generating other tumorigenic cells and also non-tumorigenic ones. However, we must highlight that the tumor digestion process can significantly affect the expression of epitopes; thus, further studies should be conducted in order to unhesitatingly affirm the ability of these two subpopulations to reestablish intra-tumoral heterogeneity. Altogether, our results suggested that the Epi-CSC cells undergo a process analogous to normal epithelial stem-cells and EMT-CSC is probably arrested in the EMT state not being able to revert their phenotype trough the mesenchymal-epithelial transition, thus possessing limited tumor-initiating capacity.

Once we characterized both subpopulations of CSC, it remained unclear what and to what extension contributes to the development and maintenance of each cell subclone. The role of microenvironment and, most important, immune cells in cancer is well recognized [45, 46]. Macrophages are the key mediators of tumor course [47] and effectively induce EMT in carcinoma cells [27]. Based on that, we hypothesized that macrophages could have a significant role in generating heterogeneity in LUC4 cells *in vitro*. As expected, LUC4 cells co-cultured with macrophages displayed increased frequency of EMT-CSC phenotype. However, further studies are necessary to assess whether these induced EMT-CSC retain the stemness traits that we observed in the Epi-CSC.

The main focus of cancer research in the past decade has been the understanding of the molecular biology of cancer. That is, the understanding of

genetic and epigenetic mutations, determination of molecules involved with proliferation and survival, and attempted to developed mechanisms that efficiently inhibit such pathways. Therefore, the knowledge of the cellular biology of cancer cells has been neglected. Before we identify what is transformed at the molecular level or even dissected signaling pathways and test new drugs, we must understand the behavior of the transformed cells and how they adapt to frequently modifying environments. Despite the knowledge that carcinoma cells in EMT are the most aggressive due to their ability to invade and migrate [30], our results suggest that the Epi-CSC are the more tumorigenic subclone and should then be considered as a potential target for future therapies. Then, the present study highlighted the significant contribution of tumor heterogeneity for cancer progression and encourages further studies on targeted therapy towards specific CSCs subpopulations.

Material and Methods

Cell culture

The human OSCC cell line SCC-9 and monocytic cell line THP-1 was obtained from the American Type Culture Collection (ATCC, Manassas, VA, USA) and maintained in 1:1 mixture of DMEM and Ham's F12 medium (Life Technologies, Carlsbad, CA, USA), 10 % fetal bovine serum (FBS), 1 % of antibiotic/antimycotic (Life Technologies) and in RPMI-C medium (RPMI 1640 medium), 10 % fetal bovine serum, 0.05 mM 2-mercaptoethanol, 2.5 mM L-glutamine, 1mM sodium pyruvate, and 1 % of antibiotic/antimycotic (all reagents from Life Technologies), respectively. The primaries cell lines, LUC4 and CA1, were derived and kindly provided by Dr. Ian Mackenzie [48]. Both cells were maintained in RM^+ medium

composed by 3:1 mixture of DMEM:F12, 10 % FBS, 1 % of antibiotic/antimycotic and mitogens (5 µg/mL transferrin, 0.4 µg/mL hydrocortisone, 0.1 mM cholera toxin, 10 ng/mL epithelial growth factor, 5 µg/mL insulin, 0.2 pM liothyronine). All cells were grown at 37° C, 5 % CO_2 in a humidified atmosphere

Immunofluorescence and confocal imaging

Cell lines were cultured in a chamber slide system (Corning, Big Flats, NY, USA) and incubated for 24-48 h to allow adherence. Cells were then fixed using 4 % paraformaldehyde and permeabilized with 0.05 % Triton-X-100 (Sigma, St Louis, MO, USA) for 10 min at room temperature. Primary antibodies were incubated for 2 h at room temperature as follows: mouse anti-human E-cadherin (1:50, clone NCH-38, Dako, Carpinteria, CA) and rabbit anti-human Vimentin (1:250, clone EPR3776, Abcam, Cambridge, UK). The proper secondary antibodies were incubated for 1 h at room temperature: anti-mouse IgG Cy™3 (1:250, Jackson ImmunoResearch, West Grove, PA, USA) and anti-rabbit IgG AlexaFluor 647® (1:250, Jackson ImmunoResearch). The nucleus was stained with 4',6-diamidino-2-phenyl-indole (DAPI, 1:250, BD Biosciences, San Jose, CA, USA) at room temperature for 30 min before mounting in ProLong® Diamond Antifade Mountant mounting medium (Life Technologies). Stained cells were examined on an inverted Leica TCS-SPE confocal microscope (Leica Microsystems GmbH, Mannheim, Baden-Württemberg, Germany) using a 40 x magnification oil lens. Images were acquired using the Leica Application Suite-Advanced Fluorescence software (LAS AF, Leica Mannheim).

Flow cytometry and fluorescence-activated cell sorting (FACS)

Cells were detached using StemPro Accutase Cell Dissociation Reagent (Life Technologies) and stained with 1:100 of mouse anti-human CD44 (clone G44-26, BD PharmigenTM, San Diego, CA, USA) and mouse anti-human ESA (clone EBA-1, BD HorizonTM), for 30 min, 4° C in the dark. The exclusion of dead cells was made using Fixable Viability Stain FVS (1:3 000, BD HorizonTM). Samples were analyzed and sorted using Becton and Dickenson FACSAriaTM Fusion Cell Sorter (BD Pharmigen) and BD FACSDivaTM 8.0 software (BD Pharmigen). FVS^{-} $CD44^{High}ESA^{High}$ and $FVS^{-}CD44^{High}ESA^{Low}$ FACS-sorted cells were collected into RM^{+} medium, 20 % FBS and 10 % antibiotic/antimycotic.

Colony formation assay

For clonogenic abilities evaluation of LUC4 Epi- and EMT-CSC, 500 cells were suspended in 3 mL of RM+ medium and added to each well of 6-well plate and incubated at 37° C, 5 % CO_2 for seven days without medium changing. Then, cells were fixed in 4% paraformaldehyde, stained with 0.04 % crystal violet in 1 % ethanol, and colonies with at least 50 cells were counted visually. The colonies´ morphology was classified as holo- (homogeneous clusters of small and tightly attached cells with regular borderlines), para- (dispersed cells with fragmented borderlines), and meroclones (intermediate morphologies) [33].

Wound-healing assay

The wound-healing assay was performed as previously described [49] with minor modifications. Briefly, 2.5 x 10^5 cells/well were plated in a 12-well plate and cultured for 24-48 h to achieve 100 %. Then, cells were incubated for 2 h with 10

µg/mL of mitomycin C to cell cycle arrestment. A 1,000 µL sterile pipette tip was used to make a scratch in the cell monolayer. Cells were then incubated in RM^+ medium diluted 1:1 in DMEM/F12. The scratch gap width was photographed at each 24 h using the CKX41 Inverted Microscope (Olympus, Tokyo, Japan). The area of the open wound was measured using ImageJ software [50], and the results were calculated as a percentage of wound closure.

3D culture and invasion assay

The 3D culture was performed using n3D bioprinting technology (Greiner Bio-One, Frickenhausen, Germany) according to the manufacturer's instructions. In brief, cells were labeled with the NanoShuttle-PL (Nano3D Biosciences, Houston, TX, USA) by three rounds of centrifugation and resuspension. 2 x 10^4 cell/200 µL were resuspended in serum-free medium and plated in triplicates in a cell-repellent 96-well plate (Greiner Bio-One). The spheroid formation was induced by placing the magnetic device (spheroid drive) under the plate followed by incubating for 30 min, at 37° C. Then, the magnetic device was removed, and the spheroids were let to stabilize for 48 h when the medium was replaced by 1:1-diluted Matrigel® matrix (Corning). Spheroids were allowed to invade for seven days and photographed each 24 h using the CKX41 Inverted Microscope (Olympus) and invasion as assessed related to 0 h using ImageJ software.

Proliferation assay

The proliferation assessment was made by EdU (5-ethynyl-2′-deoxyuridine) incorporation using the EdU Cell Proliferation Assay (Millipore, Burlington, MA, USA) according to the manufacturer's instructions. 1 x 10^4 cells were plated in

48-well plates. At 24 h, 48 h, and 72 h, EdU was added to the culture to a final concentration of 10 µM and incubated for 2 h, 37° C. Then, cells were fixed with 4 % formaldehyde/PBS, permeabilized with 0.5 % Triton X-100 and incubated with the detection solution provided by the kit. Cells were analyzed by flow cytometry.

Orthotopic xenograft model

Animal experiments were conducted in 6-8 week-old male non-obese diabetic/ severe combined immunodeficiency (NOD/SCID) mice obtained from the Animal Facility at the University of São Paulo Medical School. All animal experiments were approved by the Animal Research Ethics Committee of the Bauru School of Dentistry, University of São Paulo. Immediately after sorting, the subpopulations of LUC4 $CD44^{High}ESA^{High}$ and $CD44^{High}ESA^{Low}$ were suspended in Matrigel (5 x 10^3 cells/30 µL Matrigel, Corning) and transplanted into the tongue of anesthetized NOD/SCID mice. Animals were euthanized 60 days post-inoculation by an overdose of anesthetics.

Histopathological analysis

Tongues were collected, measured, and fixed in 10 % buffered formalin solution and paraffin embedding for histological processing. The tumor volume was calculated using the formula: V = 0.5 (L*W*W) [51]. Serial sections from tongues were stained with H&E, and tumor grade was evaluated according to the World Health Organization guidelines for OSCC [1]. H&E slides were scanned using the Aperio Scanscope CS Slide Scanner (Aperio Technologies Inc, Vista, CA, USA), and all digital images obtained in .svs format were visualized with ImageScope software (Aperio Technologies Inc).

Tumor digestion

For FACS analysis of tumors, tongues were collected and submitted to enzymatic digestion. Tumors were fragmented at 2 mm approximately using scalpels and incubated in DMEM containing 75 U/mL collagenase III (MP Biomedicals, Santa Ana, CA, USA) and 2 mg/mL dispase (Life Technologies) for two and a half hours, at 37° C under shaking. Using disposable Pasteur pipette, the solution was homogenized and cell suspension was filtered using 100 µm cell strainer (Corning), centrifuged and cells stained for flow cytometry with 2:100 of the following antibodies: rat anti-human PE-CD104 (clone 439-9B, positive selection of human epithelial cells), mouse anti-human PerCP-Cy™5.5-CD44 (clone G44-26), and mouse anti-human BV605-ESA (clone EBA-1).

Co-culture of LUC4 and macrophages

LUC4 and THP-1 derived macrophages were co-cultured using the 6-transwell system with 0.4 µm pore from Corning. 10^5 THP-1 cells were differentiated into macrophages by incubation with PMA 150 nM (Sigma) on the top of the insert for 72 h. Then, the inserts were allocated over 6-well plate containing 2 x 10^5 LUC4 cells. Cells were co-cultured for 120 h (5 days) in serum-free medium, and the phenotype of LUC4 was analyzed each 24 h.

Statistical analysis

Statistical analysis was performed using the GraphPad Prism 6 software (Graph-Pad Software, Inc., CA, USA). Quantitative data were presented as mean ± SD from three independent experiments unless otherwise stated. Comparisons between two groups were made with the t-test followed by the Mann-Whitney test

for nonparametric data or with Welch´s correction for parametric data. Comparisons of three groups were made using one-way ANOVA with the Kruskal-Wallis test followed by Dunn´s multiple comparisons test. Two-way ANOVA analyzed multiple comparisons with Tukey´s correction. p values ≤ 0.05 were considered as significant.

Acknowledgments

We thank Dr. Ian Mackenzie for the donation of the two primaries OSCC cell lines. We also acknowledge the technicians Daniele Santi Ceolin and Patrícia de Sá Mortagua for their excellent technical assistance.

Conflict of Interest

The authors declare that they have no conflict of interest.

Funding

This work was supported by São Paulo Research Foundation (FAPESP, grant #2013/07245-9), Coordination for the Improvement of Higher Education Personnel (CAPES, scholarship to N.G.A.), and National Council for Scientific and Technological Development (CNPq, grant #424158/2016-7).

Authors contributions

Conception and design: C.O. Rodini. ***Development of methodology:*** N.G. Amôr, R.F. Buzo, R.C. Ortiz, N.M. Lopes, L.M. Saito. ***Analysis and interpretation of data:*** N.G. Amôr, R.C. Ortiz, C.O. Rodini. ***Manuscript writing:*** N.G. Amôr, and C.O. Rodini.

References

1 Thompson L. World Health Organization classification of tumours: pathology and genetics of head and neck tumours. Ear Nose Throat J 2006; **85**: 74.

2 Sasahira T, Kirita T. Hallmarks of Cancer-Related Newly Prognostic Factors of Oral Squamous Cell Carcinoma. Int J Mol Sci 2018; **19**: E2413. .

3 Hannen EJ, van der Laak JA, Manni JJ, Pahlplatz MM, Freihofer HP, Slootweg PJ et al. Improved prediction of metastasis in tongue carcinomas, combining vascular and nuclear tumor parameters. Cancer 2001; **92**: 1881-1887.

4 Ortiz RC, Lopes NM, Amôr NG, Ponce JB, Schmerling CK, Lara VS et al. CD44 and ALDH1 immunoexpression as prognostic indicators of invasion and metastasis in oral squamous cell carcinoma. J Oral Pathol Med 2018; **47**:740-747.

5 Sathyanarayanan V, Neelapu SS. Cancer immunotherapy: Strategies for personalization and combinatorial approaches. Mol Oncol 2015; **9**: 2043-2053.

6 Kwong LN, Davies MA. Targeted therapy for melanoma: rational combinatorial approaches. Oncogene 2014; **33**: 1-9.

7 Heppner GH. Tumor heterogeneity. Cancer Res 1984; 44: 2259-2265.

8 Gillies RJ, Verduzco D, Gatenby RA. Evolutionary dynamics of carcinogenesis and why targeted therapy does not work. Nat Rev Cancer 2012; **12**: 487-493.

9 Tang K, Yu Y, Zhu L, Xu P, Chen J, Ma J et al. Hypoxia-reprogrammed tricarboxylic acid cycle promotes the growth of human breast tumorigenic cells. Oncogene 2019; [Epub ahead of print] doi: 10.1038/s41388-019-0932-1 .

10 Sirard C, Lapidot T, Vormoor J, Cashman JD, Doedens M, Murdoch B et al. Normal and leukemic SCID-repopulating cells (SRC) coexist in the bone marrow and peripheral blood from CML patients in chronic phase, whereas leukemic SRC are detected in blast crisis. Blood 1996; **87**: 1539-1548.

11 Valent P, Bonnet D, De Maria R, Lapidot T, Copland M, Melo JV et al. Cancer stem cell definitions and terminology: the devil is in the details. Nature reviews Cancer; 2012; **12**: 767-775.

12 Nguyen DX, Bos PD, Massagué J. Metastasis: from dissemination to organ-specific colonization. Nat Rev Cancer 2009; **9**: 274-284.

13 Batlle E, Clevers H. Cancer stem cells revisited. Nature medicine (Review) 2017; **23**: 1124-1134.

14 He W, Liang B, Wang C, Li S, Zhao Y, Huang Q et al. MSC-regulated lncRNA MACC1-AS1 promotes stemness and chemoresistance through fatty acid oxidation in gastric cancer. Oncogene 2019; **38**: 4637-4654.

15 Rodini CO, Lopes NM, Lara VS, Mackenzie IC. Oral cancer stem cells - properties and consequences. J Appl Oral Sci 2017; **25**: 708-715.

16 Labelle M, Begum S, Hynes RO. Direct signaling between platelets and cancer cells induces an epithelial-mesenchymal-like transition and promotes metastasis. Cancer Cell 2011; **20**: 576-590.

17 Tsai JH, Donaher JL, Murphy DA, Chau S, Yang J. Spatiotemporal regulation of epithelial-mesenchymal transition is essential for squamous cell carcinoma metastasis. Cancer Cell 2012; **22**: 725-736.

18 Mani SA, Guo W, Liao MJ, Eaton EN, Ayyanan A, Zhou AY et al. The epithelial-mesenchymal transition generates cells with properties of stem cells. Cell 2008; **133**: 704-715.

19 Fang X, Cai Y, Liu J, Wang Z, Wu Q, Zhang Z et al. Twist2 contributes to breast cancer progression by promoting an epithelial-mesenchymal transition and cancer stem-like cell self-renewal. Oncogene 2011; **30**: 4707-4720.

20 Thiery JP. Epithelial-mesenchymal transitions in development and pathologies. Curr Opin Cell Biol 2003; **15**: 740-746.

21 Biswas SK, Mantovani A. Macrophage plasticity and interaction with lymphocyte subsets: cancer as a paradigm. Nature immunology 2010; **11**: 889-896.

22 Christofori G. New signals from the invasive front. Nature 2006; **441**: 444-450.

23 Biddle A, Liang X, Gammon L, Fazil B, Harper LJ, Emich H et al. Cancer stem cells in squamous cell carcinoma switch between two distinct phenotypes that are preferentially migratory or proliferative. Cancer Res 2011; **71**: 5317-5326.

24 Zeisberg M, Neilson EG. Biomarkers for epithelial-mesenchymal transitions. J Clin Invest 2009; **119**: 1429-1437.

25 Zhou J, Tao D, Xu Q, Gao Z, Tang D. Expression of E-cadherin and vimentin in oral squamous cell carcinoma. Int J Clin Exp Pathol 2015; **8**: 3150-3154.

26 Amor NG, de Oliveira CE, Gasparoto TH, Vilas Boas VG, Perri G, Kaneno R et al. ST2/IL-33 signaling promotes malignant development of experimental squamous cell carcinoma by decreasing NK cells cytotoxicity and modulating the intratumoral cell infiltrate. Oncotarget 2018; **9**: 30894-30904.

27 Su S, Liu Q, Chen J, Chen F, He C, Huang D et al. A positive feedback loop between mesenchymal-like cancer cells and macrophages is essential to breast cancer metastasis. Cancer Cell 2014; **25**: 605-620.

28 Dalerba P, Cho RW, Clarke MF. Cancer stem cells: models and concepts. Annu Rev Med 2007; **58**: 267-284.

29 Prince ME, Sivanandan R, Kaczorowski A, Wolf GT, Kaplan MJ, Dalerba P et al. Identification of a subpopulation of cells with cancer stem cell properties in head and neck squamous cell carcinoma. Proc Natl Acad Sci U S A 2007; **104**: 973-978.

30 Thiery JP, Acloque H, Huang RY, Nieto MA. Epithelial-mesenchymal transitions in development and disease. Cell 2009; **139**: 871-890.

31 Papini S, Cecchetti D, Campani D, Fitzgerald W, Grivel JC, Chen S et al. Isolation and clonal analysis of human epidermal keratinocyte stem cells in long-term culture. Stem Cells 2003; **21**: 481-494.

32 Locke M, Heywood M, Fawell S, Mackenzie IC. Retention of intrinsic stem cell hierarchies in carcinoma-derived cell lines. Cancer Res 2005; **65**: 8944-8950.

33 Tan L, Sui X, Deng H, Ding M. Holoclone forming cells from pancreatic cancer cells enrich tumor initiating cells and represent a novel model for study of cancer stem cells. PLoS One 2011; **6**: e23383.

34 Tieche CC, Gao Y, Buhrer ED, Hobi N, Berezowska SA, Wyler K et al. Tumor Initiation Capacity and Therapy Resistance Are Differential Features of EMT-Related Subpopulations in the NSCLC Cell Line A549. Neoplasia 2019; **21**: 185-196.

35 Ferrer I, Verdugo-Sivianes EM, Castilla MA, Melendez R, Marin JJ, Munoz-Galvan S et al. Loss of the tumor suppressor spinophilin (PPP1R9B) increases the cancer stem cell population in breast tumors. Oncogene 2016; **35**: 2777-2788.

36 Li C, Heidt DG, Dalerba P, Burant CF, Zhang L, Adsay V et al. Identification of pancreatic cancer stem cells. Cancer Res 2007; **67**: 1030-1037.

37 Al-Hajj M, Wicha MS, Benito-Hernandez A, Morrison SJ, Clarke MF. Prospective identification of tumorigenic breast cancer cells. Proc Natl Acad Sci U S A 2003; **100**: 3983-3988.

38 Dai BW, Yang ZM, Deng P, Chen YR, He ZJ, Yang X et al. HOXC10 promotes migration and invasion via the WNT-EMT signaling pathway in oral squamous cell carcinoma. J Cancer 2019; **10**: 4540-4551.

39 Zhang J, Zheng G, Zhou L, Li P, Yun M, Shi Q et al. Notch signalling induces epithelialmesenchymal transition to promote metastasis in oral squamous cell carcinoma. Int J Mol Med 2018; **42**: 2276-2284.

40 Wang Y, Wang T, Sun Y, Sun W, Wang X. Astrocyte elevated gene-1 promotes tumour growth and invasion by inducing EMT in oral squamous cell carcinoma. Sci Rep 2017; **7**: 15447.

41 Clark AG, Vignjevic DM. Modes of cancer cell invasion and the role of the microenvironment. Curr Opin Cell Biol 2015; **36**: 13-22.

42 Hart IR. New evidence for tumour embolism as a mode of metastasis. J Pathol 2009; **219:** 275-276.

43 Knaack H, Lenk L, Philipp LM, Miarka L, Rahn S, Viol F et al. Liver metastasis of pancreatic cancer: the hepatic microenvironment impacts differentiation and self-renewal capacity of pancreatic ductal epithelial cells. Oncotarget 2018; **9**: 31771-31786.

44 McCaffrey LM, Macara IG. Epithelial organization, cell polarity and tumorigenesis. Trends Cell Biol 2011; **21**: 727-735.

45 Quail DF, Joyce JA. Microenvironmental regulation of tumor progression and metastasis. Nat Med 2013; **19**: 1423-1437.

46 Widmer DS, Hoek KS, Cheng PF, Eichhoff OM, Biedermann T, Raaijmakers MIG et al. Hypoxia contributes to melanoma heterogeneity by triggering HIF1alpha-dependent phenotype switching. J Invest Dermatol 2013; **133**: 2436-2443.

47 DeNardo DG, Ruffell B. Macrophages as regulators of tumour immunity and immunotherapy. Nat Rev Immunol 2019; **19**: 369-382.

48 Mackenzie IC. Growth of malignant oral epithelial stem cells after seeding into organotypical cultures of normal mucosa. J Oral Pathol Med 2004; **33**: 71-78.

49 Liang CC, Park AY, Guan JL. In vitro scratch assay: a convenient and inexpensive method for analysis of cell migration in vitro. Nat Protoc 2007; **2**: 329-333.

50 Schneider CA, Rasband WS, Eliceiri KW. NIH Image to ImageJ: 25 years of image analysis. Nat Methods 2012; **9**: 671-675.

51 Unger GM, Kren BT, Korman VL, Kimbrough TG, Vogel RI, Ondrey FG et al. Mechanism and efficacy of sub-50-nm tenfibgen nanocapsules for

cancer cell-directed delivery of anti-CK2 RNAi to primary and metastatic squamous cell carcinoma. Mol Cancer Ther 2014; **13**: 2018-2029.

Figure legends

Fig 1. The presence of cancer stem cells with EMT phenotype varies among OSCC cell lines. Immunofluorescence analysis of the EMT markers, E-cadherin (red) and Vimentin (white) in OSCC cell lines. SCC-9, CA1, and LUC4 cells were plated at low (10^4) and high densities (3×10^4) in slide chambers and fixed after 24-48 h. Cells were counterstained with DAPI for nuclear visualization. Photomicrographs were acquired using the inverted Leica TCS-SPE confocal microscope with the Leica Application Suite-Advanced Fluorescence software. Images acquired with x40 magnification.

Fig. 2. The proportion of epithelial and mesenchymal phenotype among OSCC cells is lineage-specific. SCC-9, CA1, and LUC4 cell lines were plated at low (2×10^4), and high densities (5×10^4) in a 24-well plate and CD44 and ESA markers were analyzed by flow cytometry 72 h after plating. **a** Phase-contrast images of the culture at the time of detachment for flow cytometry analysis. x40 magnification. Scale bar = 200 µm. **b** Dot plots and respective gate strategy for quantification of the two subpopulations of CSC: epithelial CSC (Epi-CSC) defined as $CD44^{High}ESA^{High}$ and CSC in EMT (EMT-CSC), as $CD44^{High}ESA^{Low}$. **c** Percentage of each subpopulation of CSC presented in OSCC cell lines and **d** the ratio of $CD44^{High}ESA^{High}/CD44^{High}ESA^{Low}$ analyzed at low and high confluency. Data are shown as mean ± SD from three independent experiments performed in triplicate. $*p < 0.05$.

Fig. 3. Epi-CSC and EMT-CSC LUC4 cells act uniquely *in vitro*, exhibiting different patterns of proliferation and invasive behavior. $CD44^{High}ESA^{High}$ and $CD44^{High}ESA^{Low}$ LUC4 cells were sorted for *in vitro* assays. **a** Phase-contrast images of each cell subpopulation showing the morphology differences between them. x10 magnification. Scale bar = 100 µm. Cells were plated at 5 x 10^2 cells/3 mL in a 6-well plate for **b** colony morphology assay. **c** graphic showing the counting of each clone. **d** Phase-contrast images of the wound healing assay and **e** quantification of the migratory ability of each subpopulation of CSCs. x4 magnification. Scale bar = 100µm. **f** EdU proliferation assay. **g** 3D structure formation of each cell subpopulation using the n3D bioprinting technology and pattern of Matrigel® matrix invasion. x4 magnification. Scale bar = 200 µm Data are shown as mean ± SD from three independent experiments performed in triplicate. *$p < 0.05$.

Fig. 4. Epi-CSC and EMT-CSC have different tumor-initiating capacities. Male NOD/SCID mice were inoculated in the tongue with 5 x 10^3 LUC4 cells ($CD44^{High}ESA^{High}$, n = 11; $CD44^{High}ESA^{Low}$, n = 12; Sham, n = 2). **a** Photomicrograph of the orthotopic xenograft. Graphics showing the **b** chow intake and **c** body weight. **d** Table of the frequency of tumors generated by each cancer cell subpopulation. **e** Photomicrograph of the primary tumors generated after 60 days from the xenograft. **f** Graphics showing the tumor volume. Data are representative of two independent experiments. All quantitative data are mean ± SD. *$p < 0.05$.

Fig. 5. Epi-CSC generates tumors moderately differentiate. Representative pictures are shown of H&E-stained OSCC sections that were obtained from NOD/SCID mice at 60 days after LUC4 inoculation. H&E sections were demonstrating: ulcerated areas (black arrowheads), corneal pearls (green dots), multinucleated cells (blue arrowheads), abnormal mitosis (yellow arrowheads), a small cluster of invading cells (green arrowhead). Scale bars: **a – d**, 800 µm; **e – h** and **m – p**, 200 µm; **i – l**, and **q – t**, 50 µm.

Fig. 6. Epi-CSC and EMT-CSC start to reassemble tumor heterogeneity both *in vitro* and *in vivo*. After sorting, cells that were not used for xenograft were plated and cultivated and maintained during all the *in vivo* experimental period (60 days). The phenotype of both subpopulations was analyzed by flow cytometry: **a** *in vitro* and **b** *in vivo*. ß4 integrin (CD104) was used as a positive gate for the selection of human epithelial cells from the mice´s tongues.

Fig. 7. Macrophages induce EMT-CSC phenotype *in vitro*. LUC4 cells were indirectly cultured with THP-1-derived macrophages in a transwell system for five days, and the cell´s phenotype was analyzed by flow cytometry. **a** Dot plots showing the percentage of Epi- and EMT-CSC when cultured alone (monoculture) or co-cultured with macrophages (co-culture) analyzed each day. Graphs showing the percentage of **b** Epi-CSC and **c** EMT-CSC cultured for five days alone or with macrophages. Data are representative of two independent experiments.

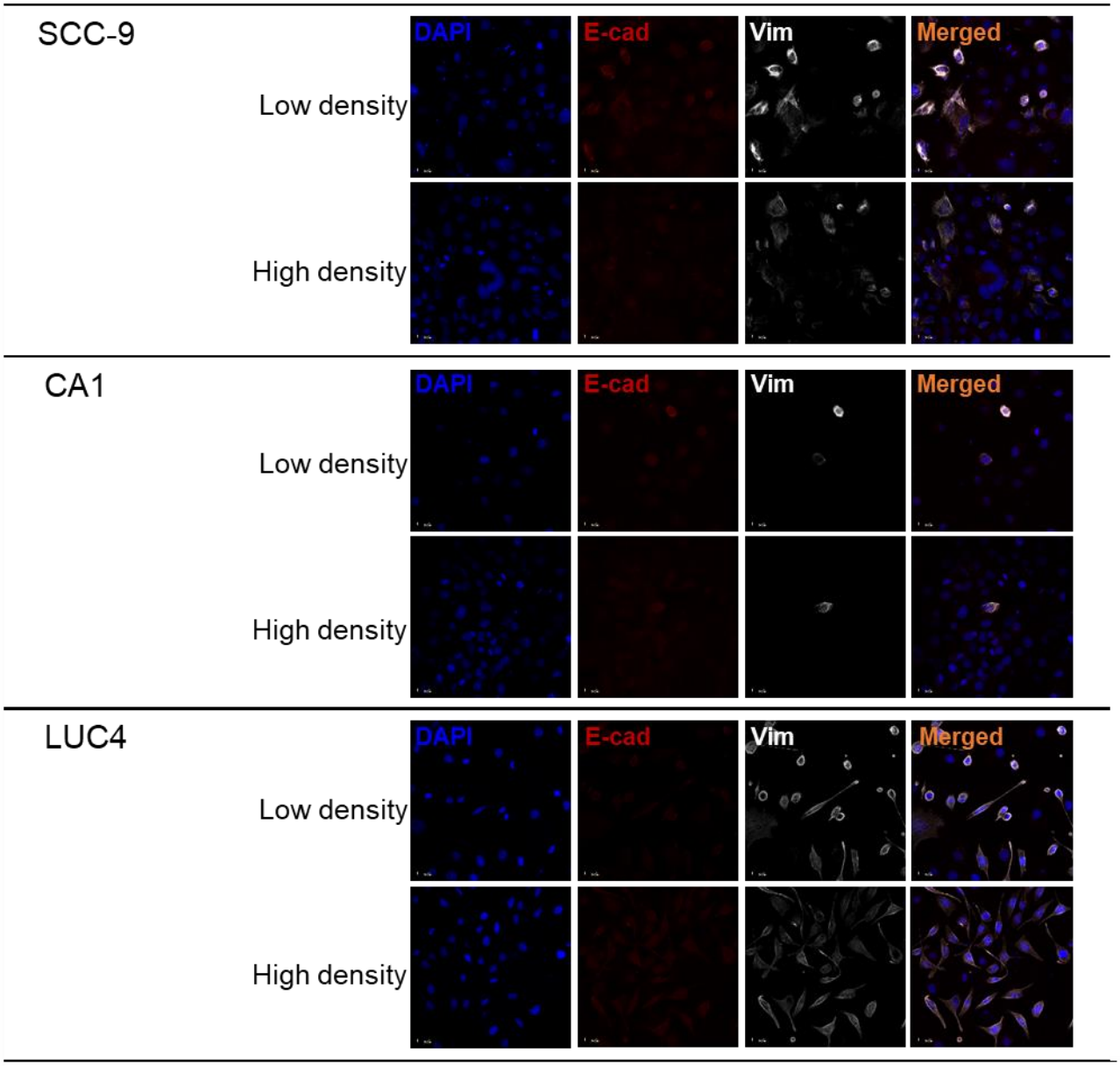
SCC-9
Low density
High density
CA1
Low density
High density
LUC4
Low density
High density
DAPI
E-cad
Vim
Merged

Fig. 1

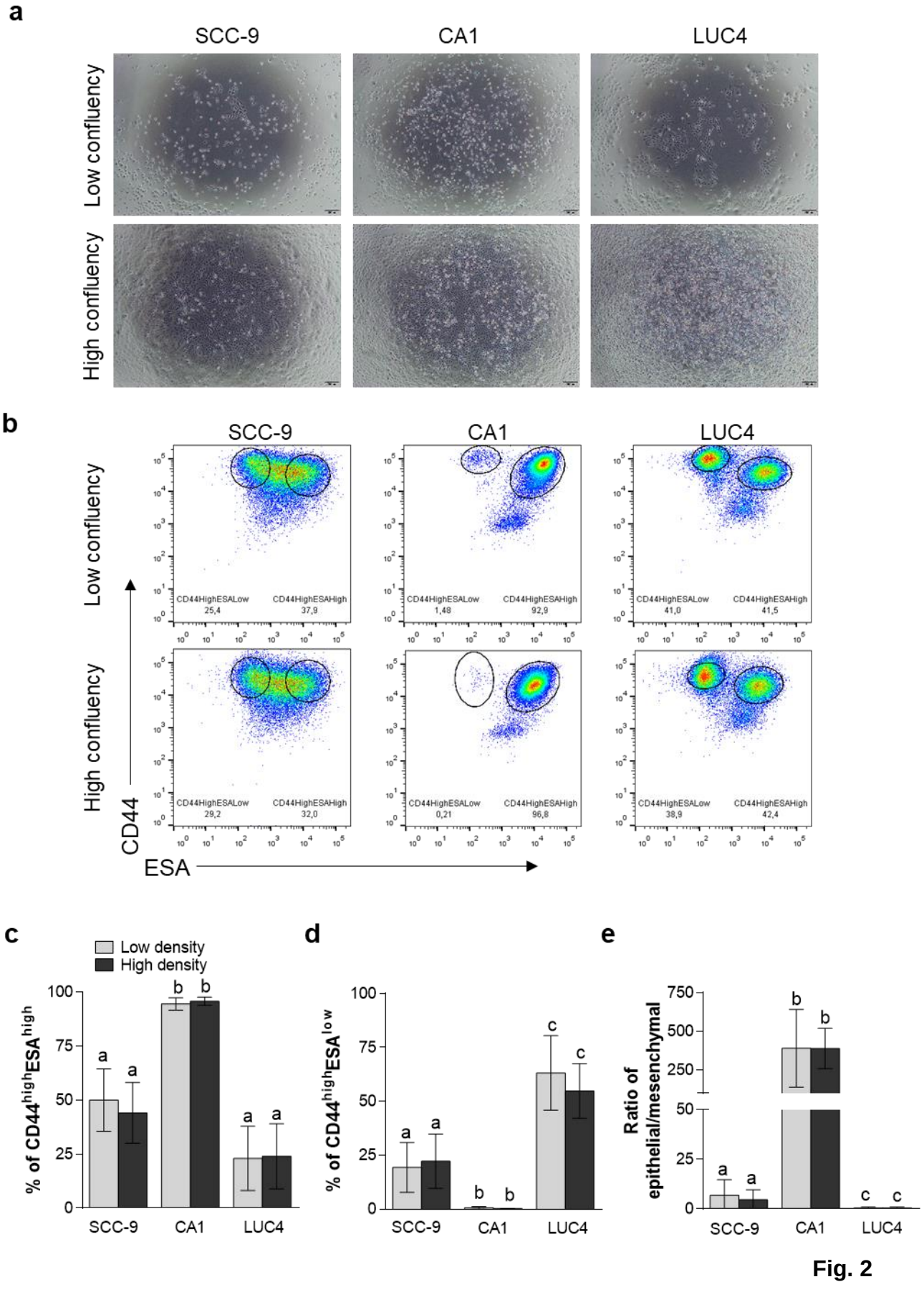
a
SCC-9
CA1
LUC4
Low confluency
High confluency
b
SCC-9
CA1
LUC4
Low confluency
High confluency
CD44
ESA
CD44HighESALow 25,4
CD44HighESAHigh 37,9
CD44HighESALow 1,48
CD44HighESAHigh 92,9
CD44HighESALow 41,0
CD44HighESAHigh 41,5
CD44HighESALow 29,2
CD44HighESAHigh 32,0
CD44HighESALow 0,21
CD44HighESAHigh 96,8
CD44HighESALow 38,9
CD44HighESAHigh 42,4
c
Low density
High density
% of CD44highESAhigh
SCC-9
CA1
LUC4
d
% of CD44highESAlow
SCC-9
CA1
LUC4
e
Ratio of epithelial/mesenchymal
SCC-9
CA1
LUC4

Fig. 2

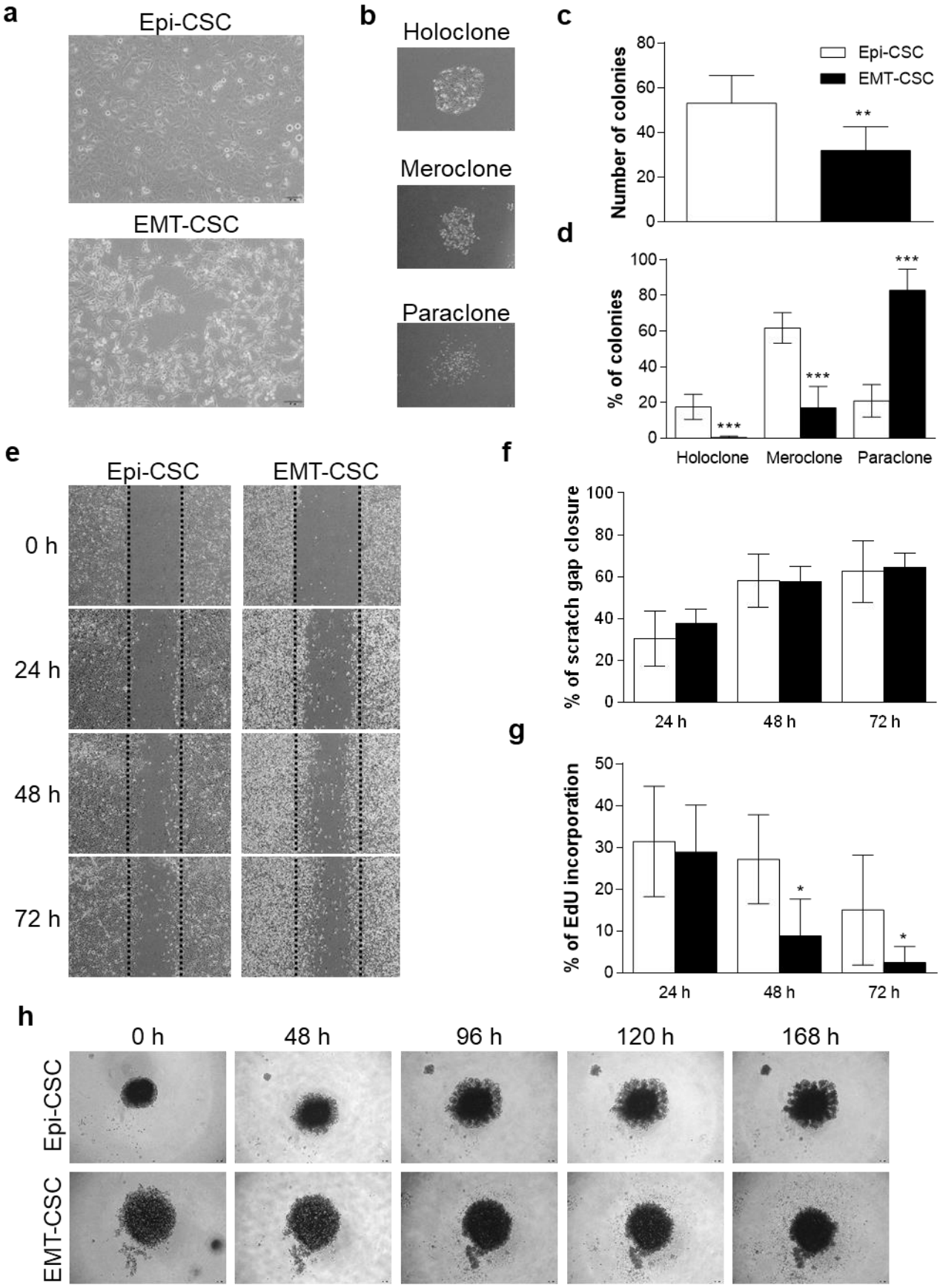
a
Epi-CSC
EMT-CSC
b
Holoclone
Meroclone
Paraclone
c
Number of colonies
Epi-CSC
EMT-CSC
**
d
% of colonies
***
Holoclone
Meroclone
Paraclone
e
Epi-CSC
EMT-CSC
0 h
24 h
48 h
72 h
f
% of scratch gap closure
24 h
48 h
72 h
g
% of EdU incorporation
*
h
0 h
48 h
96 h
120 h
168 h
Epi-CSC
EMT-CSC

Fig. 3

a

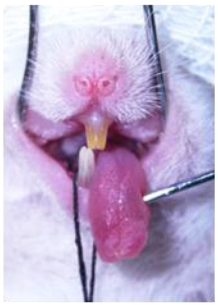

b

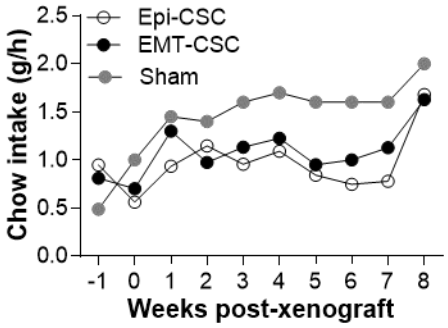

c

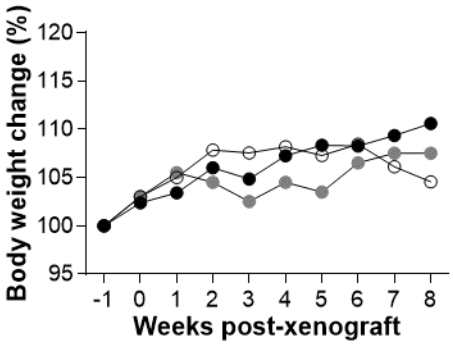

d

Subpopulation	Number of animals	Tumor incidence	
		Macroscopic	Microscopic
Epi-CSC	11	7 (63.63 %)	11 (100 %)
EMT-CSC	12	5 (41.67 %)	9 (75 %)

e

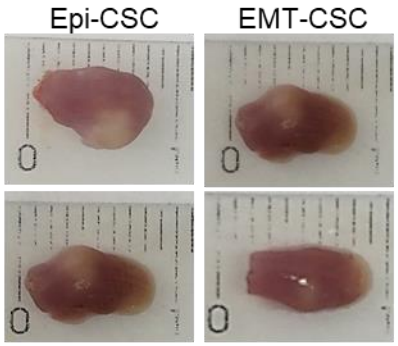

f

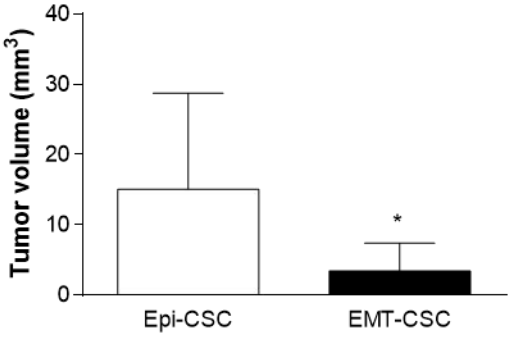

Fig. 4

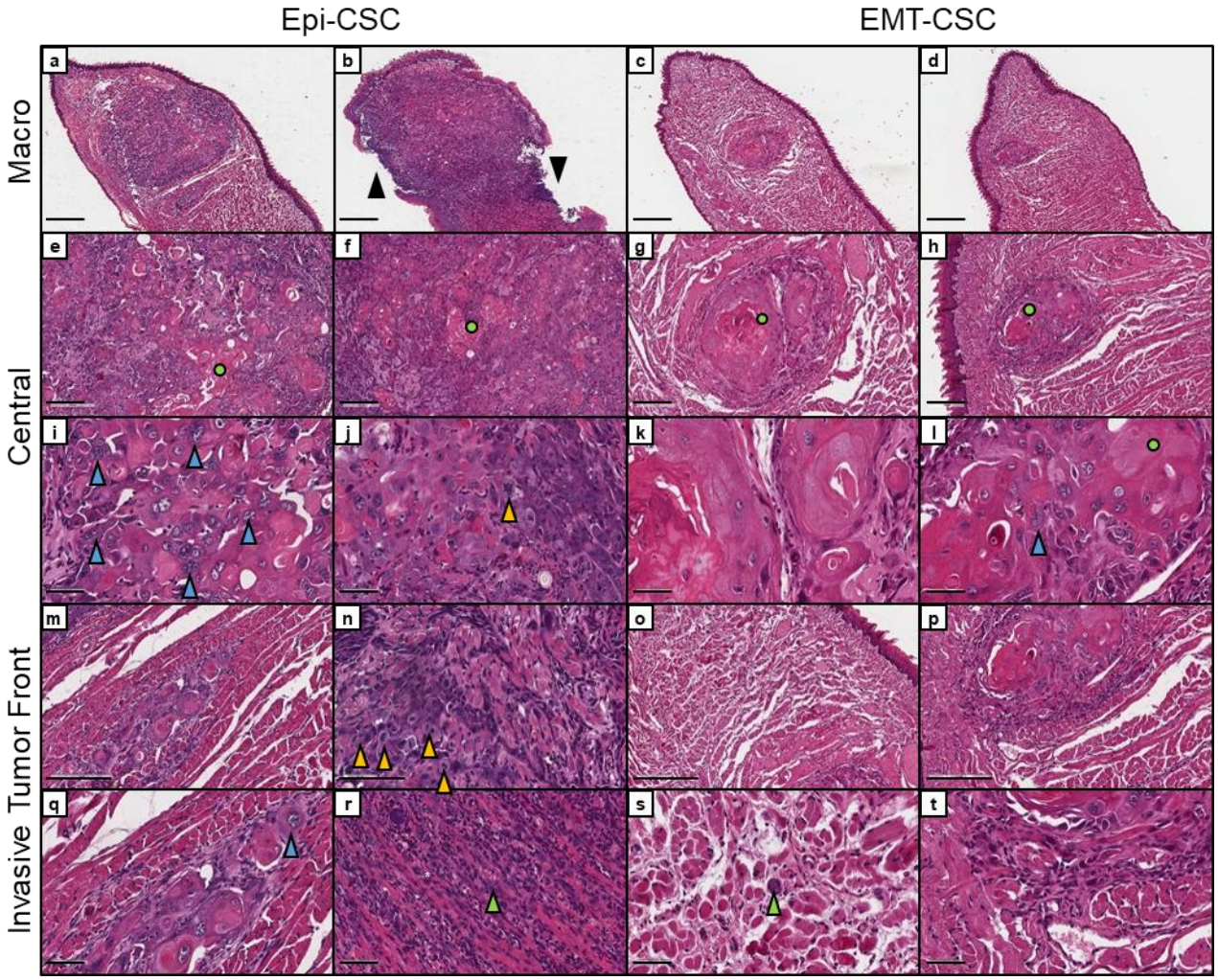
Epi-CSC
EMT-CSC
Macro
Central
Invasive Tumor Front
a
b
c
d
e
f
g
h
i
j
k
l
m
n
o
p
q
r
s
t

Fig. 5

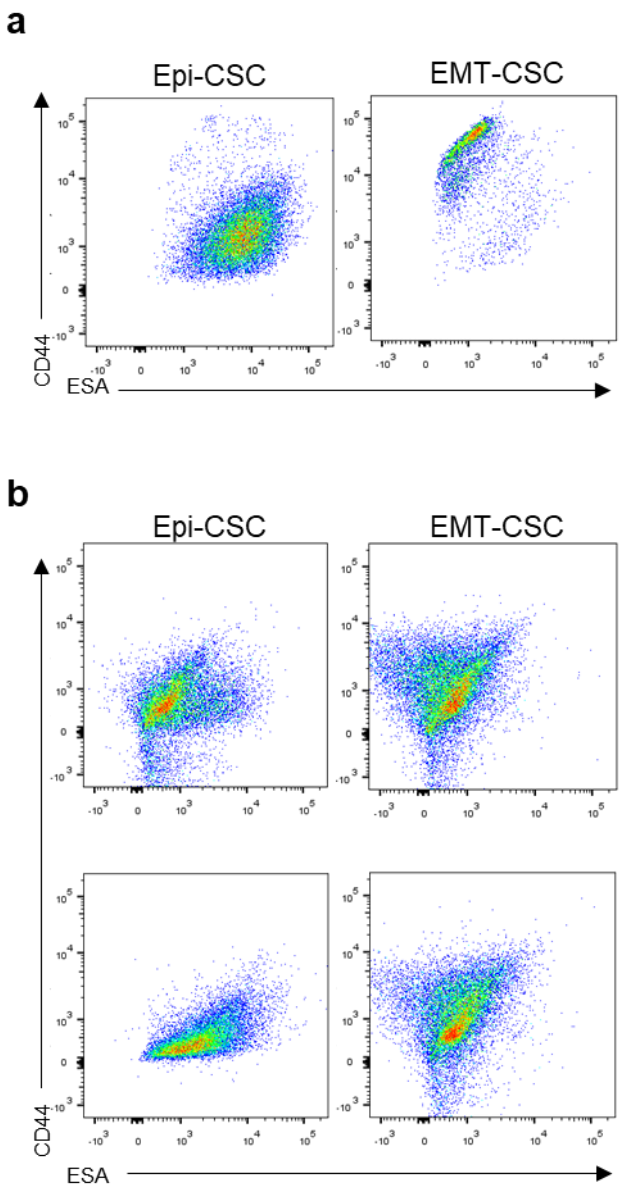

Fig. 6

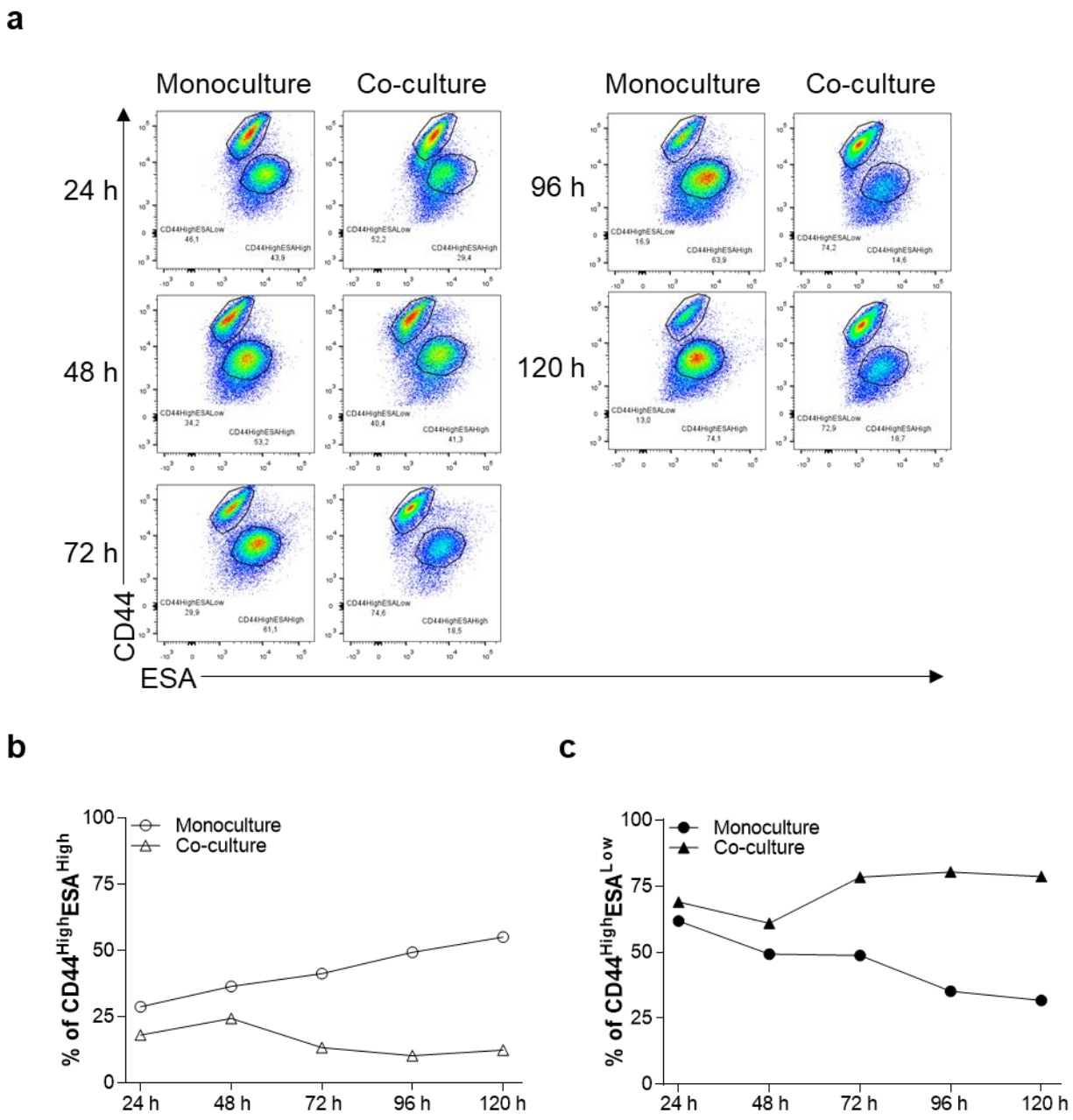
a
Monoculture
Co-culture
Monoculture
Co-culture
24 h
48 h
72 h
96 h
120 h
CD44
ESA
b
c
Monoculture
Co-culture
% of CD44HighESAHigh
% of CD44HighESALow
100
75
50
25
0
24 h
48 h
72 h
96 h
120 h

Fig. 7

Macrophages promote aggressive behavior on tumor cells via TGF-β signaling in oral squamous cell carcinoma

Nádia Ghinelli Amôr, Nathália Martins Lopes, Rafael Carneiro Ortiz, Rodrigo Fonseca Buzo, Luciana Mieli Saito and Camila Oliveira Rodini*

Department of Biological Sciences, Bauru School of Dentistry, University of São Paulo, Al. Dr. Octávio Pinheiro Brisolla, 9-75, Bauru, SP, 17012-901, Brazil

*Correspondence should be addressed to: Camila Rodini, DDS, MSc, Ph.D., Department of Biological Sciences, Bauru School of Dentistry, University of São Paulo, Av. Otavio Pinheiro Brisolla, 9-75, Bauru/SP, Brazil. Tel: +55 14 3235 8259; Email: carodini@usp.br

Running title: Macrophage-derived TGF-β and oral cancer

Keywords: Oral squamous cell carcinoma. Cancer stem-cell. Epithelial-mesenchymal transition. Macrophage. TGF-β. VEGF. Xenograft. 3D culture.

Abstract

Oral squamous cell carcinoma (OSCC) is one of the most common malignant neoplasms of the head and neck, and the major prognostic factor is the presence of metastatic lesions in cervical lymph nodes. Recent studies have shown that cancer stem cells (CSC) can be involved with migration and invasion process through the epithelial-to-mesenchymal transition (EMT) program in tumor cells. Macrophages are frequently founded at the invasive front of aggressive tumors where cancer cells undergoing EMT are found, suggesting that macrophages might influence the invasive behavior of tumor cells. In addition, macrophages are a significant source of TGF-β in the tumor microenvironment, and the signaling mediated by TGF-β has been described as essential for maintenance, differentiation, and function of CSC. In view of that, we investigated the role of macrophages and TGF-β on CSC´s behavior with epithelial phenotype or in EMT. Our results showed that macrophages improved the capacity of invasion of both phenotypes and induced EMT on the epithelial CSC phenotype. More important, inhibition of TGF-β decreased the invasion and restored the capacity of CSC on producing the vascular endothelial growth factor (VEGF). Macrophages affected the cytokine production of epithelial CSC, suggesting a possible alteration of the tumor microenvironment soluble components.

Introduction

The immune microenvironment that surrounds tumors has been revealed a critical factor driving cancer course [1]. Depending on the phenotype and activation state of the infiltrating immune cells as well the cytokine/chemokine milieu, the tumor can either progress or be suppressed [2]. The determinant toward one or another scenario is the frequently crosstalk between tumor and immune cells [3, 4]. Therefore, the knowledge of the cellular and soluble components interacting within tumor microenvironment (TME) might improve the prognosis.

Oral squamous cell carcinoma (OSCC), which arises within the oral cavity, including the tongue, upper and lower gingiva, oral floor, palate, and buccal mucosa, is the most common malignancy of the head and neck [5]. Tumorigenesis, chemoresistance, recurrence, and metastasis have been attributed to a unique subpopulation of cells with stemness properties, then called cancer stem-cells (CSC) [6, 7]. However, what contributes to the generation and maintenance of CSC in OSCC is not entirely understood.

Due to frequently commensal microorganisms challenging in the mucosa, regulation of the oral cavity immune system should be very efficient to prevent the colonization of pathogenic microorganisms and also prevent the development of chronic inflammation, maintaining immune cell activation in homeostasis [8]. In the physiological state, macrophages and monocytes are presented in the oral cavity and promote homeostasis by inducing the production of anti-inflammatory cytokines, such as IL-10 and TGF-β [8, 9]. When pathological/damage signals are presented, macrophages become pro-inflammatory and orchestrate the local immune response recruiting and activating innate and adaptive immune cells [9].

In addition, a considerable amount of evidence demonstrates that macrophages efficiently infiltrate TME of humans and experimental models [10, 11], therefore being called tumor-associated macrophages (TAM).

Preliminary work from our laboratory demonstrates that macrophages induce the epithelial-mesenchymal transition (EMT) in OSCC cell line when indirectly co-cultured *in vitro* (unpublished data). The presence of TAMs is frequently found at the invasive front of aggressive cancers [12], where tumor cells undergoing EMT are founded [13], suggesting that TAM might influence the invasive behavior of tumor cells. In addition, macrophages are a significant source of TGF-β in the tumor microenvironment [14, 15] and the signaling mediated by TGF-β have been described as essential for maintenance, differentiation and function of CSC in different types of epithelial cancers, as well regulators of EMT in normal and tumor cells [16-19]. However, several studies have also shown the tumor suppressive role of macrophages and TGF-β in tumors [20-22], but their function in OSCC remains unclear.

Based on these observations, we aimed to determine the effect of macrophages on CSC in EMT ($CD44^{High}ESA^{Low}$, EMT-CSC) or not ($CD44^{High}ESA^{High}$, Epi-CSC) sorted from the OSCC cell line, LUC4. When directly cultivated with macrophages, carcinoma cells in EMT had their motility increased. On the other hand, carcinoma cells with epithelial phenotype invade more and formed more paraclones indicating EMT. More important, inhibiting TGF-β signaling significantly reduced the invasive behavior induced by macrophages on Epi-CSC. Unexpectedly, macrophages reduced the secretion of VEGF by CSCs, although the blockage of TGF-β restored VEGF production. Our results

demonstrated a mechanism probably TGF-β-mediated by which macrophages promote EMT in carcinoma cells from OSCC.

Results

Both subpopulations founded in LUC4 cell line recruited macrophages into the TME

Analysis of tumor-associated leukocytes in mice models revealed that macrophages are the primary immune cell infiltrator [11, 23]. To determine whether Epi-CSC and EMT-CSC differently recruit macrophages into the TME, both CSC subpopulations were sorted from the LUC4 cell line and then orthotopically inoculated into the tongues of immunocompromised mice, NOD/SCID. After 60 days, mice were euthanized, the tongues were digested, and the leukocytes recovered were analyzed by flow cytometry. Despite the smaller percentage of macrophages $CD11b^{+}F4/80^{+}$ obtained from mice inoculated with EMT-CSC, we could not detect significant differences among both groups of mice (Fig. 1a-b). Next, we wonder whether these two phenotypes could modulate the differentiation of the TAM into M1 or M2. Once more, both groups of mice displayed similar percentages of M1 ($CD80^{+}$, Fig. 1c) and M2 ($CD206^{+}$, Fig. 1d) macrophages, suggesting that Epi-CSC and EMT-CSC subpopulations equally recruited and differentiated macrophages in TME.

Macrophages did not alter the invasive pattern of CSC, although increased their capacity to invade in vitro

We previously observed a significant difference in the pattern of invasive activity displayed by Epi-CSC and EMT-CSC *in vitro* and *in vivo* (unpublished data).

Once macrophages are described as potent EMT inducer [24], we hypothesized that macrophages could affect these patterns. FACS-sorted Epi-CSC and EMT-CSC (Fig, S1) were co-cultured with macrophages and cultivated in Matrigel® matrix for 21 days. Interestingly, macrophages did not changed the way that both subpopulations invaded the 3D matrix (Fig. 2a) even in long term culture (21 days); Epi-CSC directly co-cultured with macrophages still invaded as a collective group of cells, and EMT-CSC preferentially invaded as single cells (Fig. S2). However, regarding the proportion of invasion, macrophages significantly promoted more invasive behavior in both subpopulations, Epi-CSC (Fig. 2b) and EMT-CSC (Fig. 2c) in early periods. These results demonstrated a significant role of macrophages in promoting invasive behavior regardless of the CSC´s phenotype.

Macrophages induced EMT in Epi-CSC and increased the migration activity of EMT-CSC

To overcome the possibility that CSC under macrophages' influence are only proliferating rather than indeed invading the matrix, we performed a proliferation assay using the EdU incorporation technique. Epi-CSC and EMT-CSC were cultured in conditioned-medium (CM) from macrophages for 72 h, and the proliferative capacity was assessed by flow cytometry each 24 h. The proliferation rate of neither subpopulations was affected by the presence of the CM (Fig. 3a-b). To analyze whether macrophages could increase the stemness and EMT properties of both subpopulations, we performed the colony morphology assay (Fig. 3c). CM from macrophages slightly increased the number of colonies formed from both Epi-CSC and EMT-CSC; however, that difference

was not statically significant (Fig. 3d). Regarding the colony morphology, CM from macrophages induced a significant reduction of holoclone formation with concomitant increase in the frequencies of paraclones on Epi-CSC, traits frequently observed in EMT-CSC (Fig. 3e). Interestingly, the ability of EMT-CSC to form colonies was not affected by the CM from macrophages (Fig. 3f). Finally, both subpopulations were submitted to scratch assay to analyze their capacity of migration (Fig.4a). CM did not increase the ability of Epi-CSC to migrate (Fig. 4b). On the other hand, EMT-CSC has their migration capacity increased when cultured with CM for 48 h and 72 h (Fig. 4c). Collectively, these findings demonstrated that CM from macrophages increases EMT in both, Epi- and EMT-CSC.

Macrophages influenced cytokine production of Epi-CSC

Macrophages are crucial mediators of the immune balance in the TME. It is known that these cells act in other immune cells and can modulate several other cell types, such as endothelial cells, fibroblasts, and tumor cells [25]. Based on that, we investigated if macrophages could affect the cytokine production from Epi-CSC and EMT-CSC. Taken advantage of the multiplex assay, we quantified the secretion of 28 analytes in the culture supernatant after 72 h of cell culture, alone or directly co-cultured with macrophages. The most secreted cytokines (> 10 pg/mL) were: IL-1ra, IL-4, IL-8, IL-12p40, Eotaxin, G-CSF, IP-10, MCP-1, and VEGF (Fig, S3). However, despite the small amount of the analytes detected in the supernatant from the cell cultures, we observed a downregulation of IL-3, IL-6, IL-8, IL-10, IL-15, MIP-1α, MIP-1β, and VEGF in Epi-CSC cells promoted by

macrophages (Fig. 5). The cytokine/chemokine secretion of EMT-CSC was not affected by the presence of macrophages (Fig. 5).

TGF-β mediates macrophage-induced invasion in Epi-CSC

TGF-β is a well-known EMT regulator in physiological and pathological conditions [26]. Since macrophages are a significant source of TGF-β in the TME [14, 15], we hypothesized that macrophages might be inducing EMT through TGF-β signaling. To investigate the contributions of macrophages-derived TGF-β, we co-cultured Epi-CSC with macrophages and treated the culture with the TGF-β inhibitor SB431542 [27]. We founded that blocking TGF-β signaling significantly reduced the invasion displayed by Epi-CSC when co-cultured with macrophages (Fig 6a,b). Surprisingly, blocking TGF-β restored the production of VEGF from Epi-CSC (Fig. 6c), demonstrating a possible novel correlation between macrophages, TGF-β, and VEGF.

Discussion

Previous work from our lab described the behavior of two very distinct subpopulations of LUC4 oral cancer cells: $CD44^{High}ESA^{High}$, called Epi-CSC, and $CD44^{High}ESA^{Low}$, referred as EMT-CSC (unpublished data). However, what were the factors that contribute to such heterogeneity remained unclear. The relationship between cancer and macrophages, as well as the relationship between EMT and TGF-β, is well documented [28, 29]. In view of that, we pursue to investigate possible contributions of macrophages and TGF-β upon CSC and EMT phenotypes in OSCC. Using a system of direct 3D culture and cultivating cancer cells indirectly with macrophage-derived CM, we demonstrated that

macrophages increased the invasive behavior of both subpopulations of OSCC cells. Interestingly, our results also provided evidence that macrophages induced EMT, once Epi-CSC cultivated with CM derived from macrophages displayed increased frequency of paraclone formation. More importantly, we showed that the presence of macrophages significantly downregulated cytokine production from Epi-CSC and not from EMT-CSC. Finally, blocking TGF-β signaling decreased the invasion induced by macrophages in Epi-CSC and also restored the capacity of Epi-CSC to produce VEGF.

The presence of $CD206^+$ macrophages in OSCC patients was reported to be positively correlated with worst prognosis [30]. Our results showed that cultivating OSCC cells along with macrophages, regardless of their phenotype, increased their ability to invade matrix *in vitro*. Although we did not analyze the presence of metalloproteinases in the cultures, this increased invasive behavior might be explained by macrophages-derived metalloproteinases already described in the breast [31] and lung [32].

We also evaluated the colony formation and morphology capacity of both subpopulations to investigate their CSC and EMT properties [33-35]. When cultivated in the presence of CM from macrophages the ability of colony formation was not affected in both phenotypes; however, CM decreased holoclone frequency of Epi-CSC cells. In contrast with our work, macrophages have been demonstrated to increase CSC properties in different types of cancer [24, 36]. Our results might be explained by the concomitant increased frequency of paraclones observed in Epi-CSC cultivated with CM, indicating EMT. Additionally, EMT-CSC cultivated with macrophage-derived CM displayed

increased motility, suggesting that factors produced by macrophages sustained and improved EMT traits of EMT-CSC.

Due to the ability of macrophages to modulate microenvironment, we investigated the influence of macrophages in the cytokine/chemokine balance of tumor cells *in vitro*. Despite the few amounts of most analytes detected in the supernatant from the cultures, we could detect macrophage´s influence on Epi-CSC cytokine and chemokine production. When cultivated along with macrophages, Epi-CSC produced less IL-3, IL-6, IL-8, IL-10, IL-15, MIP-1α, MIP-1β, and VEGF. Opposite functions regarding tumor modulation were described for the mentioned factors. IL-6 and IL-8 were described as positive regulators of the stemness properties of breast cancer cells [37, 38]. On the other hand, IL-10, IL-15, MIP-1α, and MIP-1β are involved with activation and recruitment of crucial immune cells, such as NK cells and $CD8^+$ T lymphocytes, in several pathologies, including cancer [39-42], suggesting that macrophages, besides inducing EMT, might affect immune cells activation in TME promoting cancer progression. However, we understand that further research must be conducted in order to better characterized that cytokine/chemokine modulation and its implication in cancer progression.

Unexpected, we obtained very controversial results with the 3D cell co-culture. Macrophages are a well-known producer of VEGF, which in turn induce angiogenesis and promote tumor progression and dissemination in different types of cancers [43]. However, we detected an accentuated reduction of that protein when Epi-CSC was co-cultured with macrophages. Moreover, when we inhibited the TGF-β signaling, the VEGF production was restored, suggesting a possible compensatory mechanism exerted by both cytokines. We suggest that, since

TGF-β promotes angiogenesis in the tumor microenvironment [44, 45], blocking that signaling pathway might trigger a compensatory production of VEGF. The published data regarding the negative correlation between TGF-β and VEGF production is profoundly scarce. A study with paraffined-embedded colon cancer samples demonstrated an inverse correlation between TGF-β and VEGF [46]. The authors showed that TGF-β induced ubiquitination and degradation of VEGF in a PKA- and Smad3-dependent pathway [46]. Therefore, further molecular studies focusing on the intracellular molecules and pathways that might be involved in TGF-β/VEGF modulation are necessary. Collectively, our results show that macrophages induce preferentially EMT and that modulation is probably mediated by TGF-β. Blocking TGF-β pathway altered the invasive behavior of cancer cells and VEGF production *in vitro* which may represent a novel field for further research.

Material & Methods

Cell culture

The primary OSCC cell line, LUC4, was derived and kindly provided by Dr. Ian Mackenzie [47]. Cells were maintained in RM^+ medium composed by 3:1 mixture of DMEM:F12, 10 % FBS, 1 % of antibiotic/antimycotic and mitogens (5 µg/mL transferrin, 0.4 µg/mL hydrocortisone, 0.1 mM cholera toxin, 10 ng/mL epithelial growth factor, 5 µg/mL insulin, 0.2 pM liothyronine). The monocytic cell line, THP-1, was obtained from the American Type Culture Collection (ATCC, Manassas, VA, USA) and maintained in RPMI-C medium (RPMI 1640 medium, 10 % fetal bovine serum, 0.05 mM 2-mercaptoethanol, 2.5 mM L-glutamine, 1 mM sodium pyruvate, and 1 % of antibiotic/antimycotic (Life Technologies,

Carlsbad, CA, USA). Both cells were grown at 37° C, 5 % CO_2 in a humidified atmosphere and media replaced every 48-72 h.

Flow cytometry and fluorescence-activated cell sorting (FACS)

LUC4 cells were detached using StemPro Accutase Cell Dissociation Reagent (Life Technologies) and stained with 1:100 of mouse anti-human CD44 (clone G44-26, BD PharmigenTM, San Diego, CA, USA) and mouse anti-human ESA (clone EBA-1, BD HorizonTM), for 30 min, 4° C in the dark. The exclusion of dead cells was made using Fixable Viability Stain FVS (1:3,000, BD HorizonTM). Samples were analyzed and sorted using Becton and Dickenson FACSAriaTM Fusion Cell Sorter (BD Pharmigen) and BD FACSDivaTM 8.0 software (BD Pharmigen). FACS-sorted cells were collected into RM^+ medium, 20 % FBS and 10 % antibiotic/antimycotic.

Orthotopic xenograft model

Animal experiments were conducted in 6-8-week-old male non-obese diabetic/ severe combined immunodeficiency (NOD/SCID) mice obtained from the Animal Facility at the University of São Paulo Medical School. All animal experiments were approved by the Animal Research Ethics Committee of the Bauru School of Dentistry, University of São Paulo. Immediately after sorting, the subpopulations of LUC4 $CD44^{High}ESA^{High}$ (Epi-CSC) and $CD44^{High}ESA^{Low}$ (EMT-CSC) were suspended in of Matrigel (5 x 10^3 cells/30 µL Matrigel, Corning) and transplanted into the tongue of anesthetized NOD/SCID mice. Animals were euthanized 60 days post-inoculation by an overdose of anesthetics.

Tumor digestion

For FACS analysis of tumors, tongues were collected and submitted to enzymatic digestion. Tumors were fragmented at 2 mm approximately using scalpels and incubated in DMEM containing 75 U/mL collagenase III (MP Biomedicals, Santa Ana, CA, USA) and 2 mg/mL dispase (Life Technologies) for two and a half hours, at 37° C under shaking. Using disposable Pasteur pipette, the solution was homogenized and cell suspension was filtered using 100 µm cell strainer (Corning), centrifuged and cells stained for flow cytometry with 2:100 of the following antibodies: rat anti-mouse BV510-CD11b (clone M1/70, BD HorizonTM), rat anti-mouse PE-CF594-F4/80 (clone T45-2342, BD HorizonTM), hamster anti-mouse BV421-CD80 (clone 16-10A1, BD PharmigenTM), and rat anti-mouse AlexaFluor®647-CD206 (clone MR5D3, BD PharmigenTM).

Macrophage differentiation and conditioned medium

THP1 cells were differentiated into macrophages by incubation with RPMI-C with 150 nM phorbol 12-myristate 13-acetate (PMA) for 48 h followed by 24 h of resting in RPMI-C. Then, the macrophages were incubated with IL-4 (20 ng/mL) and IL-13 (20 ng/mL) for another 48 h. For CM, after differentiation, macrophages were incubated for 24 h with serum-free RPMI-medium. The CM was collected by centrifugation.

3D culture and invasion assay

The 3D culture was performed using n3D bioprinting technology (Greiner Bio-One, Frickenhausen, Germany) according to the manufacturer's instructions. In brief, a total of 6 x 104 cells composed only by tumor cells or mixed with 15 % of

macrophages were labeled with the NanoShuttle-PL (Nano3D Biosciences, Houston, TX, USA) by three rounds of centrifugation and resuspension. 2 x 104 cell/200 µL were resuspended in serum-free medium and plated in triplicates in a cell-repellent 96-well plate (Greiner Bio-One). The spheroid formation was induced by placing the magnetic device (spheroid drive) under the plate followed by incubating for 30 min, at 37° C. Then, the magnetic device was removed, and the spheroids were let to stabilize for 48 h. The medium of five wells of each group was replaced by RM^+:DMEM/F12 or RM^+:CM (1:1), when indicated, the TGF-β inhibitor, SB431542 (Sigma, St Louis, MO, USA), was added to a final concentration of 10µM. In another three wells, the medium was replaced by 1:1-diluted Matrigel® matrix (Corning) with or without the already mentioned treatments. The supernatant was collected and freeze with protease inhibitor for cytokine dosage. Spheroids in the well with Matrigel were allowed to migrate and invade for 21 days and photographed each 24 h using the CKX41 Inverted Microscope (Olympus).

Colony formation assay

Five-hundred cells of each subpopulation (Epi- and EMT-CSC) were suspended in 3mL of 1:1 mixture of RM^+:DMEM/F12 or in 1:1 mixture of RM^+:CM and added to each well of a 6 well plate and incubated ate 37° C, 5 % CO_2 for 7 days without medium changing. Then, cells were fixed in 4% paraformaldehyde, stained with 0.04 % crystal violet in 1 % ethanol, and colonies with at least 50 cells were counted visually. The colonies' morphology was classified as holo- (homogeneous clusters of small and tightly attached cells with regular

borderlines), para- (dispersed cells with fragmented borderlines), and meroclones (intermediate morphologies) [45].

Proliferation assay

The proliferation assessment was made by EdU (5-ethynyl-2′-deoxyuridine) incorporation using the EdU Cell Proliferation Assay (Millipore, Burlington, MA, USA) according to the manufacturer's instructions. 1 x 104 cells were plated in a 48-well plate and left to stabilize for 24-48 h. After that period, the medium was replaced by RM^+:DMEM/F12 or with RM^+:CM (both 1:1). EdU incorporation was assessed by flow cytometry at 24 h, 48 h, and 72 h.

Wound healing assay

The wound-healing assay was performed as previously described [46] with minor modifications. Briefly, 5 x 10^5 cells were plated on a 24-well plate and let to recovery for 24-48 h. Cells were then treated with 10 µg/mL of mitomycin C to inhibit proliferation. A 1,000 µL sterile pipette tip was used to make a scratch in the cell monolayer. The medium was replaced by RM^+:DMEM/F12 or for RM^+:CM (1:1). The scratch gap width was photographed at each 24 h using the CKX41 Inverted Microscope (Olympus, Tokyo, Japan). The area of the open wound was measured using ImageJ software [47], and the results were calculated as a percentage of wound closure.

Luminex

Cytokine and chemokines were analyzed in cell-free supernatant by multiplex analysis using the MILLIPLEX MAP Human Cytokine/Chemokine Magnetic Bead

Panel (Millipore, Billerica, MA, USA) according to the manufacturer's instructions. The detection and analysis were made using the Luminex 100 IS system (Luminex, Austin, TX).

Statistical analysis

Statistical analysis was performed using the GraphPad Prism 6 software (Graph-Pad Software, Inc., CA, USA). Quantitative data are presented as mean ± SD from three independent experiments unless otherwise stated. Comparisons between two groups were made with t-test followed by the Mann-Whitney test for nonparametric data or with Welch´s correction for parametric data. Comparisons of three groups were made using one-way ANOVA with the Kruskal-Wallis test followed by Dunn´s multiple comparisons test. Two-way ANOVA analyzed multiple comparisons with Tukey´s correction. p values ≤ 0.05 were considered as significant.

Acknowledgments

We thank Dr. Ian Mackenzie for the donation of the LUC4 OSCC cell. We also acknowledge the technicians Daniele Santi Ceolin and Patrícia de Sá Mortagua for their excellent technical assistance.

Conflict of Interest

The authors declare that they have no conflict of interest.

Funding

This work was supported by São Paulo Research Foundation (FAPESP, grant #2013/07245-9), Coordination for the Improvement of Higher Education Personnel (CAPES, scholarship to N.G.A.), and National Council for Scientific and Technological Development (CNPq, grant #424158/2016-7).

Authors contributions

Conception and design: C.O. Rodini. ***Development of methodology:*** N.G. Amôr, N.M. Lopes, R.F. Buzo, L.M. Saito, R. C. Ortiz. ***Analysis and interpretation of data:*** N.G. Amôr, C.O. Rodini. ***Manuscript writing:*** N.G. Amôr and C.O. Rodini.

References

1 Disis ML. Immune regulation of cancer. *J Clin Oncol* 2010; **28**: 4531-4538.

2 Knutson KL, Disis ML. Tumor antigen-specific T helper cells in cancer immunity and immunotherapy. *Cancer Immunol Immunother* 2005; **54**: 721-728.

3 Liu Y, Liang X, Dong W, Fang Y, Lv J, Zhang T *et al*. Tumor-Repopulating Cells Induce PD-1 Expression in CD8(+) T Cells by Transferring Kynurenine and AhR Activation. *Cancer Cell* 2018; **33**: 480-494.e487.

4 Barilla RM, Diskin B, Caso RC, Lee KB, Mohan N, Buttar C *et al*. Specialized dendritic cells induce tumor-promoting IL-10(+)IL-17(+) FoxP3(neg) regulatory CD4(+) T cells in pancreatic carcinoma. *Nat Commun* 2019; **10**: 1424.

5 Thompson L. World Health Organization classification of tumours: pathology and genetics of head and neck tumours. *Ear Nose Throat J* 2006; **85**: 74.

6 Batlle E, Clevers H. Cancer stem cells revisited. *Nature medicine* (Review) 2017; **23**: 1124-1134.

7 He W, Liang B, Wang C, Li S, Zhao Y, Huang Q *et al*. MSC-regulated lncRNA MACC1-AS1 promotes stemness and chemoresistance through fatty acid oxidation in gastric cancer. *Oncogene* 2019; **38**: 4637-4654.

8 Wu RQ, Zhang DF, Tu E, Chen QM, Chen W. The mucosal immune system in the oral cavity-an orchestra of T cell diversity. *Int J Oral Sci* 2014; **6**: 125-132.

9 Moutsopoulos NM, Konkel JE. Tissue-Specific Immunity at the Oral Mucosal Barrier. *Trends Immunol* 2018; **39**: 276-287.

10 Zhou J, Wang XH, Zhao YX, Chen C, Xu XY, Sun Q *et al*. Cancer-Associated Fibroblasts Correlate with Tumor-Associated Macrophages Infiltration and Lymphatic Metastasis in Triple Negative Breast Cancer Patients. *J Cancer* 2018; **9**: 4635-4641.

11 Amor NG, de Oliveira CE, Gasparoto TH, Vilas Boas VG, Perri G, Kaneno R *et al*. ST2/IL-33 signaling promotes malignant development of experimental squamous cell carcinoma by decreasing NK cells cytotoxicity and modulating the intratumoral cell infiltrate. *Oncotarget* 2018; **9**: 30894-30904.

12 Biswas SK, Mantovani A. Macrophage plasticity and interaction with lymphocyte subsets: cancer as a paradigm. *Nature immunology* (Research Support, Non-U.S. Gov't Review) 2010; **11**: 889-896.

13 Christofori G. New signals from the invasive front. *Nature* (Research Support, Non-U.S. Gov't Review) 2006; **441**: 444-450.

14 Ye XZ, Xu SL, Xin YH, Yu SC, Ping YF, Chen L *et al*. Tumor-associated microglia/macrophages enhance the invasion of glioma stem-like cells via TGF-beta1 signaling pathway. *J Immunol* 2012; 189: 444-453.

15 Zhang S, Che D, Yang F, Chi C, Meng H, Shen J *et al*. Tumor-associated macrophages promote tumor metastasis via the TGF-beta/SOX9 axis in non-small cell lung cancer. *Oncotarget* 2017; **8**: 99801-99815.

16 Ehata S, Johansson E, Katayama R, Koike S, Watanabe A, Hoshino Y *et al*. Transforming growth factor-beta decreases the cancer-initiating cell population within diffuse-type gastric carcinoma cells. *Oncogene* 2011; **30**: 1693-1705.

17 Lonardo E, Hermann PC, Mueller MT, Huber S, Balic A, Miranda-Lorenzo I *et al*. Nodal/Activin signaling drives self-renewal and tumorigenicity of pancreatic cancer stem cells and provides a target for combined drug therapy. *Cell Stem Cell* 2011; **9**: 433-446.

18 Katsuno Y, Lamouille S, Derynck R. TGF-beta signaling and epithelial-mesenchymal transition in cancer progression. *Curr Opin Oncol* 2013; **25**: 76-84.

19 Zhang H, Liu L, Wang Y, Zhao G, Xie R, Liu C *et al*. KLF8 involves in TGF-beta-induced EMT and promotes invasion and migration in gastric cancer cells. *J Cancer Res Clin Oncol* 2013; **139**: 1033-1042.

20 Markowitz SD, Roberts AB. Tumor suppressor activity of the TGF-beta pathway in human cancers. *Cytokine Growth Factor Rev* 1996; 7: 93-102.

21 Wakefield LM, Roberts AB. TGF-beta signaling: positive and negative effects on tumorigenesis. *Curr Opin Genet Dev* 2002; **12**: 22-29.

22 Bierie B, Moses HL. Tumour microenvironment: TGFbeta: the molecular Jekyll and Hyde of cancer. *Nat Rev Cancer* 2006; **6**: 506-520.

23 Linde N, Casanova-Acebes M, Sosa MS, Mortha A, Rahman A, Farias E *et al*. Macrophages orchestrate breast cancer early dissemination and metastasis. *Nat Commun* 2018; **9**: 21.

24 Fan QM, Jing YY, Yu GF, Kou XR, Ye F, Gao L *et al*. Tumor-associated macrophages promote cancer stem cell-like properties via transforming growth factor-beta1-induced epithelial-mesenchymal transition in hepatocellular carcinoma. *Cancer Lett* 2014; **352**: 160-168.

25 Ronca R, Van Ginderachter JA, Turtoi A. Paracrine interactions of cancer-associated fibroblasts, macrophages and endothelial cells: tumor allies and foes. *Curr Opin Oncol* 2018; **30**: 45-53.

26 Wendt MK, Allington TM, Schiemann WP. Mechanisms of the epithelial-mesenchymal transition by TGF-beta. *Future Oncol* 2009; **5**: 1145-1168.

27 Laping NJ, Grygielko E, Mathur A, Butter S, Bomberger J, Tweed C *et al*. Inhibition of transforming growth factor (TGF)-beta1-induced extracellular matrix with a novel inhibitor of the TGF-beta type I receptor kinase activity: SB-431542. *Mol Pharmacol* 2002; **62**: 58-64.

28 DeNardo DG, Ruffell B. Macrophages as regulators of tumour immunity and immunotherapy. *Nat Rev Immunol* 2019; **19**: 369-382.

29 Pickup M, Novitskiy S, Moses HL. The roles of TGFbeta in the tumour microenvironment. *Nat Rev Cancer* 2013; **13**: 788-799.

30 Haque A, Moriyama M, Kubota K, Ishiguro N, Sakamoto M, Chinju A *et al*. CD206(+) tumor-associated macrophages promote proliferation and invasion in oral squamous cell carcinoma via EGF production. *Sci Rep* 2019; **9**: 14611.

31 Hagemann T, Robinson SC, Schulz M, Trumper L, Balkwill FR, Binder C. Enhanced invasiveness of breast cancer cell lines upon co-cultivation with macrophages is due to TNF-alpha dependent up-regulation of matrix metalloproteases. *Carcinogenesis* 2004; **25**: 1543-1549.

32 Wang R, Zhang J, Chen S, Lu M, Luo X, Yao S *et al*. Tumor-associated macrophages provide a suitable microenvironment for non-small lung cancer invasion and progression. *Lung Cancer* (Research Support, Non-U.S. Gov't) 2011; **74**: 188-196.

33 Locke M, Heywood M, Fawell S, Mackenzie IC. Retention of intrinsic stem cell hierarchies in carcinoma-derived cell lines. *Cancer Res* 2005; **65**: 8944-8950.

34 Tan L, Sui X, Deng H, Ding M. Holoclone forming cells from pancreatic cancer cells enrich tumor initiating cells and represent a novel model for study of cancer stem cells. *PLoS One* 2011; **6**: e23383.

35 Ferrer I, Verdugo-Sivianes EM, Castilla MA, Melendez R, Marin JJ, Munoz-Galvan S *et al*. Loss of the tumor suppressor spinophilin (PPP1R9B) increases the cancer stem cell population in breast tumors. *Oncogene* 2016; **35**: 2777-2788.

36 Guo L, Cheng X, Chen H, Chen C, Xie S, Zhao M *et al*. Induction of breast cancer stem cells by M1 macrophages through Lin-28B-let-7-HMGA2 axis. *Cancer Lett* 2019; **452**: 213-225.

37 Sansone P, Storci G, Tavolari S, Guarnieri T, Giovannini C, Taffurelli M *et al*. IL-6 triggers malignant features in mammospheres from human ductal breast carcinoma and normal mammary gland. *J Clin Invest* 2007; **117**: 3988-4002.

38 Ginestier C, Liu S, Diebel ME, Korkaya H, Luo M, Brown M *et al*. CXCR1 blockade selectively targets human breast cancer stem cells in vitro and in xenografts. *J Clin Invest* 2010; **120**: 485-497.

39 Qiao J, Liu Z, Dong C, Luan Y, Zhang A, Moore C *et al*. Targeting Tumors with IL-10 Prevents Dendritic Cell-Mediated CD8(+) T Cell Apoptosis. *Cancer Cell* 2019; **35**: 901-915.e904.

40 Easom NJW, Stegmann KA, Swadling L, Pallett LJ, Burton AR, Odera D *et al*. IL-15 Overcomes Hepatocellular Carcinoma-Induced NK Cell Dysfunction. *Front Immunol* 2018; **9**: 1009.

41 Graham GJ, Wright EG, Hewick R, Wolpe SD, Wilkie NM, Donaldson D *et al*. Identification and characterization of an inhibitor of haemopoietic stem cell proliferation. *Nature* 1990; **344**: 442-444.

42 Luo X, Yu Y, Liang A, Xie Y, Liu S, Guo J *et al*. Intratumoral expression of MIP-1beta induces antitumor responses in a pre-established tumor model through chemoattracting T cells and NK cells. *Cell Mol Immunol* 2004; **1**: 199-204.

43 Qian BZ, Pollard JW. Macrophage diversity enhances tumor progression and metastasis. *Cell* 2010; **141**: 39-51.

44 Safina A, Vandette E, Bakin AV. ALK5 promotes tumor angiogenesis by upregulating matrix metalloproteinase-9 in tumor cells. *Oncogene* 2007; **26**: 2407-2422.

45 Batlle R, Andres E, Gonzalez L, Llonch E, Igea A, Gutierrez-Prat N *et al*. Regulation of tumor angiogenesis and mesenchymal-endothelial transition by p38alpha through TGF-beta and JNK signaling. *Nat Commun* 2019; **10**: 3071.

46 Geng L, Chaudhuri A, Talmon G, Wisecarver JL, Wang J. TGF-Beta suppresses VEGFA-mediated angiogenesis in colon cancer metastasis. *PLoS One* 2013; **8**: e59918.

47 Mackenzie IC. Growth of malignant oral epithelial stem cells after seeding into organotypical cultures of normal mucosa. *J Oral Pathol Med* 2004; **33**: 71-78.

Figure legends

Fig.1. Both subpopulations founded in LUC4 cell line recruited macrophages into the TME. Male NOD/SCID mice were inoculated in the tongue with 5 x 10^3 of Epi-CSC or EMT-CSC. After 60 days, the tongues were collected and submitted to enzymatic digestion for leukocyte recovery. **a** Dot plots showing the gating strategy for the identification of tumor-associated macrophages. Graphics showing the percentage of **b** total macrophages ($CD11b^+F4/80^+$), **c** M1 macrophages ($CD80^+$), and **d** M2 macrophages ($CD206^+$). Quantitative data are mean ± SD. Data are representative of two independent experiments.

Fig. 2. Macrophages did not alter the invasive pattern of CSC, although increased their capacity to invade matrix *in vitro*. $CD44^{High}ESA^{High}$ (Epi-CSC) and $CD44^{High}ESA^{Low}$ (EMT-CSC) LUC4 cells were sorted and plated using the n3D bioprinting technology. 20,000 cells were plated alone (monoculture) or with 15 % of macrophages (co-culture) and allowed to invade Matrigel® matrix for 21 days. **a** Photomicrographs from the 3D structure formed by Epi-CSC and EMT-CSC

cultured alone or associated with macrophages. x4 magnification. Scale bar = 200 µm. Graphics showing the quantification of invasion of **b** Epi-CSC and **c** EMT-CSC in monoculture or co-cultured with macrophages. Data are shown as mean ± SD from three independent experiments performed in triplicate. *$p < 0.05$; **$p < 0.01$; ***$p < 0.001$.

Fig. 3. Macrophages induce EMT in Epi-CSC cells. 10,000 cells of **a** Epi-CSC and **b** EMT-CSC subpopulation were plated in 48-well plates with normal medium (RM+) or with macrophage-derived CM. Proliferation was assessed by EdU incorporation. Also, cells were plated at 5 x 10^2 cells/3 mL in a 6-well plate for colony morphology assay. **c** Photo of the colonies. Graphics showing the **d** total number of colonies, and the frequency of each colony morphology observed in **e** Epi-CSC and **f** EMT-CSC. Data are shown as mean ± SD from three independent experiments performed in triplicate. *$p < 0.05$; **$p < 0.01$.

Fig. 4. Macrophages increased the migration of EMT-CSC. 500,000 cells of Epi- and EMT-CSC were plated in a 12-well plate. After 24 h, proliferation was inhibited using 10 µg/mL of mitomycin C. The scratch was made using a 1,000µL pipette tip and the medium was replaced by normal medium (RM+) or CM obtained from macrophages. Cells were maintained for 72 h and the percentage of migration assessed each 24 h. **a** Photomicrographs of the gaps. x10 magnification. Scale bar = 100 µm. Graphics of the quantification of the gap closure of **b** Epi-CSC and **c** EMT-CSC. Data are shown as mean ± SD from three independent experiments performed in triplicate. *$p < 0.05$.

Fig. 5. Macrophages influenced cytokine and chemokine production of Epi-CSC. 20,000 Epi-CSC or EMT-CSC were plated alone (monoculture) or with 15 % of macrophages (co-culture) using the n3D bioprinting technology. The cultures were maintained for 72 h without media changing, and the supernatant was collected and stored with protease inhibitor. Cytokine secretion was assessed using the Milliplex MAP kit. Data are shown as mean ± SD from three independent experiments, performed in five replicates. *$p < 0.05$; **$p < 0.01$.

Fig. 6. TGF-β mediated macrophage-induced invasion in Epi-CSC. 20,000 Epi-CSC cells were plated with 15 % of macrophages. The cultures were immediately treated with the TGF-β signaling inhibitor, SB431542, and allowed to invade Matrigel® matrix for three days. **a** Photomicrographs from the 3D structure formed by Epi-CSC cultured with or without TGF-β blockage. x4 magnification. Scale bar = 200 µm. **b** Graphic showing the quantification of invasion of Epi-CSC co-cultured with macrophages. The supernatant of the cultures was collected and analyzed with the Milliplex MAP kit. **c** Graphic showing VEGF concentration. Data are shown as mean ± SD from three independent experiments performed in triplicate. *$p < 0.05$; **$p < 0.01$.

Fig. S1. Gate strategy and photomicrographs (x 4 magnification, scale bar = 200 µm) of the subpopulations $CD44^{High}ESA^{High}$ (Epi-CSC) and $CD44^{High}ESA^{Low}$ (EMT-CSC) sorted from the OSCC cell line LUC4.

Fig. S2. Macrophages did not alter the pattern of invasion displayed by both CSC subclones. Epi- and EMT-CSC LUC4 cells were plated using the n3D bioprinting

technology. 20,000 Epi-CSC or EMT-CSC were plated alone (monoculture) or with 15 % of macrophages (co-culture) and allowed to invade Matrigel® matrix for 21 days without media changing. Photomicrographs from the 3D structure formed by Epi-CSC and EMT-CSC. X 4 magnification. Scale bar = 200 µm.

Fig. S3. Analysis of the cytokine secretion in cultures of Epi-CSC and EMT-CSC alone or associated with macrophages. Epi- and EMT-CSC LUC4 cells were sorted for 3D culture using the n3D bioprinting technology. 20,000 Epi-CSC or EMT-CSC were plated alone (monoculture) or with 15 % of macrophages (co-culture) and maintained for 72 h without media changing. After that period, the supernatant of the cultures was collected and stored with protease inhibitor. Cytokine secretion was assessed using the Milliplex MAP kit. Data are shown as mean ± SD from three independent experiments, performed in five replicates.

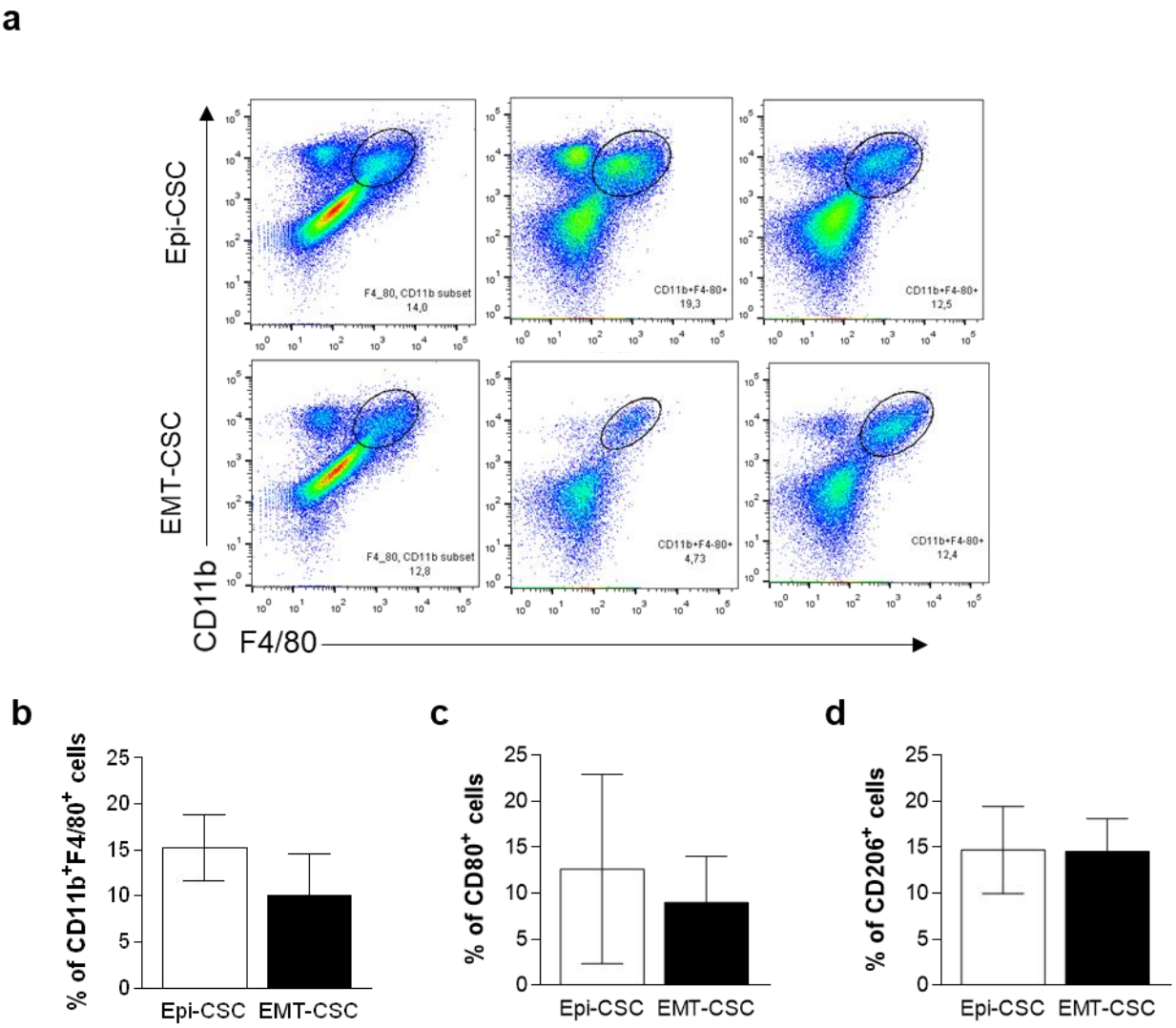
a
Epi-CSC
EMT-CSC
CD11b
F4/80
F4_80, CD11b subset
14,0
CD11b+F4-80+
19,3
CD11b+F4-80+
12,5
F4_80, CD11b subset
12,8
CD11b+F4-80+
4,73
CD11b+F4-80+
12,4
b
% of CD11b+F4/80+ cells
c
% of CD80+ cells
d
% of CD206+ cells
Epi-CSC
EMT-CSC

Fig. 1

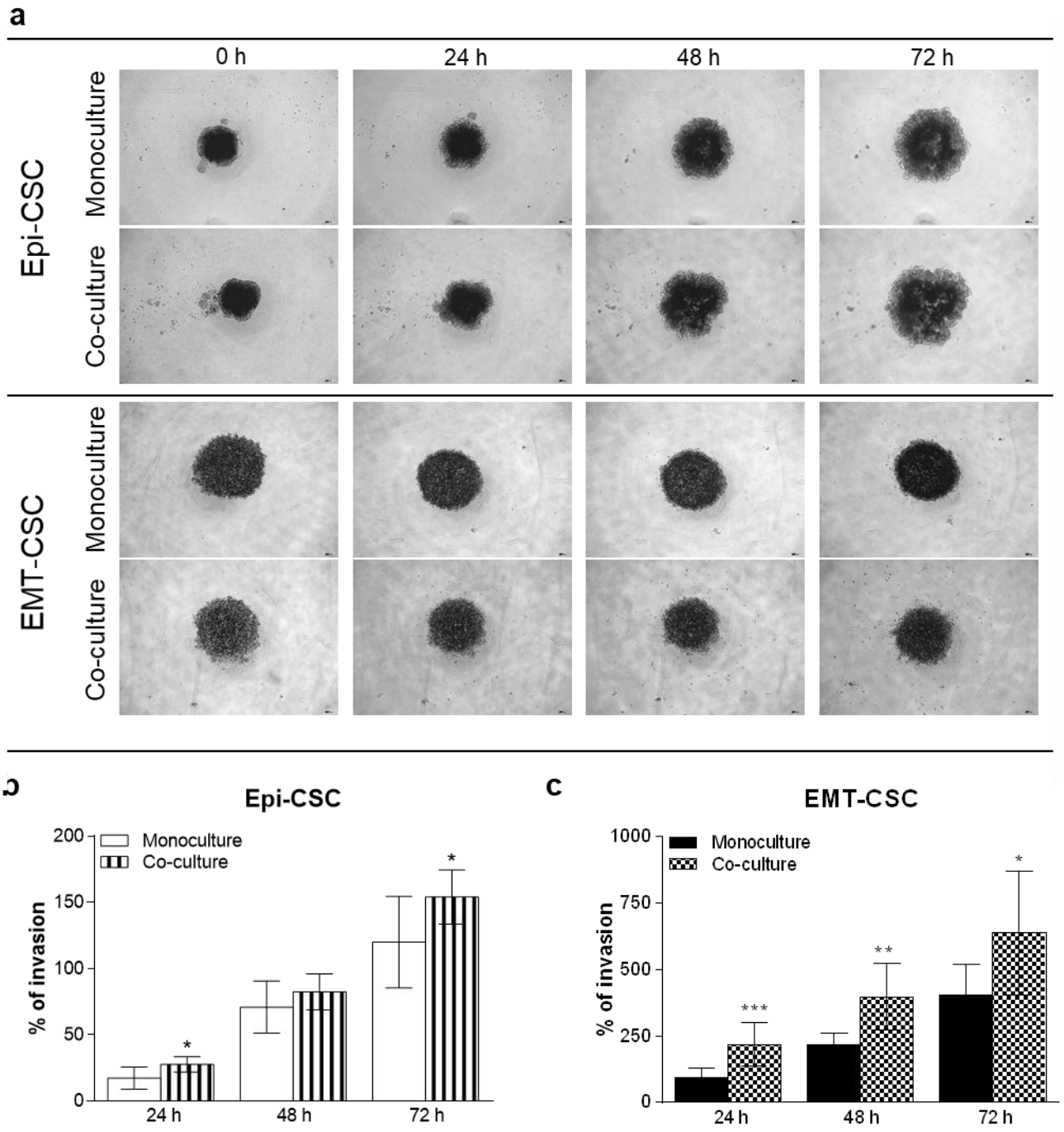
a
0 h
24 h
48 h
72 h
Epi-CSC
Monoculture
Co-culture
EMT-CSC
Monoculture
Co-culture
b
Epi-CSC
Monoculture
Co-culture
% of invasion
200
150
100
50
0
24 h
48 h
72 h
c
EMT-CSC
Monoculture
Co-culture
% of invasion
1000
750
500
250
0
24 h
48 h
72 h

Fig. 2

Fig. 2

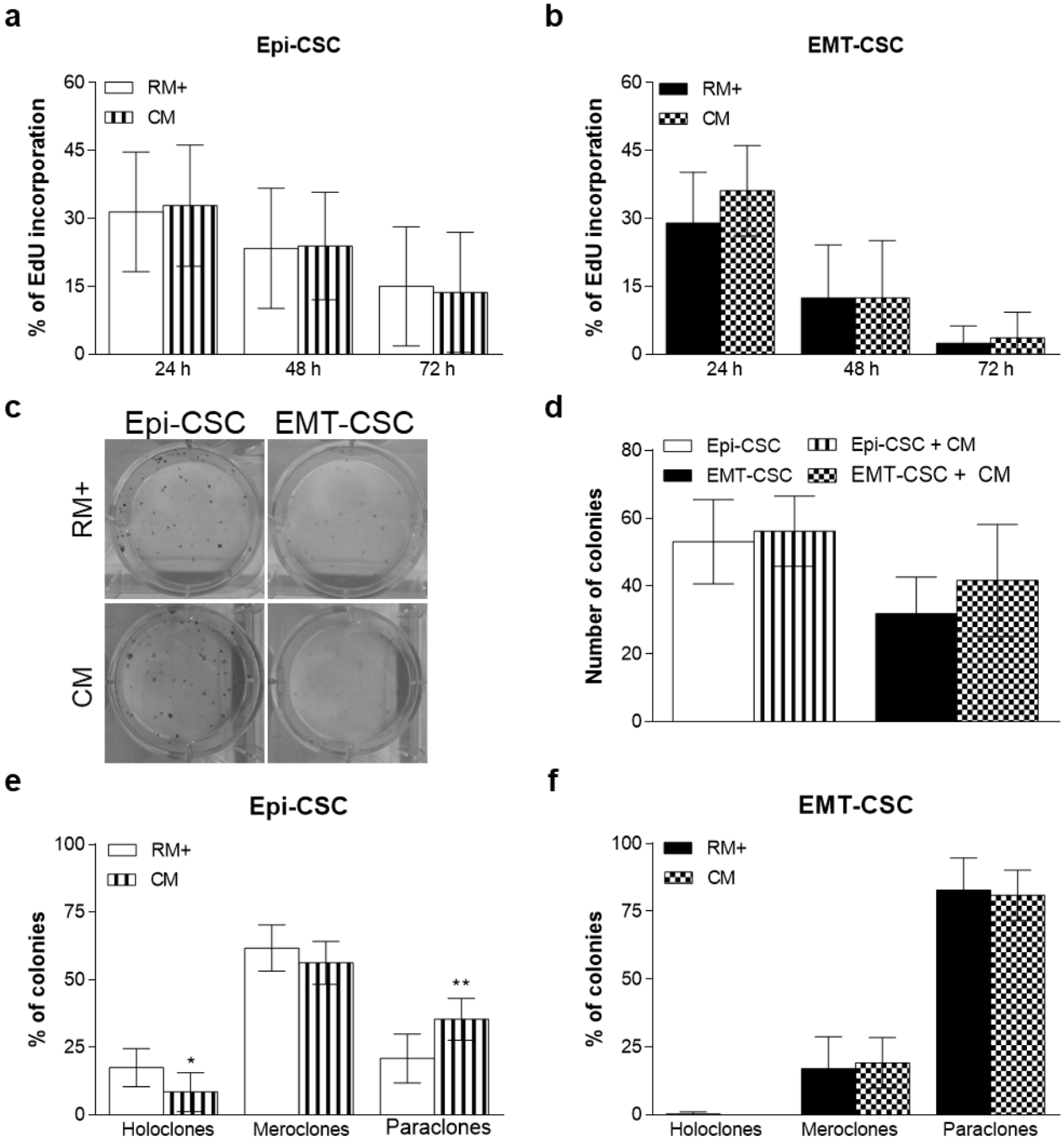
a
Epi-CSC
RM+
CM
% of EdU incorporation
60
45
30
15
0
24 h
48 h
72 h
b
EMT-CSC
RM+
CM
% of EdU incorporation
60
45
30
15
0
24 h
48 h
72 h
c
Epi-CSC
EMT-CSC
RM+
CM
d
Epi-CSC
Epi-CSC + CM
EMT-CSC
EMT-CSC + CM
Number of colonies
80
60
40
20
0
e
Epi-CSC
RM+
CM
% of colonies
100
75
50
25
0
*
**
Holoclones
Meroclones
Paraclones
f
EMT-CSC
RM+
CM
% of colonies
100
75
50
25
0
Holoclones
Meroclones
Paraclones

Fig. 3

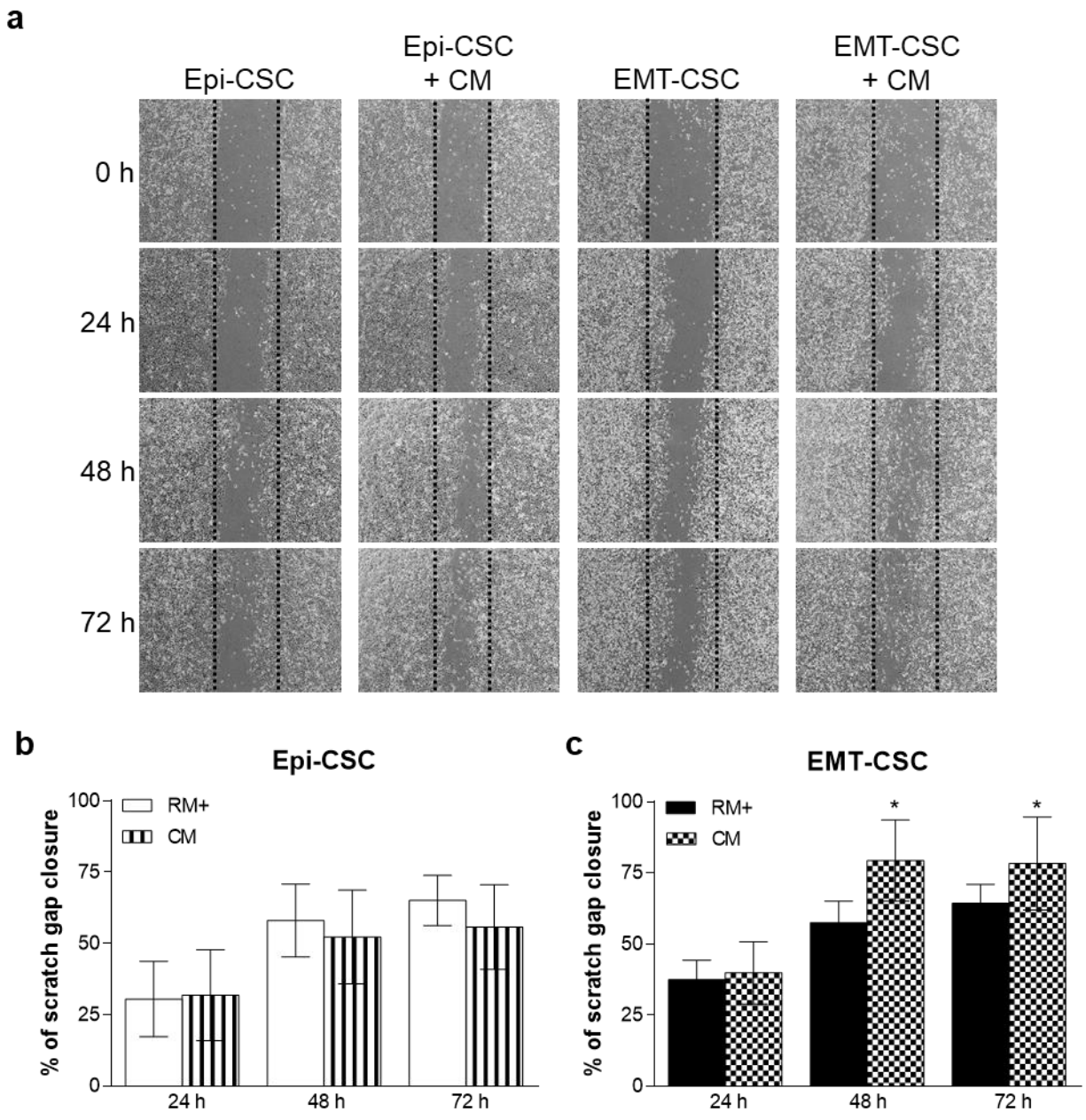
a
Epi-CSC
Epi-CSC + CM
EMT-CSC
EMT-CSC + CM
0 h
24 h
48 h
72 h
b
Epi-CSC
RM+
CM
% of scratch gap closure
100
75
50
25
0
24 h
48 h
72 h
c
EMT-CSC
RM+
CM
% of scratch gap closure
100
75
50
25
0
*
*
24 h
48 h
72 h

Fig. 4

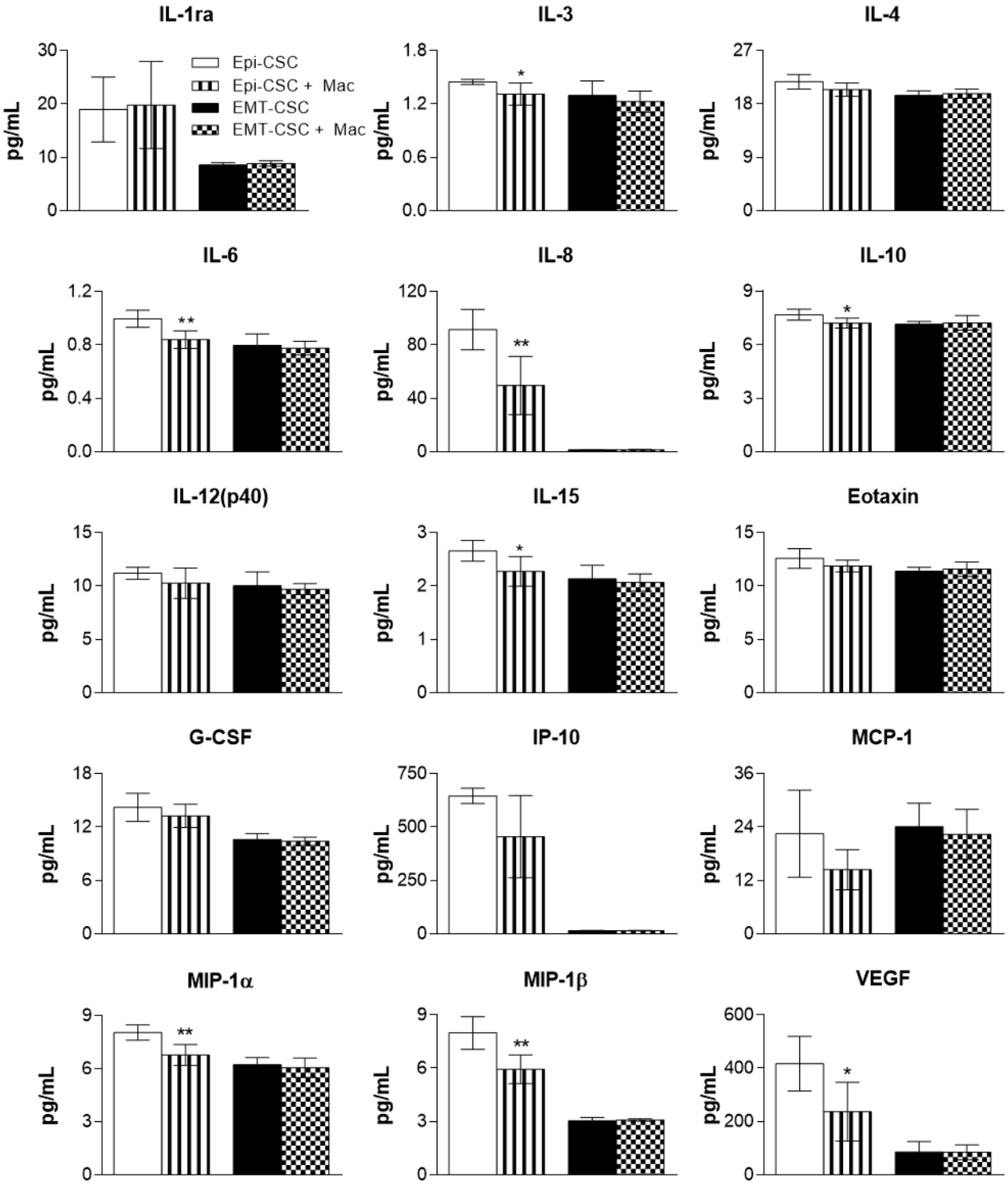
IL-1ra
IL-3
IL-4
IL-6
IL-8
IL-10
IL-12(p40)
IL-15
Eotaxin
G-CSF
IP-10
MCP-1
MIP-1α
MIP-1β
VEGF
Epi-CSC
Epi-CSC + Mac
EMT-CSC
EMT-CSC + Mac
pg/mL

Fig. 5

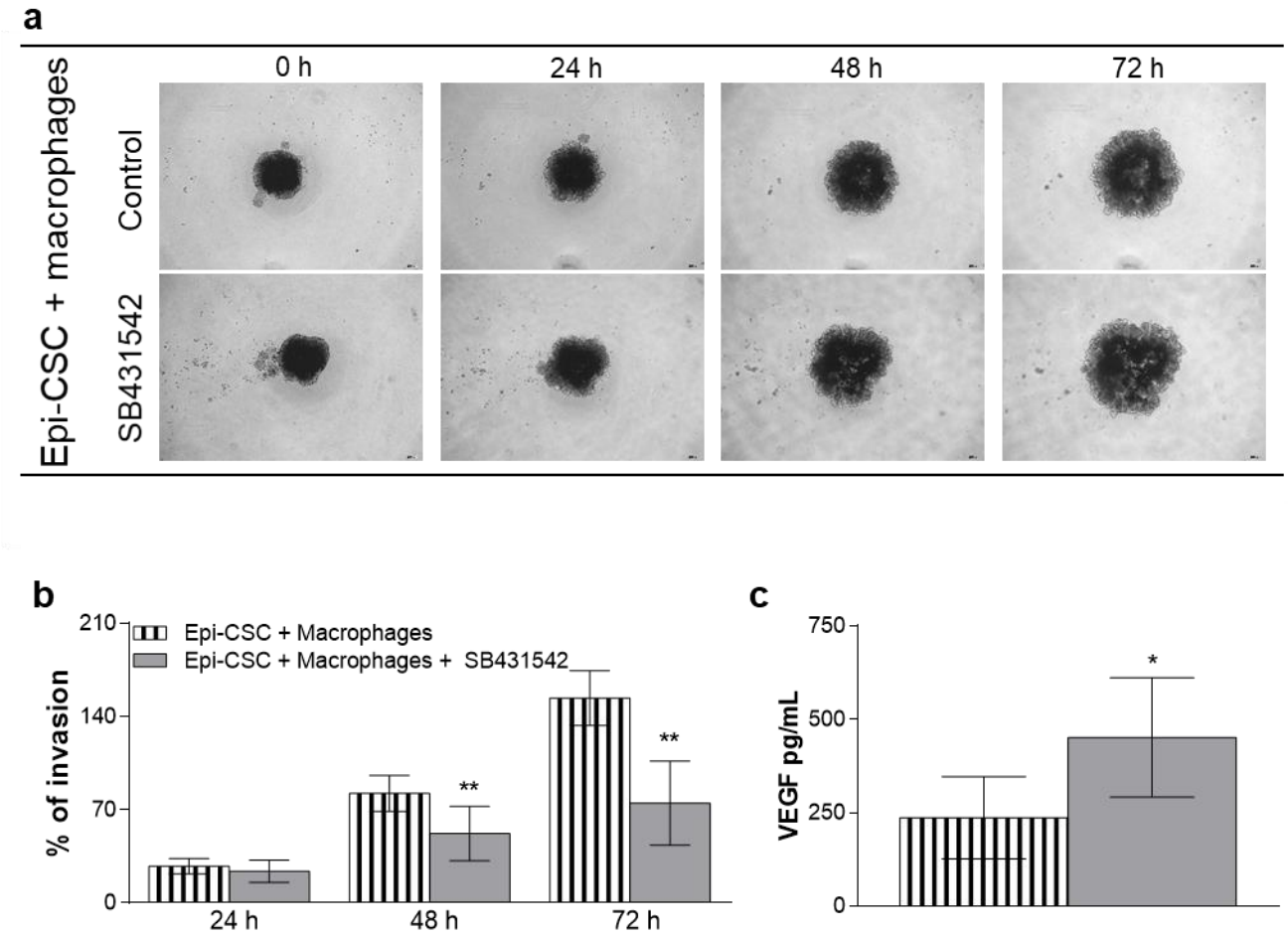
a
Epi-CSC + macrophages
Control
SB431542
0 h
24 h
48 h
72 h
b
% of invasion
210
140
70
0
Epi-CSC + Macrophages
Epi-CSC + Macrophages + SB431542
**
**
24 h
48 h
72 h
c
VEGF pg/mL
750
500
250
0
*

Fig, 6

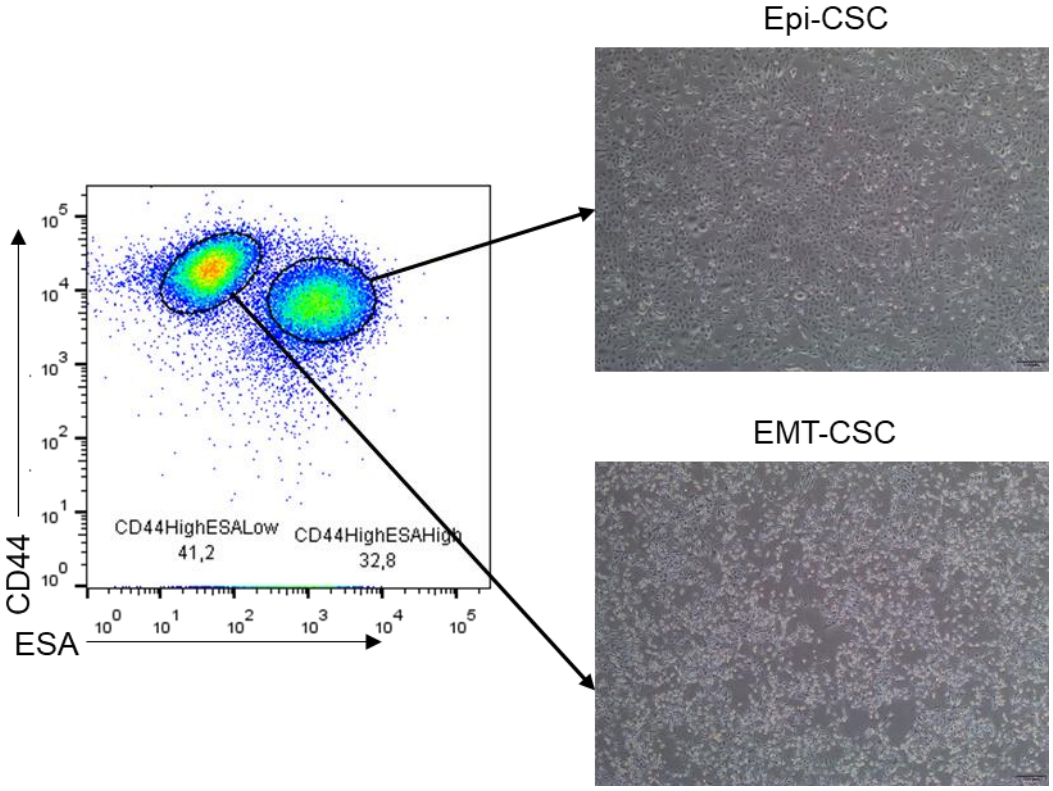
Epi-CSC
EMT-CSC
CD44
ESA
CD44HighESALow
41,2
CD44HighESAHigh
32,8

Fig. S1

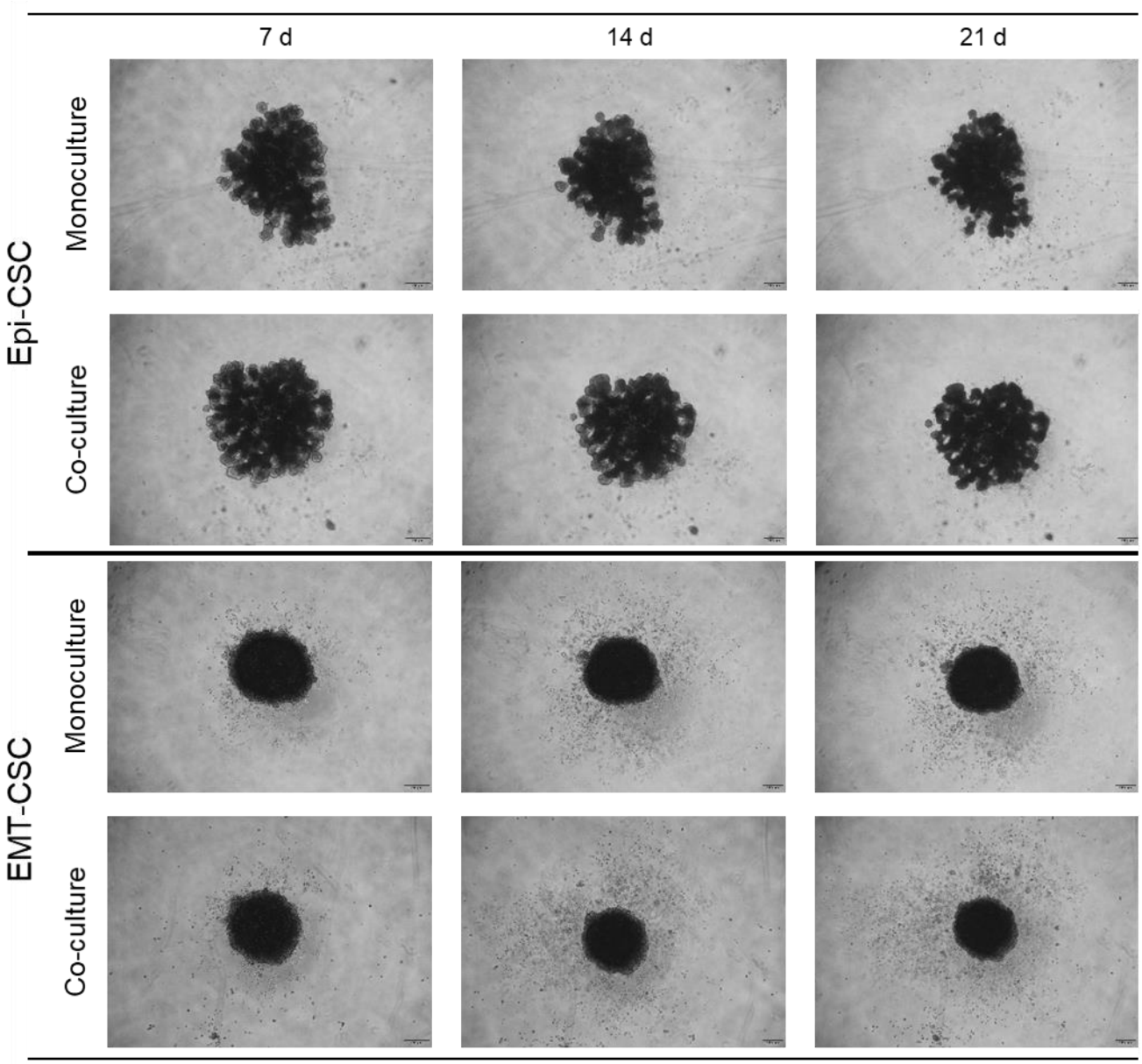
7 d
14 d
21 d
Epi-CSC
Monoculture
Co-culture
EMT-CSC
Monoculture
Co-culture

Fig. S2

a

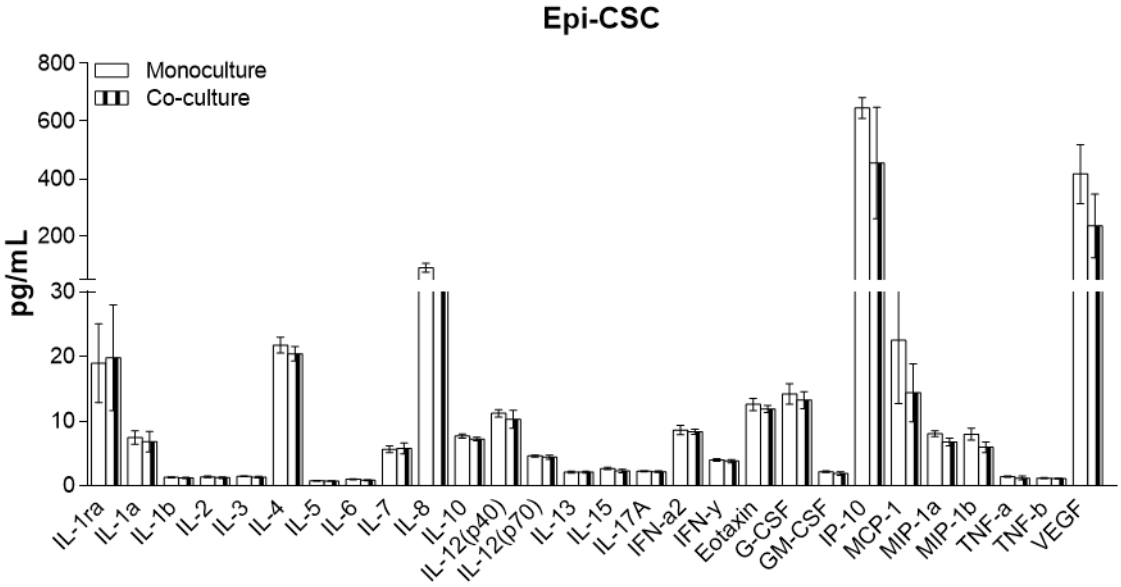
Epi-CSC
Monoculture
Co-culture
pg/mL
800
600
400
200
30
20
10
0
IL-1ra
IL-1a
IL-1b
IL-2
IL-3
IL-4
IL-5
IL-6
IL-7
IL-8
IL-10
IL-12(p40)
IL-12(p70)
IL-13
IL-15
IL-17A
IFN-a2
IFN-y
Eotaxin
G-CSF
GM-CSF
IP-10
MCP-1
MIP-1a
MIP-1b
TNF-a
TNF-b
VEGF

b

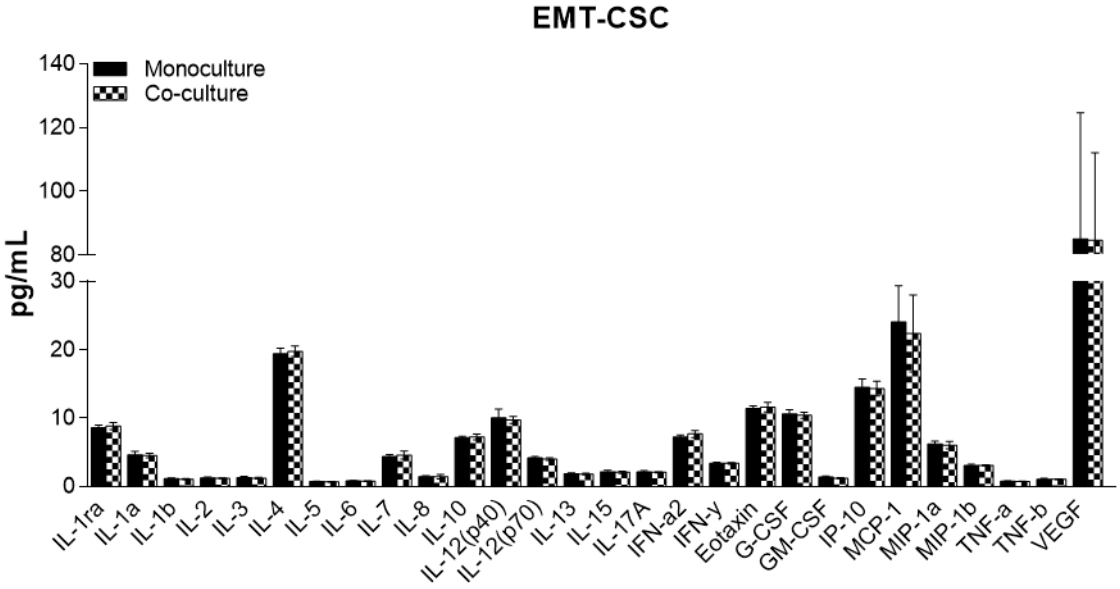
EMT-CSC
Monoculture
Co-culture
pg/mL
140
120
100
80
30
20
10
0
IL-1ra
IL-1a
IL-1b
IL-2
IL-3
IL-4
IL-5
IL-6
IL-7
IL-8
IL-10
IL-12(p40)
IL-12(p70)
IL-13
IL-15
IL-17A
IFN-a2
IFN-y
Eotaxin
G-CSF
GM-CSF
IP-10
MCP-1
MIP-1a
MIP-1b
TNF-a
TNF-b
VEGF

Fig. S3

3 Discussion

In the present thesis, we focused on the identification and understanding of tumor diversity and how tumor microenvironment can modulate intra-tumoral heterogeneity in OSCC. Tumor heterogeneity has been revealed as critical for metastasis, drug responses, and clinical outcomes (MARUSYK; ALMENDRO; POLYAK, 2012). In head and neck cancers, Prince et al. (PRINCE; SIVANANDAN; KACZOROWSKI; WOLF et al., 2007) have demonstrated the existence of cancer cells with distinct tumor-initiating capacities. When xenografted into immunocompromised mice, only $CD44^{+}$ cells were able to generate tumors with similar characteristics to the original one and restore intra-tumoral heterogeneity (PRINCE; SIVANANDAN; KACZOROWSKI; WOLF et al., 2007). More importantly, using CD44 associated with ESA (EpCAM, epithelial marker) and ALDH1 (CSC marker), Biddle et al. (BIDDLE; LIANG; GAMMON; FAZIL et al., 2011) have demonstrated the existence of four different subclones of CSC in OSCC cell lines and described the dynamics that regulate the transition between them. Here, we described the behavior of two of these subpopulations in the LUC4 cell line, $CD44^{High}ESA^{High}$, named Epi-CSC; and $CD44^{High}ESA^{Low}$, named EMT-CSC, and demonstrated that the tumorigenic ability of LUC4 cells resided mostly in the Epi-CSC phenotype. In addition, we provided evidence that macrophages could interfere in the balance of Epi/EMT-CSC *in vitro* and that TGF-β possibly mediated this modulation.

Studies on CSC have correlated SC properties with the morphology of colonies generated from single cells (LOCKE; HEYWOOD; FAWELL; MACKENZIE, 2005; PAPINI; CECCHETTI; CAMPANI; FITZGERALD et al., 2003), and CSC was demonstrated to reside mostly in holoclones (FERRER; VERDUGO-SIVIANES; CASTILLA; MELENDEZ et al., 2016; TAN; SUI; DENG; DING, 2011; TIECHE; GAO; BUHRER; HOBI et al., 2019). Our results showed that the Epi-CSC phenotype formed considerably more holoclones than EMT-CSC, which in turn formed significant more percentages of paraclones, thus allowing us to correlate Epi-CSC with tumor-initiating cells and paraclone formation with EMT state. However, it remained unclear what contributes to the development and maintenance of each cell subclone. The presence of TAMs is frequently detected at the invasive front of aggressive cancers (BISWAS; MANTOVANI, 2010), where tumor cells undergoing EMT are found

(CHRISTOFORI, 2006), suggesting a positive correlation between TAM and EMT. To investigate the role of macrophages on Epi/EMT-CSC balance, LUC4 cells were indirectly co-cultured with macrophages. Our results showed that macrophages increased the frequency of EMT-CSC phenotype on LUC4 cells whole population. When cultivated in the presence of conditioned medium (CM) from macrophages, the colony formation ability of LUC4 cells was not affected in both CSC phenotypes; however, CM decreased the holoclone frequency of Epi-CSC cells and increased the percentage of paraclones. In contrast with our work, macrophages have been demonstrated to increase CSC properties in different types of cancer (FAN; JING; YU; KOU et al., 2014; GUO; CHENG; CHEN; CHEN et al., 2019). Our results might be explained by the concomitant increased frequency of paraclones observed in Epi-CSC cultivated with CM, indicating EMT.

Despite the well-described migration capacity of carcinoma cells in EMT (THIERY; ACLOQUE; HUANG; NIETO, 2009), EMT-CSC migrated at the same ratio as Epi-CSC. However, EMT-CSC cultivated with macrophages-derived CM migrate more than EMT-CSC cultivated in normal medium, supporting the notion that macrophages promote tumor aggressiveness (BISWAS; MANTOVANI, 2010). Regarding invasive behavior, Epi-CSC and EMT-CSC invaded very differently. While Epi-CSC invaded Matrigel matrix collectively, that means as a compact group of cells, EMT-CSC invaded as single cells. A considerable amount of work pointed single-cell invasion, typically observed in carcinoma cells in EMT, as essential for cancer metastasis (DAI; YANG; DENG; CHEN et al., 2019; WANG; WANG; SUN; SUN et al., 2017; ZHANG; ZHENG; ZHOU; LI et al., 2018). However, tumor border of carcinomas is frequently dominated by multicellular agglomerates and, consequently, there is a predominance of collective cell invasion (CLARK; VIGNJEVIC, 2015). Additionally, the presence of tumor cell emboli in lymph and blood vessels suggests that collective invasion may be necessary for tumor spread (HART, 2009). Again, macrophages contributed for tumor aggressive behavior by increasing the ability of both subpopulations, Epi-CSC and EMT-CSC, to invade matrix. Although we did not analyze the presence of metalloproteinases in the cultures, this increased invasive behavior might be probably explained by macrophages-derived

metalloproteinases already described in the breast (HAGEMANN; ROBINSON; SCHULZ; TRUMPER et al., 2004) and lung (WANG; ZHANG; CHEN; LU et al., 2011).

Due to the ability of macrophages to modulate microenvironment, we also investigated the role of macrophages in affecting the cytokine and chemokine balance of tumor cells *in vitro*. Despite the fewer amount of most analytes detected in the supernatant from the cultures, we could detect macrophage´s influence on Epi-CSC cytokine production. When cultivated along with macrophages, Epi-CSC produced less IL-3, IL-6, IL-8, IL-10, IL-15, MIP-1α (macrophage inflammatory protein), MIP-1β, and VEGF. Opposite functions regarding tumor modulation were described for all cytokines listed above. IL-6 and IL-8 were described as positive regulators of the stemness properties of breast cancer cells (GINESTIER; LIU; DIEBEL; KORKAYA et al., 2010; SANSONE; STORCI; TAVOLARI; GUARNIERI et al., 2007). On the other hand, IL-6, IL-10, IL-15, MIP-1α, and MIP-1β are involved with activation and recruitment of crucial immune cells, such as NK (natural killer) cells and $CD8^+$ T lymphocytes in several diseases, including cancer (EASOM; STEGMANN; SWADLING; PALLETT et al., 2018; FISHER; CHEN; SKITZKI; MUHITCH et al., 2011; GRAHAM; WRIGHT; HEWICK; WOLPE et al., 1990; LUO; YU; LIANG; XIE et al., 2004; QIAO; LIU; DONG; LUAN et al., 2019). It suggested that macrophages, besides inducing EMT, also might affect immune cells activation in tumor microenvironment promoting cancer progression.

Macrophages are a well-known producer of VEGF, which in turn induce angiogenesis and promote tumor progression and dissemination in different types of neoplasia (QIAN; POLLARD, 2010). However, we detected an accentuated reduction of that protein when CSC were co-cultured with macrophages. Moreover, when we inhibited the TGF-β signaling, the VEGF production was restored, suggesting a possible compensatory mechanism exerted by both cytokines. We suggest that, since TGF-β promotes angiogenesis in the tumor microenvironment (BATLLE; ANDRES; GONZALEZ; LLONCH et al., 2019; SAFINA; VANDETTE; BAKIN, 2007), blocking that signaling pathway might trigger a compensatory production of VEGF. The published data regarding the negative correlation between TGF-β and VEGF production is profoundly scarce.

A study with colon cancer demonstrated an inverse correlation between TGF-β and VEGF in paraffine-embedded samples (GENG; CHAUDHURI; TALMON; WISECARVER et al., 2013). The authors showed that TGF-β induced ubiquitination and degradation of VEGF in a PKA- (protein kinase A) and Smad3-dependent pathway (GENG; CHAUDHURI; TALMON; WISECARVER et al., 2013). Therefore, further molecular studies focusing on the intracellular molecules and pathways that might be involved in TGF-β/VEGF modulation are necessary. Collectively, our results showed that macrophages induced preferentially EMT rather than CSC properties. More importantly, that modulation was probably mediated by TGF-β, and blocking that pathway altered the invasive behavior of cancer cells and VEGF production *in vitro*.

To finally determine whether Epi-CSC and EMT-CSC have tumor-initiating capacity, both subpopulations were xenografted into the tongues of NOD/SCID mice. As expected, the Epi-CSC phenotype effectively generated tumors in all xenografted mice. On the other hand, only 75% of mice inoculated with the EMT-CSC phenotype formed tumors. Knaack et al. (KNAACK; LENK; PHILIPP; MIARKA et al., 2018) obtained similar results; they observed efficient tumor formation when inoculating holoclone in immunocompromised mice and only a few animals inoculated with paraclones formed tumors. Moreover, at the end of the experimental period, the tumors generated by Epi-CSC cells were considerably larger than the ones formed by EMT-CSC, probably due to its high proliferative activity. Although we did not analyze ALDH1 expression on EMT-CSC cells, Biddle et al. (BIDDLE; LIANG; GAMMON; FAZIL et al., 2011) demonstrated that some subclones of $CD44^{High}ESA^{Low}$ cells did not express ALDH-1 and do not undergo MET, thus cannot generate tumor. Once normal epithelial SC are responsible for restoring tissue heterogeneity (MCCAFFREY; MACARA, 2011), we assumed that CSC should also be able to reestablish tumor heterogeneity. Indeed, analysis of tumor cells recovered from the tongue of the mice revealed a heterogenous pattern of cells regarding CD44 and ESA expression. Tumors recovered from Epi-CSC-xenografted mice were more heterogeneous than the tumors recovered from EMT-CSC inoculated mice. Similar results were obtained in studies with breast cancer (AL-HAJJ; WICHA; BENITO-HERNANDEZ; MORRISON et al., 2003), where the authors

documented a high capacity of tumorigenic $ESA^+CD44^+CD24^-$ cells in generating other tumorigenic cells and also non-tumorigenic ones. The lower tumor-initiating capacity of EMT-CSC cells is probably due to its arrestment in the EMT state. However, we must highlight that the tumor digestion process can significantly affect the expression of epitopes; thus, further studies should be conducted to unhesitatingly affirm the ability of these two subpopulations to reestablish intra-tumoral heterogeneity. Altogether, our results suggested that the Epi-CSC cells rather than EMT-CSC undergo processes analogous to normal epithelial stem-cells. In accordance with our work, $CD44^+ESA^+$ cancer cells were also demonstrated to be highly tumorigenic and described as cancer stem cells in pancreatic (LI; HEIDT; DALERBA; BURANT et al., 2007) and breast cancer (AL-HAJJ; WICHA; BENITO-HERNANDEZ; MORRISON et al., 2003).

Personalized antitumor therapies considering intrinsic characteristics from each patient have been revealed as a promising approach to improve cancer treatment, especially immunotherapies (KWONG; DAVIES, 2014; SATHYANARAYANAN; NEELAPU, 2015). Before we identified what is transformed at the molecular level or even dissected signaling pathways and test new drugs, we must understand the behavior of the transformed cells and how they adapt to frequently modifying environments. Despite the knowledge that carcinoma cells in EMT are the most aggressive due to their ability to invade and migrate (THIERY; ACLOQUE; HUANG; NIETO, 2009), our results suggest that the Epi-CSC are the more tumorigenic subclone and should then be considered as a potential target for future therapies. Additionally, macrophages and TGF-β seem to play a critical role in modulating EMT on Epi-CSC which might increase the metastasis rate *in vivo*. In summary, the present study highlighted the significant contribution of tumor heterogeneity and stroma components for cancer progression.

4 Conclusions

In the present work we showed that:

1. The OSCC cell line, LUC4, is composed of two very distinguishable phenotypes regarding the CSC marker, CD44, and the epithelial marker, ESA: $CD44^{High}ESA^{High}$ (Epi-CSC) and $CD44^{High}ESA^{Low}$ (EMT-CSC);

2. The tumorigenic property of LUC4 cells resides in the Epi-CSC phenotype, and the EMT-CSC fraction is probably arrested in the EMT state, thus not able to revert their phenotype and generate tumor efficiently;

3. Macrophages induce EMT in the Epi-CSC phenotype and increased the motility of EMT-CSC;

4. TGF-β mediates the modulation effects of macrophages on CSC in OSCC;

5. Inhibition of TGF-β signaling alters the VEGF production showing a novel correlation between TGF-β and VEGF on tumor context.

References

AL-HAJJ, M.; WICHA, M. S.; BENITO-HERNANDEZ, A.; MORRISON, S. J. *et al.* Prospective identification of tumorigenic breast cancer cells. **Proc Natl Acad Sci U S A**, 100, n. 7, p. 3983-3988, Apr 1 2003.

ALBERS, A. E.; CHEN, C.; KOBERLE, B.; QIAN, X. *et al.* Stem cells in squamous head and neck cancer. **Crit Rev Oncol Hematol**, 81, n. 3, p. 224-240, Mar 2012.

BATLLE, R.; ANDRES, E.; GONZALEZ, L.; LLONCH, E. *et al.* Regulation of tumor angiogenesis and mesenchymal-endothelial transition by p38alpha through TGF-beta and JNK signaling. **Nat Commun**, 10, n. 1, p. 3071, Jul 11 2019.

BIDDLE, A.; GAMMON, L.; LIANG, X.; COSTEA, D. E. *et al.* Phenotypic Plasticity Determines Cancer Stem Cell Therapeutic Resistance in Oral Squamous Cell Carcinoma. **EBioMedicine**, 4, p. 138-145, Feb 2016.

BIDDLE, A.; LIANG, X.; GAMMON, L.; FAZIL, B. *et al.* Cancer stem cells in squamous cell carcinoma switch between two distinct phenotypes that are preferentially migratory or proliferative. **Cancer Res**, 71, n. 15, p. 5317-5326, Aug 1 2011.

BIERIE, B.; MOSES, H. L. Transforming growth factor beta (TGF-beta) and inflammation in cancer. **Cytokine Growth Factor Rev**, 21, n. 1, p. 49-59, Feb 2010.

BISWAS, S. K.; MANTOVANI, A. Macrophage plasticity and interaction with lymphocyte subsets: cancer as a paradigm. **Nat Immunol**, 11, n. 10, p. 889-896, Oct 2010.

BLANPAIN, C.; HORSLEY, V.; FUCHS, E. Epithelial stem cells: turning over new leaves. **Cell**, 128, n. 3, p. 445-458, Feb 9 2007.

BONAVITA, E.; GALDIERO, M. R.; JAILLON, S.; MANTOVANI, A. Phagocytes as Corrupted Policemen in Cancer-Related Inflammation. **Adv Cancer Res**, 128, p. 141-171, 2015.

BONAVITA, E.; GENTILE, S.; RUBINO, M.; MAINA, V. *et al.* PTX3 is an extrinsic oncosuppressor regulating complement-dependent inflammation in cancer. **Cell**, 160, n. 4, p. 700-714, Feb 12 2015.

BRABLETZ, T.; JUNG, A.; SPADERNA, S.; HLUBEK, F. *et al.* Opinion: migrating cancer stem cells - an integrated concept of malignant tumour progression. **Nat Rev Cancer**, 5, n. 9, p. 744-749, Sep 2005.

BRUNA, A.; GREENWOOD, W.; LE QUESNE, J.; TESCHENDORFF, A. *et al.* TGFbeta induces the formation of tumour-initiating cells in claudinlow breast cancer. **Nat Commun**, 3, p. 1055, 2012.

CHRISTOFORI, G. New signals from the invasive front. **Nature**, 441, n. 7092, p. 444-450, May 25 2006. Research Support, Non-U.S. Gov't
Review.

CLARK, A. G.; VIGNJEVIC, D. M. Modes of cancer cell invasion and the role of the microenvironment. **Curr Opin Cell Biol**, 36, p. 13-22, Oct 2015.

CUFI, S.; VAZQUEZ-MARTIN, A.; OLIVERAS-FERRAROS, C.; MARTIN-CASTILLO, B. *et al.* Metformin against TGFbeta-induced epithelial-to-mesenchymal transition (EMT): from cancer stem cells to aging-associated fibrosis. **Cell Cycle**, 9, n. 22, p. 4461-4468, Nov 15 2010.

DAI, B. W.; YANG, Z. M.; DENG, P.; CHEN, Y. R. *et al.* HOXC10 promotes migration and invasion via the WNT-EMT signaling pathway in oral squamous cell carcinoma. **J Cancer**, 10, n. 19, p. 4540-4551, 2019.

DALAL, B. I.; KEOWN, P. A.; GREENBERG, A. H. Immunocytochemical localization of secreted transforming growth factor-beta 1 to the advancing edges of primary tumors and to lymph node metastases of human mammary carcinoma. **Am J Pathol**, 143, n. 2, p. 381-389, Aug 1993.

DENARDO, D. G.; RUFFELL, B. Macrophages as regulators of tumour immunity and immunotherapy. **Nat Rev Immunol**, 19, n. 6, p. 369-382, Jun 2019.

DRIESSENS, G.; BECK, B.; CAAUWE, A.; SIMONS, B. D. *et al.* Defining the mode of tumour growth by clonal analysis. **Nature**, 488, n. 7412, p. 527-530, Aug 23 2012.

EASOM, N. J. W.; STEGMANN, K. A.; SWADLING, L.; PALLETT, L. J. *et al.* IL-15 Overcomes Hepatocellular Carcinoma-Induced NK Cell Dysfunction. **Front Immunol**, 9, p. 1009, 2018.

EHATA, S.; JOHANSSON, E.; KATAYAMA, R.; KOIKE, S. *et al.* Transforming growth factor-beta decreases the cancer-initiating cell population within diffuse-type gastric carcinoma cells. **Oncogene**, 30, n. 14, p. 1693-1705, Apr 7 2011.

FAN, Q. M.; JING, Y. Y.; YU, G. F.; KOU, X. R. *et al.* Tumor-associated macrophages promote cancer stem cell-like properties via transforming growth factor-beta1-induced epithelial-mesenchymal transition in hepatocellular carcinoma. **Cancer Lett**, 352, n. 2, p. 160-168, Oct 1 2014.

FERRER, I.; VERDUGO-SIVIANES, E. M.; CASTILLA, M. A.; MELENDEZ, R. *et al.* Loss of the tumor suppressor spinophilin (PPP1R9B) increases the cancer stem cell population in breast tumors. **Oncogene**, 35, n. 21, p. 2777-2788, May 2016.

FIDLER, I. J.; KRIPKE, M. L. Metastasis results from preexisting variant cells within a malignant tumor. **Science**, 197, n. 4306, p. 893-895, Aug 26 1977.

FISHER, D. T.; CHEN, Q.; SKITZKI, J. J.; MUHITCH, J. B. *et al.* IL-6 trans-signaling licenses mouse and human tumor microvascular gateways for trafficking of cytotoxic T cells. **J Clin Invest**, 121, n. 10, p. 3846-3859, Oct 2011.

FUCHS, E.; RAGHAVAN, S. Getting under the skin of epidermal morphogenesis. **Nat Rev Genet**, 3, n. 3, p. 199-209, Mar 2002.

GENG, L.; CHAUDHURI, A.; TALMON, G.; WISECARVER, J. L. *et al.* TGF-Beta suppresses VEGFA-mediated angiogenesis in colon cancer metastasis. **PLoS One**, 8, n. 3, p. e59918, 2013.

GIANCOTTI, F. G.; TARONE, G. Positional control of cell fate through joint integrin/receptor protein kinase signaling. **Annu Rev Cell Dev Biol**, 19, p. 173-206, 2003.

GINESTIER, C.; LIU, S.; DIEBEL, M. E.; KORKAYA, H. *et al.* CXCR1 blockade selectively targets human breast cancer stem cells in vitro and in xenografts. **J Clin Invest**, 120, n. 2, p. 485-497, Feb 2010.

GORDON, S.; MARTINEZ, F. O. Alternative activation of macrophages: mechanism and functions. **Immunity**, 32, n. 5, p. 593-604, May 28 2010.

GRAHAM, G. J.; WRIGHT, E. G.; HEWICK, R.; WOLPE, S. D. *et al.* Identification and characterization of an inhibitor of haemopoietic stem cell proliferation. **Nature**, 344, n. 6265, p. 442-444, Mar 29 1990.

GRILLE, S. J.; BELLACOSA, A.; UPSON, J.; KLEIN-SZANTO, A. J. *et al.* The protein kinase Akt induces epithelial mesenchymal transition and promotes enhanced motility and invasiveness of squamous cell carcinoma lines. **Cancer Res**, 63, n. 9, p. 2172-2178, May 1 2003.

GUO, L.; CHENG, X.; CHEN, H.; CHEN, C. *et al.* Induction of breast cancer stem cells by M1 macrophages through Lin-28B-let-7-HMGA2 axis. **Cancer Lett**, 452, p. 213-225, Jun 28 2019.

HAGEMANN, T.; ROBINSON, S. C.; SCHULZ, M.; TRUMPER, L. *et al.* Enhanced invasiveness of breast cancer cell lines upon co-cultivation with macrophages is due to TNF-alpha dependent up-regulation of matrix metalloproteases. **Carcinogenesis**, 25, n. 8, p. 1543-1549, Aug 2004.

HANNEN, E. J.; VAN DER LAAK, J. A.; MANNI, J. J.; PAHLPLATZ, M. M. *et al.* Improved prediction of metastasis in tongue carcinomas, combining vascular and nuclear tumor parameters. **Cancer**, 92, n. 7, p. 1881-1887, Oct 2001.

HAQUE, A.; MORIYAMA, M.; KUBOTA, K.; ISHIGURO, N. *et al.* CD206(+) tumor-associated macrophages promote proliferation and invasion in oral squamous cell carcinoma via EGF production. **Sci Rep**, 9, n. 1, p. 14611, Oct 10 2019.

HART, I. R. New evidence for tumour embolism as a mode of metastasis. **J Pathol**, 219, n. 3, p. 275-276, Nov 2009.

HELDIN, C. H.; LANDSTROM, M.; MOUSTAKAS, A. Mechanism of TGF-beta signaling to growth arrest, apoptosis, and epithelial-mesenchymal transition. **Curr Opin Cell Biol**, 21, n. 2, p. 166-176, Apr 2009.

HEPPNER, G. H. Tumor heterogeneity. **Cancer Res**, 44, n. 6, p. 2259-2265, Jun 1984.

HERMANN, P. C.; HUBER, S. L.; HERRLER, T.; AICHER, A. *et al.* Distinct populations of cancer stem cells determine tumor growth and metastatic activity in human pancreatic cancer. **Cell Stem Cell**, 1, n. 3, p. 313-323, Sep 13 2007.

IKENOUCHI, J.; MATSUDA, M.; FURUSE, M.; TSUKITA, S. Regulation of tight junctions during the epithelium-mesenchyme transition: direct repression of the gene expression of claudins/occludin by Snail. **J Cell Sci**, 116, n. Pt 10, p. 1959-1967, May 15 2003.

IKUSHIMA, H.; TODO, T.; INO, Y.; TAKAHASHI, M. *et al.* Autocrine TGF-beta signaling maintains tumorigenicity of glioma-initiating cells through Sry-related HMG-box factors. **Cell Stem Cell**, 5, n. 5, p. 504-514, Nov 6 2009.

Instituto Nacional de Câncer - INCA. Estatísticas de câncer, Brazil, 2019. Acesso em: March, 28th.

JONES, K. B.; KLEIN, O. D. Oral epithelial stem cells in tissue maintenance and disease: the first steps in a long journey. **Int J Oral Sci**, 5, n. 3, p. 121-129, Sep 2013.

KANG, Y.; MASSAGUE, J. Epithelial-mesenchymal transitions: twist in development and metastasis. **Cell**, 118, n. 3, p. 277-279, Aug 6 2004.

KATSUNO, Y.; LAMOUILLE, S.; DERYNCK, R. TGF-beta signaling and epithelial-mesenchymal transition in cancer progression. **Curr Opin Oncol**, 25, n. 1, p. 76-84, Jan 2013.

KNAACK, H.; LENK, L.; PHILIPP, L. M.; MIARKA, L. *et al.* Liver metastasis of pancreatic cancer: the hepatic microenvironment impacts differentiation and self-renewal capacity of pancreatic ductal epithelial cells. **Oncotarget**, 9, n. 60, p. 31771-31786, Aug 3 2018.

KROHN, A.; SONG, Y. H.; MUEHLBERG, F.; DROLL, L. *et al.* CXCR4 receptor positive spheroid forming cells are responsible for tumor invasion in vitro. **Cancer Lett**, 280, n. 1, p. 65-71, Jul 18 2009.

KWONG, L. N.; DAVIES, M. A. Targeted therapy for melanoma: rational combinatorial approaches. **Oncogene**, 33, n. 1, p. 1-9, Jan 2 2014.

LI, C.; HEIDT, D. G.; DALERBA, P.; BURANT, C. F. *et al.* Identification of pancreatic cancer stem cells. **Cancer Res**, 67, n. 3, p. 1030-1037, Feb 1 2007.

LIU, H.; PATEL, M. R.; PRESCHER, J. A.; PATSIALOU, A. *et al.* Cancer stem cells from human breast tumors are involved in spontaneous metastases in orthotopic mouse models. **Proc Natl Acad Sci U S A**, 107, n. 42, p. 18115-18120, Oct 19 2010.

LOCKE, M.; HEYWOOD, M.; FAWELL, S.; MACKENZIE, I. C. Retention of intrinsic stem cell hierarchies in carcinoma-derived cell lines. **Cancer Res**, 65, n. 19, p. 8944-8950, Oct 1 2005.

LONARDO, E.; HERMANN, P. C.; MUELLER, M. T.; HUBER, S. *et al.* Nodal/Activin signaling drives self-renewal and tumorigenicity of pancreatic cancer stem cells and provides a target for combined drug therapy. **Cell Stem Cell**, 9, n. 5, p. 433-446, Nov 4 2011.

LU, F. X.; JACOBSON, R. S. Oral mucosal immunity and HIV/SIV infection. **J Dent Res**, 86, n. 3, p. 216-226, Mar 2007.

LUO, X.; YU, Y.; LIANG, A.; XIE, Y. *et al.* Intratumoral expression of MIP-1beta induces antitumor responses in a pre-established tumor model through chemoattracting T cells and NK cells. **Cell Mol Immunol**, 1, n. 3, p. 199-204, Jun 2004.

MARUSYK, A.; ALMENDRO, V.; POLYAK, K. Intra-tumour heterogeneity: a looking glass for cancer? **Nat Rev Cancer**, 12, n. 5, p. 323-334, Apr 19 2012.

MASSAGUE, J. TGFbeta in Cancer. **Cell**, 134, n. 2, p. 215-230, Jul 25 2008.

MATTIJSSEN, V.; PETERS, H. M.; SCHALKWIJK, L.; MANNI, J. J. *et al.* E-cadherin expression in head and neck squamous-cell carcinoma is associated with clinical outcome. **Int J Cancer**, 55, n. 4, p. 580-585, Oct 1993.

MCCAFFREY, L. M.; MACARA, I. G. Epithelial organization, cell polarity and tumorigenesis. **Trends Cell Biol**, 21, n. 12, p. 727-735, Dec 2011.

MOREL, A. P.; LIÈVRE, M.; THOMAS, C.; HINKAL, G. *et al.* Generation of breast cancer stem cells through epithelial-mesenchymal transition. **PLoS One**, 3, n. 8, p. e2888, Aug 2008.

NAKAYAMA, S.; SASAKI, A.; MESE, H.; ALCALDE, R. E. *et al.* Establishment of high and low metastasis cell lines derived from a human tongue squamous cell carcinoma. **Invasion Metastasis**, 18, n. 5-6, p. 219-228, 1998-1999 1998.

NANCI, A. **Ten Cate, histologia oral**. 8th ed. Rio de Janeiro: Elsevier, 2013. 400 p.

NOWELL, P. C. The clonal evolution of tumor cell populations. **Science**, 194, n. 4260, p. 23-28, Oct 1 1976.

OFT, M.; HEIDER, K. H.; BEUG, H. TGFbeta signaling is necessary for carcinoma cell invasiveness and metastasis. **Curr Biol**, 8, n. 23, p. 1243-1252, Nov 19 1998.

OKAMOTO, M.; NISHIMINE, M.; KISHI, M.; KIRITA, T. *et al.* Prediction of delayed neck metastasis in patients with stage I/II squamous cell carcinoma of the tongue. **J Oral Pathol Med**, 31, n. 4, p. 227-233, Apr 2002.

ORTIZ, R. C.; LOPES, N. M.; AMÔR, N. G.; PONCE, J. B. *et al.* CD44 and ALDH1 immunoexpression as prognostic indicators of invasion and metastasis in oral squamous cell carcinoma. **J Oral Pathol Med**, May 2018.

PAPINI, S.; CECCHETTI, D.; CAMPANI, D.; FITZGERALD, W. *et al.* Isolation and clonal analysis of human epidermal keratinocyte stem cells in long-term culture. **Stem Cells**, 21, n. 4, p. 481-494, 2003.

POLLARD, J. W. Tumour-educated macrophages promote tumour progression and metastasis. *In*: **Nat Rev Cancer**. England, 2004. v. 4, p. 71-78.

PORTELLA, G.; CUMMING, S. A.; LIDDELL, J.; CUI, W. *et al.* Transforming growth factor beta is essential for spindle cell conversion of mouse skin carcinoma in vivo: implications for tumor invasion. **Cell Growth Differ**, 9, n. 5, p. 393-404, May 1998.

PRINCE, M. E.; AILLES, L. E. Cancer stem cells in head and neck squamous cell cancer. **J Clin Oncol**, 26, n. 17, p. 2871-2875, Jun 10 2008.

PRINCE, M. E.; SIVANANDAN, R.; KACZOROWSKI, A.; WOLF, G. T. *et al.* Identification of a subpopulation of cells with cancer stem cell properties in head and neck squamous cell carcinoma. **Proc Natl Acad Sci U S A**, 104, n. 3, p. 973-978, Jan 16 2007.

QIAN, B. Z.; POLLARD, J. W. Macrophage diversity enhances tumor progression and metastasis. **Cell**, 141, n. 1, p. 39-51, Apr 2 2010.

QIAO, J.; LIU, Z.; DONG, C.; LUAN, Y. *et al.* Targeting Tumors with IL-10 Prevents Dendritic Cell-Mediated CD8(+) T Cell Apoptosis. **Cancer Cell**, 35, n. 6, p. 901-915.e904, Jun 10 2019.

REYA, T.; CLEVERS, H. Wnt signalling in stem cells and cancer. **Nature**, 434, n. 7035, p. 843-850, Apr 14 2005.

REYA, T.; MORRISON, S. J.; CLARKE, M. F.; WEISSMAN, I. L. Stem cells, cancer, and cancer stem cells. **Nature**, 414, n. 6859, p. 105-111, Nov 1 2001.

RODINI, C. O.; LOPES, N. M.; LARA, V. S.; MACKENZIE, I. C. Oral cancer stem cells - properties and consequences. **J Appl Oral Sci**, 25, n. 6, p. 708-715, Nov-Dec 2017.

RONCA, R.; VAN GINDERACHTER, J. A.; TURTOI, A. Paracrine interactions of cancer-associated fibroblasts, macrophages and endothelial cells: tumor allies and foes. **Curr Opin Oncol**, 30, n. 1, p. 45-53, Jan 2018.

SAFINA, A.; VANDETTE, E.; BAKIN, A. V. ALK5 promotes tumor angiogenesis by upregulating matrix metalloproteinase-9 in tumor cells. **Oncogene**, 26, n. 17, p. 2407-2422, Apr 12 2007.

SANSONE, P.; STORCI, G.; TAVOLARI, S.; GUARNIERI, T. *et al.* IL-6 triggers malignant features in mammospheres from human ductal breast carcinoma and normal mammary gland. **J Clin Invest**, 117, n. 12, p. 3988-4002, Dec 2007.

SASAHIRA, T.; KIRITA, T. Hallmarks of Cancer-Related Newly Prognostic Factors of Oral Squamous Cell Carcinoma. **Int J Mol Sci**, 19, n. 8, Aug 2018.

SATHYANARAYANAN, V.; NEELAPU, S. S. Cancer immunotherapy: Strategies for personalization and combinatorial approaches. **Mol Oncol**, 9, n. 10, p. 2043-2053, Dec 2015.

SHIN, K.; FOGG, V. C.; MARGOLIS, B. Tight junctions and cell polarity. **Annu Rev Cell Dev Biol**, 22, p. 207-235, 2006.

SHIOZAWA, Y.; NIE, B.; PIENTA, K. J.; MORGAN, T. M. *et al.* Cancer stem cells and their role in metastasis. **Pharmacol Ther**, 138, n. 2, p. 285-293, May 2013.

SICA, A.; MANTOVANI, A. Macrophage plasticity and polarization: in vivo veritas. **J Clin Invest**, 122, n. 3, p. 787-795, Mar 2012.

SU, S.; LIU, Q.; CHEN, J.; CHEN, F. *et al.* A positive feedback loop between mesenchymal-like cancer cells and macrophages is essential to breast cancer metastasis. **Cancer Cell**, 25, n. 5, p. 605-620, May 12 2014.

TAN, L.; SUI, X.; DENG, H.; DING, M. Holoclone forming cells from pancreatic cancer cells enrich tumor initiating cells and represent a novel model for study of cancer stem cells. **PLoS One**, 6, n. 8, p. e23383, 2011.

THIERY, J. P. Epithelial-mesenchymal transitions in tumour progression. **Nat Rev Cancer**, 2, n. 6, p. 442-454, Jun 2002.

THIERY, J. P. Epithelial-mesenchymal transitions in development and pathologies. **Curr Opin Cell Biol**, 15, n. 6, p. 740-746, Dec 2003.

THIERY, J. P.; ACLOQUE, H.; HUANG, R. Y.; NIETO, M. A. Epithelial-mesenchymal transitions in development and disease. **Cell**, 139, n. 5, p. 871-890, Nov 25 2009.

TIECHE, C. C.; GAO, Y.; BUHRER, E. D.; HOBI, N. *et al.* Tumor Initiation Capacity and Therapy Resistance Are Differential Features of EMT-Related Subpopulations in the NSCLC Cell Line A549. **Neoplasia**, 21, n. 2, p. 185-196, Feb 2019.

VAN MEIR, E. G.; HADJIPANAYIS, C. G.; NORDEN, A. D.; SHU, H. K. *et al.* Exciting new advances in neuro-oncology: the avenue to a cure for malignant glioma. **CA Cancer J Clin**, 60, n. 3, p. 166-193, May-Jun 2010.

VENKATESH, V.; NATARAJ, R.; THANGARAJ, G. S.; KARTHIKEYAN, M. *et al.* Targeting Notch signalling pathway of cancer stem cells. **Stem Cell Investig**, 5, p. 5, 2018.

WANG, R.; ZHANG, J.; CHEN, S.; LU, M. *et al.* Tumor-associated macrophages provide a suitable microenvironment for non-small lung cancer invasion and progression. **Lung Cancer**, 74, n. 2, p. 188-196, Nov 2011. Research Support, Non-U.S. Gov't.

WANG, Y.; WANG, T.; SUN, Y.; SUN, W. *et al.* Astrocyte elevated gene-1 promotes tumour growth and invasion by inducing EMT in oral squamous cell carcinoma. **Sci Rep**, 7, n. 1, p. 15447, Nov 13 2017.

WANGSA, D.; RYOTT, M.; AVALL-LUNDQVIST, E.; PETERSSON, F. *et al.* Ki-67 expression predicts locoregional recurrence in stage I oral tongue carcinoma. **Br J Cancer**, 99, n. 7, p. 1121-1128, Oct 7 2008.

WATT, F. M. Role of integrins in regulating epidermal adhesion, growth and differentiation. **Embo j**, 21, n. 15, p. 3919-3926, Aug 1 2002.

WU, K.; DING, J.; CHEN, C.; SUN, W. *et al.* Hepatic transforming growth factor beta gives rise to tumor-initiating cells and promotes liver cancer development. **Hepatology**, 56, n. 6, p. 2255-2267, Dec 2012.

YANAMOTO, S.; KAWASAKI, G.; YAMADA, S.; YOSHITOMI, I. *et al.* Isolation and characterization of cancer stem-like side population cells in human oral cancer cells. **Oral Oncol**, 47, n. 9, p. 855-860, Sep 2011.

YU, C. C.; CHANG, Y. C. Enhancement of cancer stem-like and epithelial-mesenchymal transdifferentiation property in oral epithelial cells with long-term nicotine exposure: reversal by targeting SNAIL. **Toxicol Appl Pharmacol**, 266, n. 3, p. 459-469, Feb 1 2013.

ZHANG, H.; LIU, L.; WANG, Y.; ZHAO, G. *et al.* KLF8 involves in TGF-beta-induced EMT and promotes invasion and migration in gastric cancer cells. **J Cancer Res Clin Oncol**, 139, n. 6, p. 1033-1042, Jun 2013.

ZHANG, J.; ZHENG, G.; ZHOU, L.; LI, P. *et al.* Notch signalling induces epithelialmesenchymal transition to promote metastasis in oral squamous cell carcinoma. **Int J Mol Med**, 42, n. 4, p. 2276-2284, Oct 2018.

Appendixes

DECLARAÇÃO DE USO EXCLUSIVO DE ARTIGO EM TESE

Declaramos estarmos cientes de que o trabalho ***Cancer stem-cells subpopulations differentially affect oral squamous carcinoma behavior* in vivo *and* in vitro** será apresentado na ***Tese*** da aluna ***Nádia Ghinelli Amôr***, e que não foi e nem será utilizado em outra dissertação/tese dos Programas de Pós-Graduação da FOB-USP.

Bauru, 30 de outubro de 2019.

Nádia Ghinelli Amôr	Nádia G. Amôr Assinatura
Rodrigo Fonseca Buzo	Rodrigo Fonseca Buzo Assinatura
Rafael Carneiro Ortiz	Rafael Ortiz Assinatura
Nathália Martins Lopes	Nathália Lopes Assinatura
Luciana Mieli Saito	Assinatura
Dra. Camila de Oliveira Rodini Pegoraro	Camila O. Rodini Pegoraro Assinatura

DECLARAÇÃO DE USO EXCLUSIVO DE ARTIGO EM TESE

Declaramos estarmos cientes de que o trabalho ***Macrophages promote aggressive behavior on tumor cells via TGF-β signaling in oral squamous cell carcinoma***, e que não foi e nem será utilizado em outra dissertação/tese dos Programas de Pós-Graduação da FOB-USP.

Bauru, 30 de outubro de 2019.

Nádia Ghinelli Amôr	Nádia G. Amôr Assinatura
Nathália Martins Lopes	Nathália Lopes Assinatura
Rafael Carneiro Ortiz	Rafael Ortiz Assinatura
Rodrigo Fonseca Buzo	Rodrigo Fonseca Buzo Assinatura
Luciana Mieli Saito	Assinatura
Dra. Camila Oliveira Rodini	Camila Rodrigo Assinatura

Annexes

Gmail

Nádia Ghinelli Amôr <nadiaghiamor@gmail.com>

ONC-2019-02232 Approved MS Receive

Oncogene@us.nature.com <Oncogene@us.nature.com> Wed, Oct 30, 2019 at 8:34 AM
Reply-To: Oncogene@us.nature.com
To: nadiaghiamor@gmail.com

Dear Miss Amôr,

On 30th Oct 19, the manuscript entitled "Cancer stem-cells subpopulations differentially affect oral squamous carcinoma behavior in vivo and in vitro" by Nádia Amôr, Rodrigo Buzo, Rafael Ortiz, Nathália Lopes, Luciana Saito, and Camila Rodini was submitted by the author.

The manuscript has been assigned the Paper #: ONC-2019-02232.

Your manuscript will now undergo internal review by one of our Deputy Editors. This initial screening has been put in place due to the high volume of manuscripts we receive and will determine whether your paper is suitable to proceed to full peer review. If successful, the editorial office will quality check your manuscript and then assign to an Associate Editor who will allocate reviewers.
If unsuccessful, a decision will be returned to you promptly allowing you to submit elsewhere in a timely manner.

You may check on the status of this manuscript by selecting the "Check Manuscript Status" link under the following URL:

https://mts-onc.nature.com/cgi-bin/main.plex?el=A1BT2WLb5A1BnpX7F6A9ftdo8ZPALNzzIywUYHCI6ywbAZ

(Press/Click on the above link to be automatically sent to the web page.)

You can now use a single sign-on for all your accounts, view the status of all your manuscript submissions and reviews, access usage statistics for your published articles and download a record of your refereeing activity for the Nature journals. Please check your account regularly and ensure that we have your current contact information.

In addition, Springer Nature encourages all authors and reviewers to associate an Open Researcher and Contributor Identifier (ORCID) to their account. ORCID is a community-based initiative that provides an open, non-proprietary and transparent registry of unique identifiers to help disambiguate research contributions.

Sincerely,

Dr Justin Stebbing
Dr George Miller
Editors-in-Chief
Oncogene
oncogene@natureny.com

ONC - This email has been sent through the Springer Nature Tracking System NY-610A-NPG&MTS

Confidentiality Statement:

This e-mail is confidential and subject to copyright. Any unauthorised use or disclosure of its contents is prohibited. If you have received this email in error please notify our Manuscript Tracking System Helpdesk team at

Universidade de São Paulo
Faculdade de Odontologia de Bauru

Comissão de Ética no Ensino e Pesquisa em Animais

CEEPA-Proc. Nº 002/2017.

Bauru, 5 de maio de 2017.

Senhora Professora,

Informamos que Projeto de Pesquisa denominado ***"Caracterização da Relação Funcional entre Macrófagos, Fenótipo Célula-Tronco de Câncer e Fenômeno de Transição Epitélio-Mesenquimal no Carcinoma Epidermóide de Boca"*** tendo Vossa Senhoria como Pesquisador Responsável, que envolve a utilização de animais (roedores), para fins de pesquisa científica, encontra-se de acordo com os preceitos da Lei nº 11.794, de 8 de outubro de 2008, do Decreto nº 6.899, de 15 de julho de 2009, e com as normas editadas pelo Conselho Nacional de Controle da Experimentação Animal (CONCEA), foi analisado e considerado APROVADO em reunião ordinária da Comissão de Ética no Ensino e Pesquisa em Animais (CEEPA), realizada nesta data.

Vigência do projeto:	*Maio/2017 a Maio/2020*
Espécie/Linhagem:	*Camundongos imunodeficientes NOD/SCID*
Nº de animais:	*300*
Peso/Idade	*20g/6-8 semanas*
Sexo:	*Machos e fêmeas*
Origem:	*Centro de Bioterismo da Faculdade de Medicina da USP*

Esta CEEPA solicita que ao final da pesquisa seja enviado um Relatório com os resultados obtidos para análise ética e emissão de parecer final, o qual poderá ser utilizado para fins de publicação científica.

Atenciosamente,

Profª Drª Ana Paula Campanelli

Presidente da Comissão de Ética no Ensino e Pesquisa em Animais

Profa. Dra. Camila de Oliveira Rodini Pegoraro
Docente do Departamento de Ciências Biológicas

Al. Dr. Octávio Pinheiro Brisolla, 9-75 – Bauru-SP – CEP 17012-901 – C.P. 73
e-mail: ceepa@fob.usp.br – Fone/FAX (0xx14) 3235-8356
http://www.fob.usp.br